UNIVERSITÀ
DEGLI STUDI
DI TRIESTE

UNIVERSITÀ DEGLI STUDI DI TRIESTE

XXXVIII CICLO DEL DOTTORATO DI RICERCA IN BIOMEDICINA MOLECOLARE

Set up of a celiac disease derived organoid model to study ER stress

Settore scientifico-disciplinare: BIO/13

DOTTORANDO

Samuele Pellizzaro

COORDINATORE

PROF. Alessandro Tossi

SUPERVISORE DI TESI

PROF. Daniele Sblattero

ANNO ACCADEMICO 2024/2025

ABSTRACT

Celiac disease (CD) is a systemic autoimmune disorder caused by the ingestion of gluten in genetically predisposed individuals carrying the human leukocyte antigen (**HLA) DQ2 and/or DQ8**. With an overall average prevalence of 1% it is one of the **most diffused chronic diseases** worldwide. It affects the proximal small intestine leading to intestinal damage, malnutrition and other intestinal symptoms frequently accompanied by a wide variety of extraintestinal symptoms. To date, there is **no cure for CD**, and the only available therapy is a lifelong gluten-free diet which, despite working, is difficult to follow and has side-effects both physically and mentally on the patient.

CD pathogenesis has an important **immune component** that is well known but the autoimmune response can't fully explain CD pathogenesis, meaning that **over components must be involved** in CD pathogenesis. Among these, it is still unclear what the effect of gluten peptides is on intestinal cells, possibly due to the **lack of a suitable model**. Recently, the development of organoid technology allowed the generation of **intestinal organoids** derived from duodenal or colonic tissue, giving a useful tool to study intestinal cells in a more faithful *in vitro* model.

In this PhD thesis, we evaluated the **induction of ER stress in enterocytes in a patient's derived organoid from control and CD patients by a digest of gliadin with pepsin and trypsin** (peptic-tryptic gliadin digest, PTG) to mimic gliadin peptides. First, we showed induction of ER stress in a cell model using CaCo-2, in an animal model using gluten-sensitive mouse intestine in the gut *ex-vivo* system (GEVS) after PTG stimulation, and in patients biopsies.

Then we established reproducible **protocols for organoids generation** from control and CD patient's duodenal biopsies, **culturing and expanding them maintaining their stemness**. To obtain an organoid resembling intestinal tissue cellular composition, we established a **differentiation protocol** to differentiate intestinal stem cells into the other intestinal cell types. This is **confirmed by principal component analysis** (PCA) on staminal organoids versus differentiated ones, **and qPCR** analysis of differentiation marker gene for enterocytes, confirming the presence of Goblet cells too, and of a small population of Paneth cells. From this analysis we didn't observe differences between control and CD

organoids, meaning that organoids of both groups are generated and differentiated with the same efficiency.

To resemble intestinal cell organization and mimic the interaction between gliadin peptides and enterocytes' apical surface, we **inverted the polarity of our organoids** exposing the apical surface outside (apical-out organoids) while previously it was facing the inner cavity of the organoid (basal-out organoids), confirming the inversion through **immunofluorescence.**

With our protocols set up and verified, **organoids from 7 control patients and 6 CD patients** have been generated, expanded, differentiated and inverted: these are stimulated with **PTG for 1h and 8h or left untreated**, then analyzed by qPCR to evaluate ER stress induction and of a CD marker to check if the organoids retain some typical celiac characteristics. The data obtained suggests a **trend in CD patients detecting ER stress after 8h.** However, these data have high standard deviations, indicating a **heterogeneous sensibility to PTG across CD patients** not restricted to ER stress induction but as a response to PTG as a whole since CD marker has also high standard deviation.

Overall, we **established protocols to generate and work with organoids** obtained from patients' biopsies, developing a human model that can replicate the heterogeneity found in patients, the complexity present in the intestine, in combination with the accessibility given by an *in vitro* model. With this model, we studied **ER stress induction in CD patients' derived organoids, that is present but with heterogeneity** across CD samples, establishing a trend that needs to be studied more in depth.

TABLE OF CONTENTS

1. INTRODUCTION

1.1 Celiac disease

Celiac disease (CD) is a systemic autoimmune disorder caused by the ingestion of gluten in genetically predisposed individuals [1], [2], characterized by the presence of human leukocyte antigen (HLA) DQ2 and DQ8. It affects the proximal small intestine, leading to villus atrophy and crypt hyperplasia, together with increased numbers of lamina propria and intraepithelial lymphocytes (IELs) [3] and a variety of intestinal and extraintestinal symptoms in response to gluten [4], [5]. Previously considered a rare pediatric disease predominantly found in Europe, now, thanks to the increasing availability of sensitive and specific screening tests, raising significantly the diagnoses of CD [2], it is recognized as one of the most common lifelong disorders worldwide, affecting people of all ages [6].

The most common intestinal symptoms of CD include diarrhea, abdominal pain, weight loss, nausea, constipation and malnutrition [7], together with many different extraintestinal symptoms, mainly caused by malabsorption, affecting the body at a systemic level. Despite being the most known, less than 50% of patients present with gastrointestinal symptoms [4] (that are more common in children), making CD diagnosis challenging [4], [7]. Untreated CD for long periods of time can lead to the development of complications like malignant tumors and other comorbidities, prevalently autoimmune diseases like type 1 diabetes [1], [8]. The only available therapy for CD is the complete removal of gluten from the diet, adopting a gluten-free diet, that although being effective in most cases in recovering the normal mucosal phenotype, is difficult to follow, has different side-effect on the physical and psychosocial side and not every patient respond to it, showing the need for new therapies for the treatment of CD [9].

1.1.1 Epidemiology

In the past decades, CD was considered an uncommon disease affecting children and restricted to the European population. Thanks to the diffusion of serological tests and a simplification of the diagnostic criteria, CD has been identified in countries outside Europe all over the world and in patients at different ages, establishing the **overall average prevalence** of CD in the global population at 1% [10]. Observing the distribution of prevalence across the world, it varies based on geographic location, ranging from 0,4% in

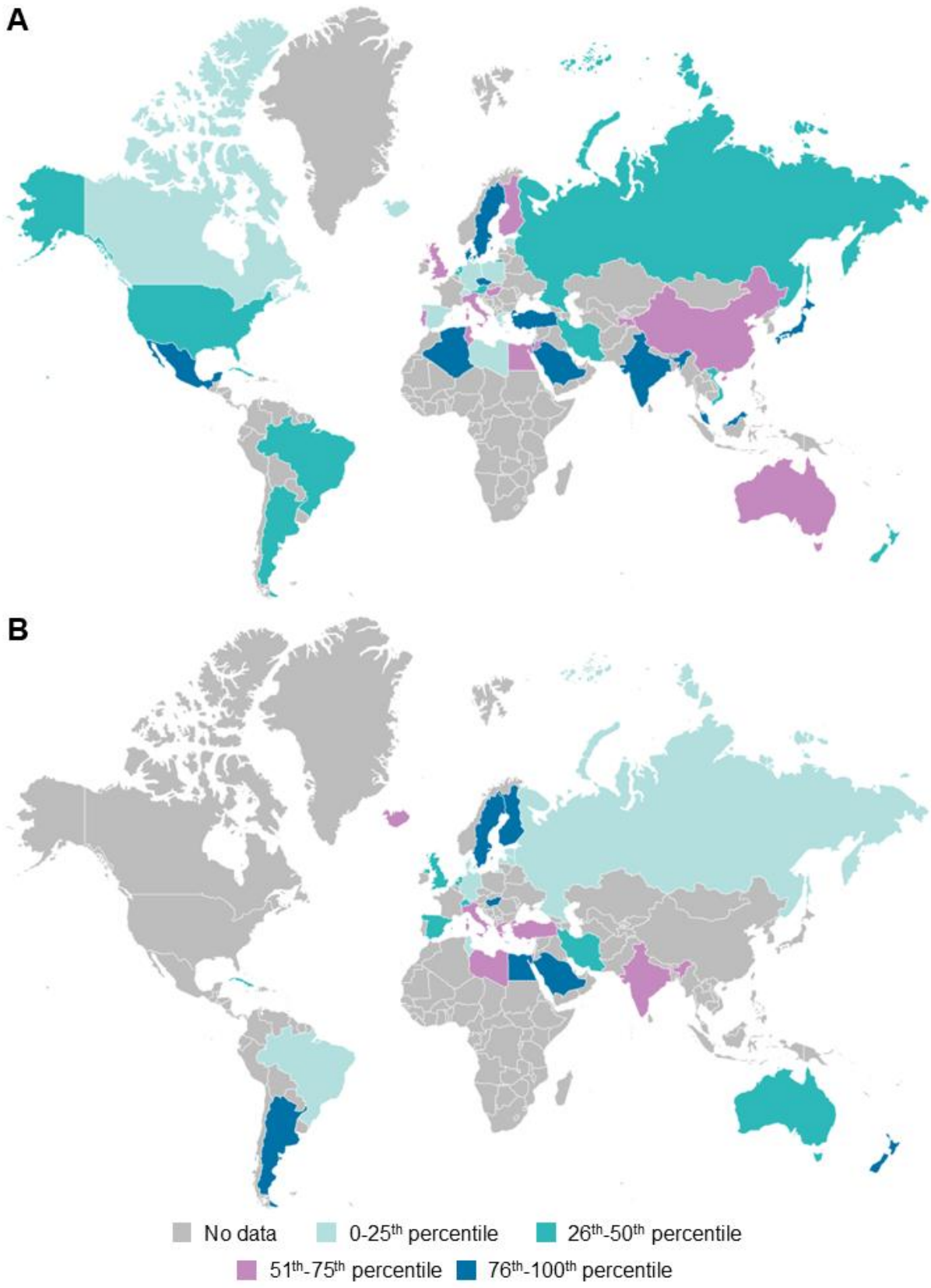

Figure 1: A) *worldwide prevalence of CD determined by seropositivity: corresponding prevalence values for each percentile are 0,8% (25th percentile), 1,1% (50th percentile), 2,0% (75th percentile) and 8,5% (100th percentile).* ***B)*** *worldwide prevalence of CD diagnosed based on biopsy analysis: corresponding prevalence values for each percentile are 0,36% (25th percentile), 0,6% (50th percentile), 1,1% (75th percentile) and 3,0% (100th percentile). Data and graphs obtained from [11].*

South America to 0,8% in Europe and Oceania (Figure 1). These differences in prevalence are even higher when focusing on singular countries, suggesting the involvement of environmental factors in etiology of the disease [11], [12].

CD is also diagnosed more frequently in women than men, with a ratio between 1,5 and 2, and a higher prevalence in children than adults [13]. In accordance with the genetic predisposition characteristic of CD, it has been noted a higher risk of developing CD in first-degree CD relatives (10-15%) [14], which is further confirmed by investigating CD development in twins, especially in monozygotic twins where the concordance rate of HLA and non-HLA genes confirms a high heritability in CD [15], [16].

1.1.2 Clinical manifestations

Clinical manifestations of CD are classified as intestinal and extraintestinal. While intestinal symptoms are the most well-known, most patients present with extraintestinal symptoms, which are more common, especially when CD manifests itself in adulthood. The disease can presents at any particular age but there are two peaks of onset, one is in the first 2 years of life after encountering gluten, the second one is in the second or third decade of life, which diagnosis can be challenging given the variety of symptoms from patient to patient [17].

Intestinal symptoms (Figure 2) are found more frequently in children and include diarrhea, nausea, vomiting, bloating, abdominal pain, malabsorption, and consequent malnutrition, which can cause involuntary weight loss in some patients. Despite malnutrition being a frequent manifestation of CD, being underweight isn't directly associated with it, on the contrary a higher percentage of patients show overweight and obesity at the diagnosis of CD, in which the classical intestinal symptoms, like diarrhea, are less common, contributing to a delayed diagnosis of the disease [18].

Extraintestinal symptoms are more varied, some manifestations can be explained by malabsorption caused by CD, while other symptoms can be a consequence of the immune reactions in the autoimmune processes that characterize CD. The extraintestinal manifestations can be (Figure 2):

- General symptoms.
- Oral symptoms.
- Bone metabolic disorders.
- Dermatological conditions.

- Endocrine and gynecological disorders.
- Hematological disorders.
- Neurological and psychiatric disorders.
- Vitamin deficiencies with related consequences.

The adoption and the continuos following of a rigid gluten-free diet usually resolve these manifestations, even though some symptoms can last for longer periods of time despite the elimination of gluten in a subgroup of patients, of which some do not respond to the treatment, showing a persistence of the symptoms [2], [7], [19].

Based on symptomatology, CD has been classified into five types:

- **classical CD**, that presents symptoms of malabsorption (diarrhea, steatorrhea, weight loss or growth failure is required), therefore including some intestinal manifestations but also disorders derived from deficiencies, like anemia.
- **Non classical CD** on the opposite side presents without signs or symptoms of malabsorption, like constipation or abdominal pain.

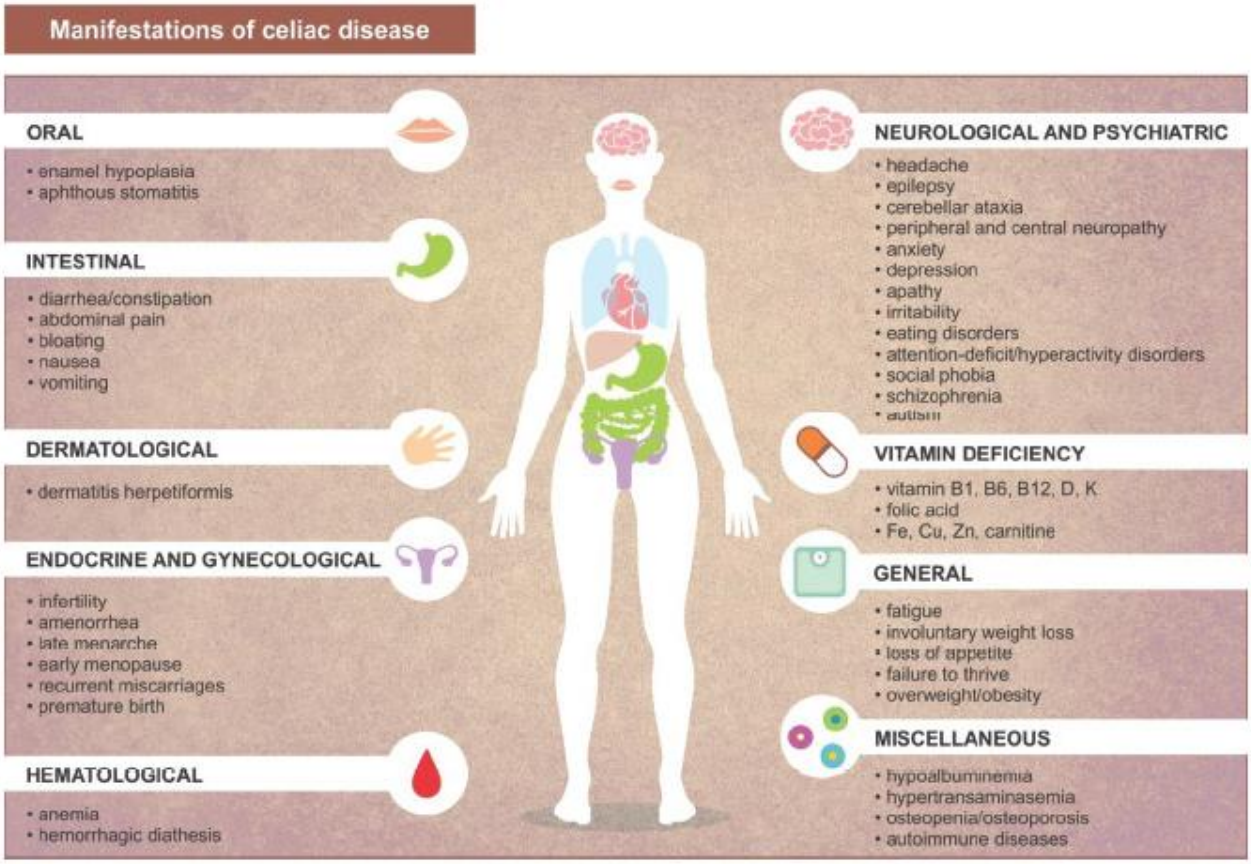

***Figure 2**: intestinal and extraintestinal manifestations of CD [7].*

- **Subclinical CD** refers to patients presenting with extraintestinal symptoms or some clinical/laboratory signs but without symptoms, although having these characteristics they are below the threshold of detection without signs or symptoms sufficient to start CD testing.
- **Potential CD** presents with a normal small intestinal mucosa but also with positive CD serology, indicating an increased risk of CD development.
- **Refractory CD** refers to patients with persistent or recurrent malabsorption symptoms accompanied by villous atrophy despite following a rigid gluten-free diet for more than 12 months. Refractory CD is diagnosed after excluding other possible causes for villous atrophy and confirming the initial diagnosis of CD. Usually, these patients are negative for CD serology markers because of being on a gluten-free diet, even though the persistence of positivity does not exclude refractory CD, but it requires confirming the absence of accidental gluten exposure or dietary adherence [20]. Refractory CD is divided into two categories, type I characterized by a normal intra-epithelial lymphocyte phenotype and type II, in which there is a clonal expansion of an aberrant intra-epithelial lymphocyte population and is associated with the development of enteropathy-associated T-cell lymphoma [21].

1.1.3 Gluten characteristics

Gluten is the term used to indicate the storage proteins present in wheat, rye and barley. Wheat gluten is divided into **glutenins** and **gliadins**. Rye gluten contains prolamins called secalins while barley prolamins are termed hordeins. These proteins are characterized by a high proportion of proline (Pro) and glutamine (Gln) residues. This composition does not allow gastric and pancreatic enzymes to fully break them, and because of their immunogenicity, an immune response is started [12], [22].

Wheat gluten, being one of the most used cereals in food, has been well characterized. Due to protein polymorphism, multigene families and post-translational modifications, up to 1300 wheat grain proteins have been detected, with glutenins and gliadins representing around 70-80% of total grain proteins; the remaining proteins are albumins, globulins and residual insoluble proteins. This subdivision is based on the solubility of these protein fractions (Figure 3A). Albumins and globulins are both soluble in diluted salt solutions and albumins also in solely water; glutenins and gliadins are insoluble in aqueous solutions but are soluble

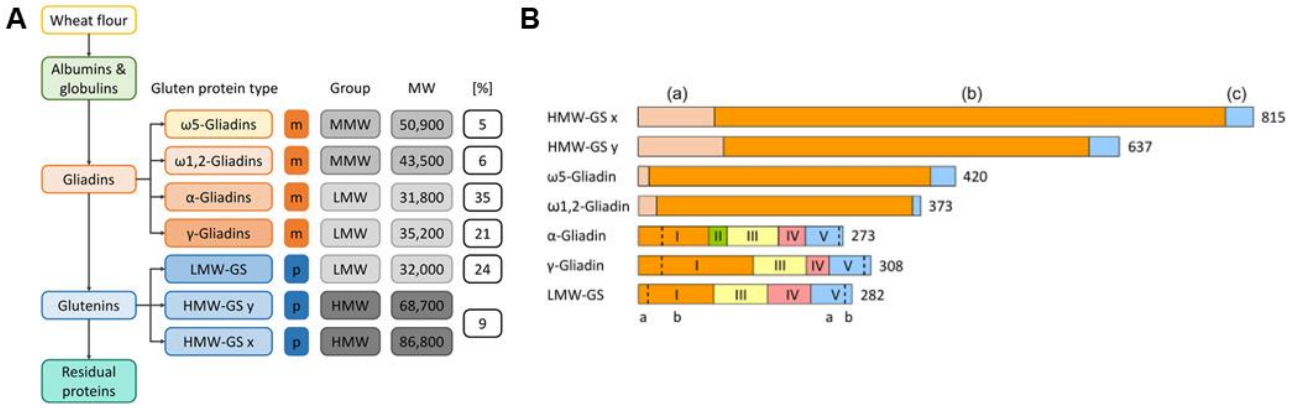

***Figure 3**: **A)** wheat grain proteins classification: wheat proteins can be grouped in albumins and globulins, gliadin and glutenins (called gluten proteins) based on their aqueous solubility, with a small fraction being residual insoluble proteins. Gliadin proteins can be further subdivided in α-, γ-, ω1,2-, and ω5-gliadins, whereas glutenins are divided in LMW-GS and HMW-GS, which are subdivided in x- and y-type. Each gluten protein type is monomeric (m) or polymeric (p), classified based on their MW in LMW, MMW and HMW group and have a relative abundance in the totality of gluten proteins [23]. **B)** gluten proteins composition. HWS-GS x- and y-type, as well as ω1,2-, and ω5-gliadins have a non-repetitive N-term domain (a) and C-term domain (c) and a repetitive central domain (b), while LMW-GS and α- and γ-gliadin have an N-term domain that includes segment I (subdivided in an homologous section Ia and repetitive one Ib) and segment II in α-gliadins, and a C-term domain that is composed by the homologous segment III, IV and V (divided in an homologous section Va and a unique one for each protein type [23].*

only in aqueous alcohols, with glutenins becoming soluble only after reduction of disulfide bonds. Glutenins are divided into **low-molecular-weight glutenin subunits (LMW-GS) and high-molecular-weight glutenin subunits (HMW-GS)** based on their mobility on sodium dodecyl sulfate-polyacrylamide gel electrophoresis (SDS-PAGE), with HMW-GS being further subdivided into x-type and y-type, whereas gliadins are subdivided into **α-, γ-, ω1,2-, and ω5-gliadins** based on their mobility on acid-polyacrylamide gel electrophoresis (A-PAGE) (Figure 3A). Considering their molecular weight of each protein type, they are also grouped in three classes being low-, medium- and high- molecular weight (LMW, MMW and HMW) [23].

HMW-GS organization consists of an N-terminal domain A, a repetitive central domain B and a C-terminal domain C (Figure 3B): domains A and C are non-repetitive and contains most cysteines and charged amino acids, while domain B has a repetitive sequence as a backbone that is frequently modified by a single amino acid, with one repetitive unit separated from the other by nonapeptides or tripeptides in the HMW-GS x-type, and by hexapeptides in the y-type that usually shows a shorter B domain. ω1,2-, and ω5-gliadins are similar (Figure 3B), being composed of a short non-repetitive N-terminal and C-terminal domains called A and C respectively, and a repetitive central domain B that is shorter in ω1,2-gliadins.

α-, γ-gliadins and LMW-GS have partly homologous sequences that can be divided into an N-terminal domain containing segments I and II, and a C-terminal domain with segments III, IV and V (Figure 3B). The N-terminal domain starts with a short non-repetitive sequence (Ia) characteristic of each type, followed by unique repetitive units constituting segment Ib. The C-terminal domain shows non-repetitive sequences and a more balanced amino-acid composition, with segment III being the most homologous of the segments, segment IV containing a homologous section and a unique one for each type, as well as segment V (the homologous sequence is identified as Va while the unique one as Vb) [23].

ω1,2-, and ω5-gliadins have no or few cysteines, therefore there aren't disulfide bonds in their structure, on the contrary, the other gluten proteins have interchain disulfide bonds that have an important role in the determination of their structure. HMW-GS can also establish disulfide bonds with other HMW-GS and LMW-GS molecules, creating a network of proteins bound with each other [23].

1.1.4 Gliadin toxic peptides

Among these gliadin peptides, the α-gliadin 56-88 peptide (called **33mer**) and the α-gliadin 31-43 peptide (**p31-43**) have shown properties that could contribute to the pathogenic mechanisms of CD [24]. Especially p31-43 has been extensively studied: it showed to induce Ca^{2+} mobilization from intracellular stores in enterocytes, activating type 2 transglutaminase (TG2) and inducing ER stress [25], [26]; it is able to form stable aggregates that activate the inflammasome consequently inducing inflammation and mucosal damage [24], [27]; it has inflammatory effects on the cell, inducing the production of inflammatory cytokines and reactive oxygen species (ROS), making cells more susceptible to apoptosis [3]. Additionally, it has been shown that enterocytes of CD patients are constitutively more susceptible to inflammation and more sensible to inflammatory stimuli given by gluten peptides [28].

Among gliadin peptides, some have shown resistance to digestive enzyme and have been studied to discover their role in CD and its pathogenesis. The α-gliadin 56-88 peptide (called **33mer**) and the α-gliadin 31-43 peptide (**p31-43**) have been the main focus, especially p31-43 have many effects directly affecting cells [24]:

- **It activates the innate immunity**, inducing increased expression of interleukin-15 (IL-15), intercellular adhesion molecule 1 (ICAM1) which is essential for leukocytes

motility, an of HLA, leading to increased death of the enterocytes in CD patients [29]. The ability of p31-43 to activate the innate immunity was further confirmed in a mouse model where it was administered via intraluminal injection, and in response it caused an **increase of intraepithelial lymphocytes** (IELs) and the reduction of villous height/crypt depth ratio [30].

- It induces **mast cells degranulation** from CD patients and the expression of **proinflammatory cytokines and chemokines** [31].
- **It increases the expression of major histocompatibility complex class I polypeptide-related sequence A** (MICA), a molecule expressed on the surface of cells in response to stress conditions, signaling damage and inducing IELs activation to eliminate the stressed cell through the interaction with receptors on natural killer cells (NK cells). MICA expression is increased also in response to IL-15 [32].
- It can **mobilize Ca^{2+}** from endoplasmic reticulum and mitochondrial stores, causing ER stress and leading to activation of **type 2 transglutaminase (TG2)**, a Ca^{2+} dependent enzyme important in CD pathogenesis [25], [26]. It also causes cellular stress through the **production of reactive oxygen species** (ROS) [33].
- It can **bind to TG2** activated by Ca^{2+}, covalent binding with TG2 promotes the formation of complexes between the enzyme and a subunit of cystic fibrosis transmembrane conductance regulator (CFTR), a membrane channel regulating Cl^- flux, inhibiting its function: this causes increased ROS production, TG2 activation leading to nuclear factor κ B (NF-κB) pathway activation. This pathway induces the transcription of proinflammatory cytokines, among which there is IL-15, and of the components of the inflammasome [34].
- It localizes in early vesicles, interfering with their maturation and **slowing down early to late endocytic trafficking** [35], this in consequence delays epidermal growth factor receptor (EGFR) turnover on cell surface, which can remain active for longer **increasing enterocytes proliferation** in CD patients [35], [36], [37]. Moreover, EGFR tends to form complexes with other receptors, among these there's IL-15 receptor, which complex with EGFR is essential for enterocytes proliferation in intestinal crypts; p31-43 can increase the formation of this complex and by doing so, both EGF and IL-15 can start the signaling that leads to their mutual transcription, increasing intestinal crypt proliferation [36].

1.1.5 Pathogenesis

CD is an autoimmune enteropathy; multiple factors are responsible for its pathogenesis. The main event triggering the disease is the ingestion of gluten in genetically susceptible individuals, in which an immune response begins against undigested gluten proteins that interact directly on the enterocytes too. Gluten intake, genetic predisposition and the consequent immune reaction aren't the only factors involved in CD pathogenesis, and although being necessary they are not sufficient for the development of CD, suggesting that other factors are involved in its pathogenesis [16].

1.1.5.1 Genetics

CD has an important genetic component in its pathogenesis, as shown by a strong hereditability since it is characterized by a high familial recurrence between 10-15% and a high concordance of the disease among monozygotic twins, between 75-80%. The most important genes to date involved in CD are the HLA-DQ haplotypes **HLA-DQ2 and HLA-DQ8** [2], [38]. They are dimeric class II major histocompatibility complex (MHC-II) molecules expressed on the surface of human antigen-presenting cells (APC), with the task to recognize exogenous proteins and allow their presentation to T lymphocyte receptor; in particular, HLA-II presents molecules to CD4+ T cells [39]. The two glycosylated chains forming HLA-II create a pocket, where the recognition of the antigen happens, rich in positively charged aminoacidic residues, therefore the negative aminoacidic residues in the gluten peptides originated by their deamidation binds with higher affinity to the HLA-II pocket [12].

Approximately 90% of individuals diagnosed with CD have a variant of HLA-DQ2 called HLA-DQ2.5 encoded by the genes HLA-DQA1*05:01 and HLA-DQB1*02:01 either on the same chromosome (*cis* position) or on different chromosome (*trans* position), while half of the remaining patients possess the variant HLA-DQ8, encoded by genes HLA-DQA1*03 and HLA-DQB1*03:02. The remaining cases of CD have either HLA-DQ2.2 or HLA-DQ7.5, both characterized by carrying one of the two chains of HLA-DQ2.5, in particular the first has the gene for HLA-DQB1*02:01 while the latter carry the gene for HLA-DQA1*05:01 (Figure 4) [12], [40], [41]. The HLA-DQ2 and HLA-DQ8 genotypes have been identified in all CD patients and in approximately 40% of the population, but only around 3% of those with one of these genotypes develop CD, making them a necessary but not sufficient factor for the development of CD [42].

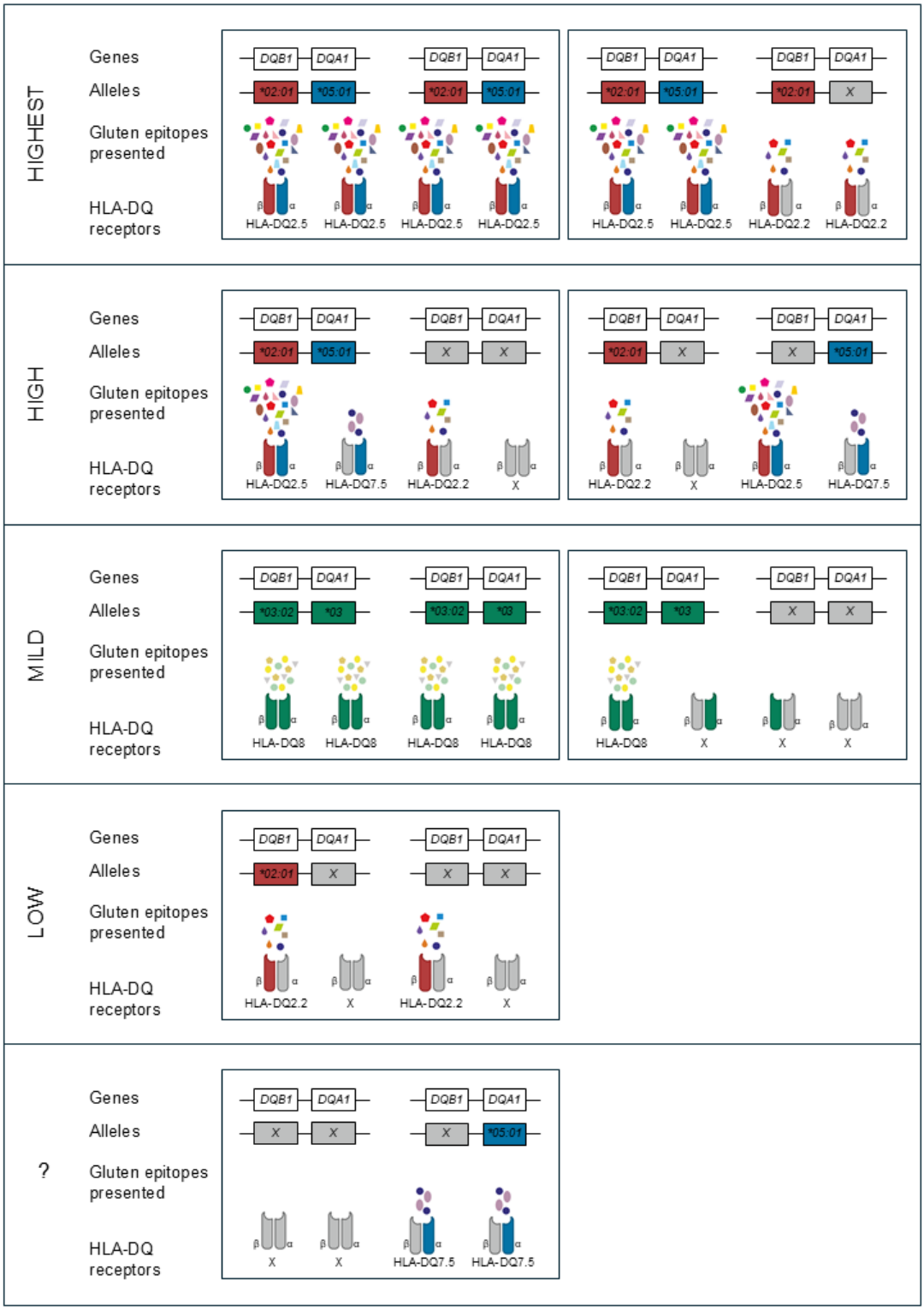

***Figure 4**: HLA genotyping and associated risk to develop CD. Depending on the HLA genotype, it has been proposed that each HLA is able to recognize a different number of gluten peptides with a corresponding higher or lower risk to develop CD. Each section shows the genes on the two chromosomes with the corresponding alleles for each gene on each chromosome, and the various HLA-DQ encoded by the different allele combinations for each chromosomes couple. Homozygosis for HLA-DQ2.5 alleles (DQA1*02:01 and DQB1*05:01) shows the highest risk since all HLA encoded are the DQ2.5 variant; even in heterozygosis, carrying the two alleles represents a high risk for CD. The HLA-DQ8 variant as the second most common variant in CD is associated with a mild risk to develop CD, hypothesizing that this variant recognizes a lower number of gluten peptides compared to the DQ2.5 variant. Lastly, the DQ2.2 and the DQ7.5 variants, despite carrying only one of the two alleles of the DQ2.5 variant, are still associated with a low risk to develop CD, even though it happens rarely and there are fewer patients carrying these genotypes [29].*

Genome-wide association studies have identified 42 more non-HLA regions related to CD with predisposing or protecting effects, mainly involved in the regulation at different levels of the immune system and the intestinal epithelial barrier since these variants are not located in the coding regions but rather in the regulatory ones, impacting the severity and the phenotype of the disease. These non-HLA loci are estimated to contribute to approximately 15% of the genetic variance for CD, however, even considering them together with HLA genes into the genetic factors contributing to CD development, only about 50% of the genetic variance in the disease is explained, suggesting that additional unknown hereditary factors may be involved [42], [43].

1.1.5.2 Immune response

The immune component in the pathogenesis of CD is one of the main damage mechanisms of the disease. The immune response in celiac patients revolves mainly on the adaptive immunity, with specific T cells able to recognize undigested gluten peptides. An autoimmune component is also present, with the generation of different autoantibodies during the immune response, Moreover, there are evidences of the involvement of the innate immunity during the induction of the adaptive immune response, although still uncertain [44].

Gluten peptides arrive in the intestinal lumen where they can't be further digested in smaller sizes: here they are able to cross the intestinal epithelial barrier through paracellular and transcellular transportation [45], arriving in the lamina propria. Here, the immunogenicity of gluten peptides is enhanced by the action of **type 2 transglutaminase (TG2)**, a ubiquitous Ca^{2+} dependent enzyme which expression is increased in response to inflammatory stimuli.

TG2 is a transamidase that forms isopeptide bonds between a glutamine (Gln) residue and lysine (Lys) residue of the same protein or different ones. In rare conditions, like slightly acid pH and virtual absence of aminic groups, TG2 deamidates a Gln, forming a glutamate (Glu) residue (Figure 5) [46]. When this modification happens on gluten peptides, the net negative charge created makes them more affine to HLA-DQ2 and HLA-DQ8 recognition pocket rich in positive charges, greatly enhancing the antigen presentation to the immune system [12].

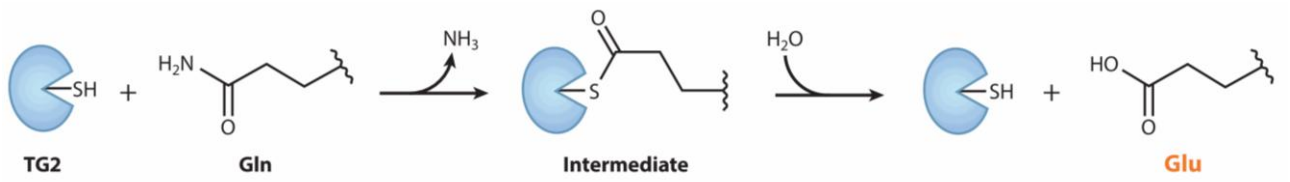

***Figure 5**: deamidation reaction mechanism for TG2-mediated conversion of Gln residue into Glu (modified from [45]).*

Additionally, TG2 can create complexes between itself and the deamidated gluten peptides thanks to its crosslinking activity; these complexes are recognized by APCs, supporting the formation of autoantibodies against TG2 by specific B-cell [12], [26]. The production of autoantibodies against TG2 can be caused by molecular mimicry of certain deamidated gliadin peptides, that show similar 3D structure with TG2, leading B-cell to produce antibodies against the enzyme and gliadin deamidated peptides [47].

In the lamina propria, deamidated gluten peptides and unmodified ones are recognized by **antigen-presenting cells (APCs)** with HLA-DQ2 or DQ8 that then activate specific CD4+ T cells (Figure 6). These immune cells constitute a part of the IELs present in the small intestine, that comprehend an adaptive component (consisting of TCRαβ+ T cells divided in CD8αβ+ and CD4+ T cells) and an innate component (consisting of TCRγ/δ+ T cells and NK cells). The adaptive component is activated by the APCs presenting gluten peptides through the HLA-DQ2 and DQ8, while the innate component is activated by cytokines and NK receptors [3], [48].

CD4+ T cells, after being activated by APCs, proliferate and expand starting the **adaptive immune response** and releasing several **pro-inflammatory cytokines** in the lamina propria. Among these, interferon-γ (IFN- γ) is the main protagonist of the chronic inflammation present in the intestinal mucosal, having also a direct pro-apoptotic effect on intestinal epithelial cells in CD patients [3], [49]. Other cytokines produced upon CD4+ T cells activation are: interleukin-2 (IL-2), that can also be used as a marker for the activation of the immune response after gluten ingestion [50] and together with interleukin-12 (IL-12), interleukin-21 (IL-21) and TNF-α direct CD4+ T cell to a T helper type 1 lymphocyte phenotype in CD and induce proliferation and the expansion of IELs [51]; interleukin-15 (IL-15) has also the same effects on IELs and shows an increased expression both in lamina propria and epithelium in CD patients. Additionally, IL-15 has a reprogramming effect acting on the NK cell receptors of many IELs, causing a decrease of cells expressing the inhibitory receptors CD94/NKG2A and an increase of cells expressing the activating receptors CD94/NKG2C and CD94/NKG2D [12], [52]. These receptors allow IELs to bind to non-classical HLA molecules like MICA, MICB and HLA-E that are upregulated in infectious and inflammatory conditions in intestinal epithelial cells, inducing the cytotoxic activity of IELs, contributing to tissue destruction and intestinal mucosal remodeling (Figure 6) [6].

Mucosal remodeling is caused also by CD4+ T cells that, when interacting with gluten peptides in the lamina propria, induce production by stromal cells of proinflammatory

cytokines, metalloproteases and keratinocyte growth factor. In combination with the cytotoxic effect of IELs, crypt hyperplasia and villous blunting is induced, that is typical of CD. The hyperplasia of the crypts is characterized by an expansion of the immature progenitor cells compartment and is possibly a consequence of an imbalance between the continuos damage caused by the immune response and the inability of stem cells to compensate for the cells destroyed [2].

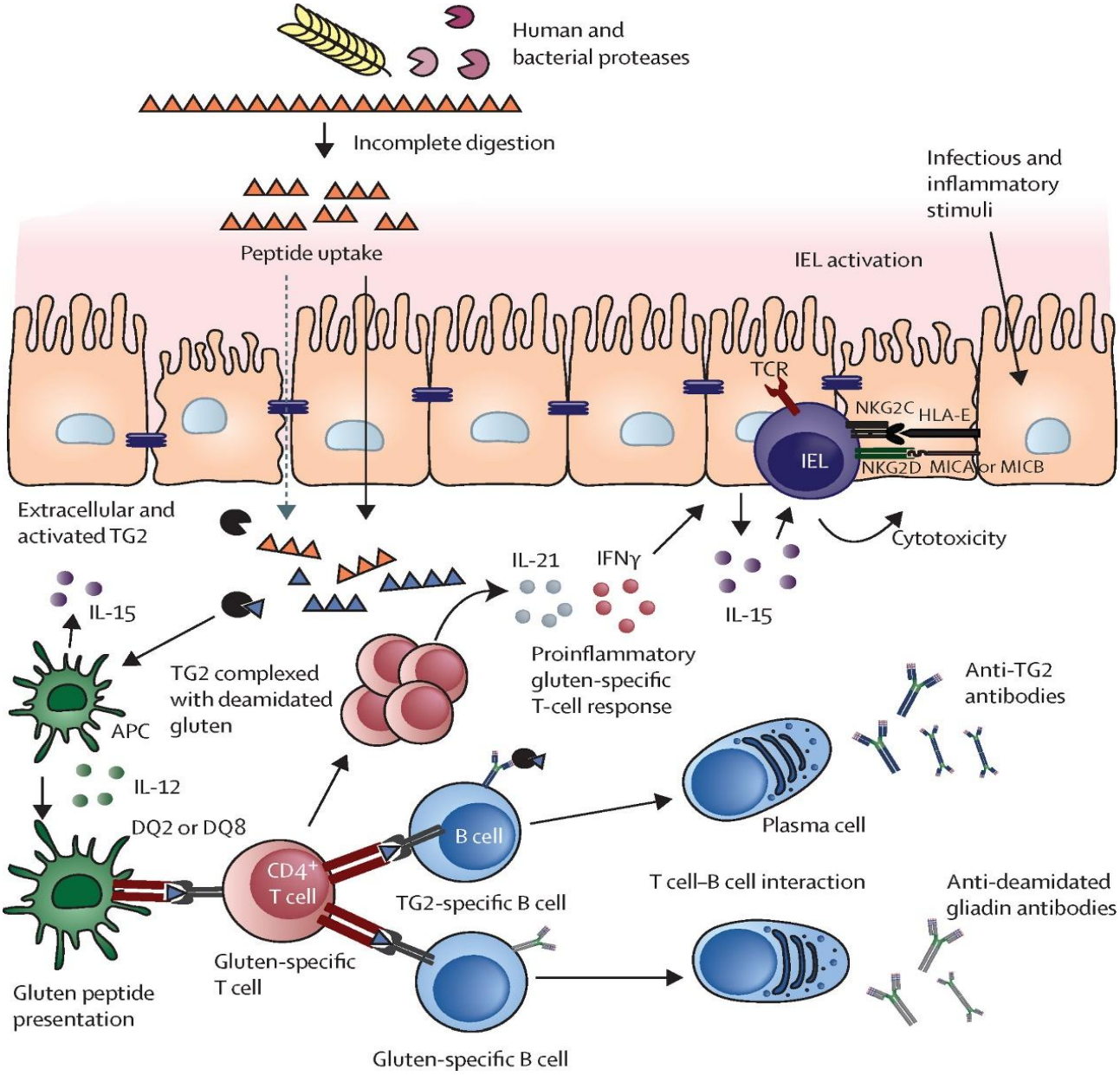

***Figure 6**: CD immune reaction: gluten is digested in gliadin peptides that travels through the intestinal epithelium via paracellular and transcellular transportation, arriving in the lamina propria. Here, they are modified by TG2 and recognized alone or complexed with TG2 by resident APCs with the HLA-DQ2 or DQ8, that present the recognized epitopes to gluten-specific CD4+ T cells, starting the immune response against gluten peptides. Activated CD4+ T cells proliferate and produce pro-inflammatory cytokine, further amplifying the immune response and activating IELs, that exert their cytotoxic action on intestinal epithelial cells, exposing non-classical HLA molecules (MICA, MICB and HLA-E) under inflammatory conditions, recognized by IELs. Gluten-specific CD4+ T cells activate also TG2-specific and gluten-specific B cells that mature in antibodies producing plasmacells [6].*

Gluten-specific CD4+ T cells have a role in the **activation of B cells** present in the lamina propria (Figure 6): the production of gluten-specific and TG2-specific antibodies happens in response to gluten exposure and rely on the interaction between their respective B cells with gluten specific CD4+ T cells. Gluten-specific B cells receive cognate help directly from gluten-specific CD4+ T cells, indeed, they both recognize preferably deamidated gluten peptides. On the other hand, TG2-specific B cells recognize TG2-gluten peptide complexes through their B cell receptor with a hapten-carrier like mechanism and then presenting deamidated gluten peptides to T cells.

B-cells functions include the production of anti-TG2 and anti-deamidated gluten peptides (anti-DGP) antibodies, but also the role of APCs for T cells, most likely after an initial priming against gluten and an initial expansion of antigen-specific T cells and B-cells. The interactions between T cells and B cells as APCs lead to the presentation of DGPs by TG2-specific B cells lead to the activation of gluten-specific T cells, that would then activate gluten-specific and TG2-specific B cells, resulting in the amplification of the immune response and the differentiation of these cells into their effector phenotype [53], [54].

The **innate immunity** has a role in the immune response in CD too, starting an initial local inflammation in the small intestine, that prime the adaptive immune response. Despite being still unclear how the innate immunity operate in the pathogenesis of CD [44], cytokine produced through the innate response have a role in CD, like IL-15 which can polarize dendritic cells to induce the typical CD4+ T cells inflammatory response against gluten. IL-15 showed also to increase the expression of NK cell receptors on enterocytes promoting their killing by IELs as said before, and IL-15 increase the expression of anti-apoptotic molecules, promoting survival and expansion of IELs [55]. The toxic peptide p31-43 in particular is considered to be the main protagonist in the interaction with the innate immunity, enhancing it via Toll-like receptor 7 (TLR7) [56], activating TG2, inducing Il-15 production and NF-κB nuclear translocation [44], and activation of the inflammasome through the formation of oligomeric structures [24]. Nonetheless, a receptor for p31-43 that mediates the interaction is still unknown, and it is supposed that it is internalization happens thanks to membrane composition and organization [57].

Another effect on the innate immunity is given by amylase-trypsin inhibitors (ATIs) that are present in wheat and other cereals together with gluten peptides. ATIs engage via TLR4, activating them and inducing an innate immune response thanks to the release of pro-

inflammatory cytokines. ATIs cause also epithelial barrier dysfunction, allowing the passage of gluten peptides in the lamina propria, helping to start CD enteropathy [2], [58].

1.1.5.3 Additional factors

Genetic factors and the immune response are fundamental in the pathogenesis of CD, but they are not sufficient to explain the series of events happening in the disease and additional factors have been considered in contributing to the damage observed in patients.

An important component involved in the digestive processes is the **intestinal microbiota**: the latter is comprised of different microorganisms, including multiple strains of bacteria, viruses, fungi, protists and archaea, contributing to digestion processes, production of vitamin, bile acid metabolism and the development of tolerance and the immune system [59]. To date, despite being extensively studied, a unique microbiome signature of CD has not been identified since there is a high variability across studies due to multiple factors that differ between study to study (like clinical trial design, sampling site and population) [60]. Generally, a common trait observed in CD patients when compared to healthy subjects is a dysbiosis consisting in a decrease of good bacterial strains and an increase of pro-inflammatory bacterial strains [61] and a similar effect has been observed in both healthy subjects and celiac patients as a consequence of following a gluten-free diet, causing in the subjects studied numerous gastrointestinal side effects [1], [62]. Dysbiosis in the intestinal microbiota is relevant because some bacterial strains take part in the digestion of gluten: indeed, many bacteria produce endopeptidases and hydrolases that contribute to the digestion of peptides derived from the gliadin degradation, while other bacteria produce proteases that increase gluten antigenicity and enhance the reactivity of gluten-specific T cells [63]. Additionally, bacteria can also influence the immune system, for example some bacteria express epitopes that mimic gliadin, potentially triggering an immune response against gluten [64]. Gram negative bacteria have lipopolysaccharide on the outer membrane, that can start both an innate and an adaptive immune response through IL-15 production, creating a pro-inflammatory environment [65]. Finally, intestinal microbiota can induce the release of zonulin, a protein that increases paracellular permeability by inducing tight junction disassembly, influencing intestinal permeability, another key factor in CD pathogenesis. Despite all these considerations on intestinal microbiota and CD, it is still unclear if there is a causation between them, or if the dysbiosis and all its consequences are an effect of CD [2], [65].

Another important factor in the pathogenesis of CD is the role of the **intestinal barrier and the alteration of its permeability**. The integrity of the intestinal barrier prevents the entrance of gluten peptides in the lamina propria where they meet the immune system, starting the immune response typical of CD: unfortunately, in CD patients there is an increased gut permeability that allows an easier passage of gluten peptides [16]. Gluten trafficking from intestinal lumen to the lamina propria occurs via paracellular and transcellular transport. Paracellular transport is impaired due to dysregulation of tight junctions proteins expression: these proteins (claudins) contribute to forming a barrier for the paracellular transport of solutes and water, as well as to constitute paracellular channels to allow the passage of water and ions across the epithelial barrier. During CD, barrier-forming claudins have been found to be down-regulated, increasing paracellular transport, while channel-forming claudins, like claudin-2 (CLDN2), are upregulated, increasing the leakage of ions and water [45]. On the other hand, transcellular transport happens after gluten tolerance has been broken through transferrin receptor CD71. CD71, while normally expressed on the basolateral side of enterocytes, it is overexpressed on the luminal side in CD patients enterocytes during active CD, leading to the apical-basal retrotranscytosis of gliadin-IgA complexes, that protects gliadin peptides from lysosomal degradation, allowing their transport to the lamina propria where they can continue the ongoing inflammation [2], [66].

1.1.6 Diagnosis

CD diagnosis consists in a combination of **CD serology** testing and the observation of the small **intestinal mucosa morphology** in biopsies [16].

1.1.6.1 Serological tests

Right now, serological tests are based on the research of **anti-TG2 antibodies and anti-endomysial antibodies (anti-EMA)**, both of IgA class antibodies [7].

The first screening test for CD diagnosis is testing for the presence of **anti-TG2 IgA** antibodies, this is one of most diffuse and standardized serological tests available, and paired with the evaluation of total serum IgA, to exclude IgA deficiency, has high sensitivity and specificity (shown in Table 1) in patients on a gluten-containing diet [5], [67]. An high level of anti-TG2 IgA antibodies is strongly associated with intestinal mucosa remodeling. In

case of patients with IgA deficiency, testing for the presence of anti-TG2 IgG antibodies can be done for diagnostic purposes, despite being less accurate [6].

The other antibodies utilized for diagnostic purposes are **anti-EMA IgA** antibodies. These antibodies recognize TG2 found in the endomysium in a tissue section. Their presence is detected through an indirect immunofluorescence assay on monkey esophageal or human umbilical cord tissue sections. Despite not being as sensitive as the testing for anti-TG2 IgA antibodies, it has a specificity of almost 100% (shown in Table 1). However, this test is not the most appropriate for initial screening for CD diagnosis because of its labor intensity and its operator dependent variability, thus it is used preferably as a confirmatory test for the pathology [67], [68].

The **anti-DGP IgG** antibodies, typical of CD, can be used for diagnostic purposes too, especially in case of patients with selective IgA deficiency or for children younger than 2 years old, since anti-DGP IgG antibodies appear earlier than anti-TG2 IgA antibodies, showing high sensitivity and specificity (shown in Table 1) [6], [67], [69].

1.1.6.2 Histological test

Histological evaluation of duodenal biopsies remains the best tool in combination with a positive result from a serological test to confirm CD diagnosis, given the typical modification of the intestinal mucosa in CD [70]. The characteristics of CD are **mucosal villous atrophy, crypt hypertrophy and an increase in IELs** [71]. The quantification of intestinal damage is done using intestinal morphology as a reference, evaluating the count of IELs, villous height, crypts depth and the ratio between villous height and crypts depth.

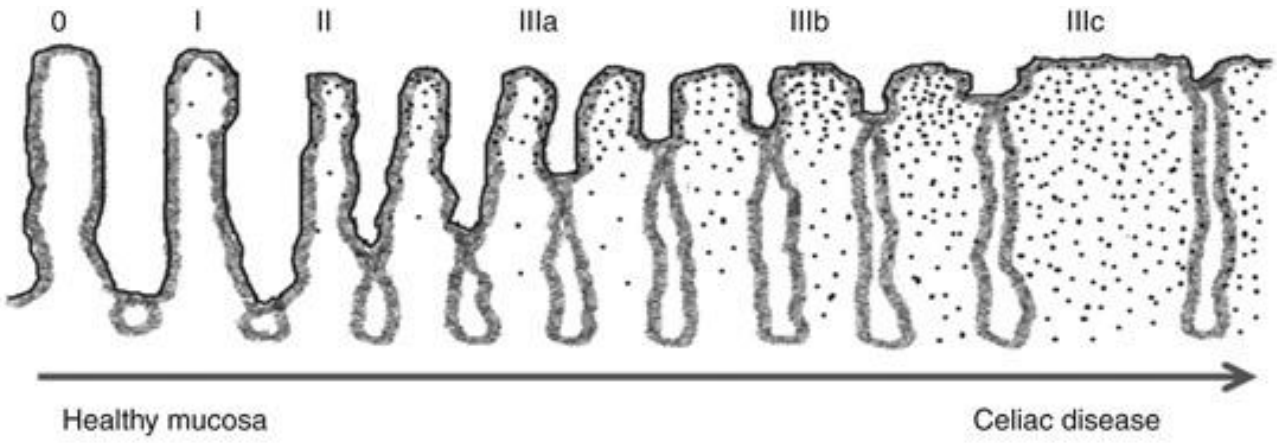

***Figure 7**: schematic representation of Marsh-Oberhuber stages of the intestinal epithelium morphology [61].*

The grading of the intestinal damage is then based on the **Marsh-Oberhuber scoring system** (Figure 7), which comprehends five grades of damage:

- **Grade 0**, which has no damage and shows normal intestinal histology, the number of IELs is less than 40 per 100 enterocytes.
- **Grade 1**, which has infiltrative damage and is characterized by an increased number of IELs, over 40 IELs per 100 enterocytes, while the mucosal structure is still normal.
- **Grade 2**, which has hyperplastic damage and is defined by an increased number of IELs and crypt hyperplasia, villous structure is normal, and the ratio villous-crypts is three to one.
- **Grade 3**, which has destructive damage, shows any degree of villous atrophy in addition to an increased number of IELs and crypt hyperplasia. It is further subdivided into:
    - Grade 3a, with partial villous atrophy.
    - Grade 3b, with almost complete villous atrophy.
    - Grade 3c, with total villous atrophy.
- **Grade 4**, which has hypoplastic and atrophic damage, shows complete villous atrophy but a normal crypt structure and a normal number of IELs [72].

Biopsies to be analyzed are collected during upper gastrointestinal endoscopy, and they are taken from two main areas of the small intestine: at least one sample is taken from the duodenal bulb to ensure accuracy of the diagnosis, and a minimum of four are collected from the descending portion of the duodenum [73].

1.1.6.3 Genetic screening and HLA typing

HLA typing in CD is an important factor for the development of the disease, the presence of HLA DQ2 and HLA DQ8 haplotypes is **essential, but alone it does not guarantee CD** insurgence, since they are present in approximately 40% of the population [42]. Therefore, HLA genetic testing is done when there are discrepancies between serological and histological tests, in patients who started a gluten-free diet before testing or in patients in risk groups, and rather than confirming CD diagnosis, it is more useful in ruling it out in patients who are seronegative but with typical histological changes [1], [7].

1.1.6.4 Diagnostic criteria

Given these different tests to diagnose CD, the diagnostic criteria to do so follow the **guidelines established by the European Society for Pediatric Gastroenterology, Hepatology and Nutrition** (ESPGHAN) (Figure 8). In case of adult patients, the diagnosis

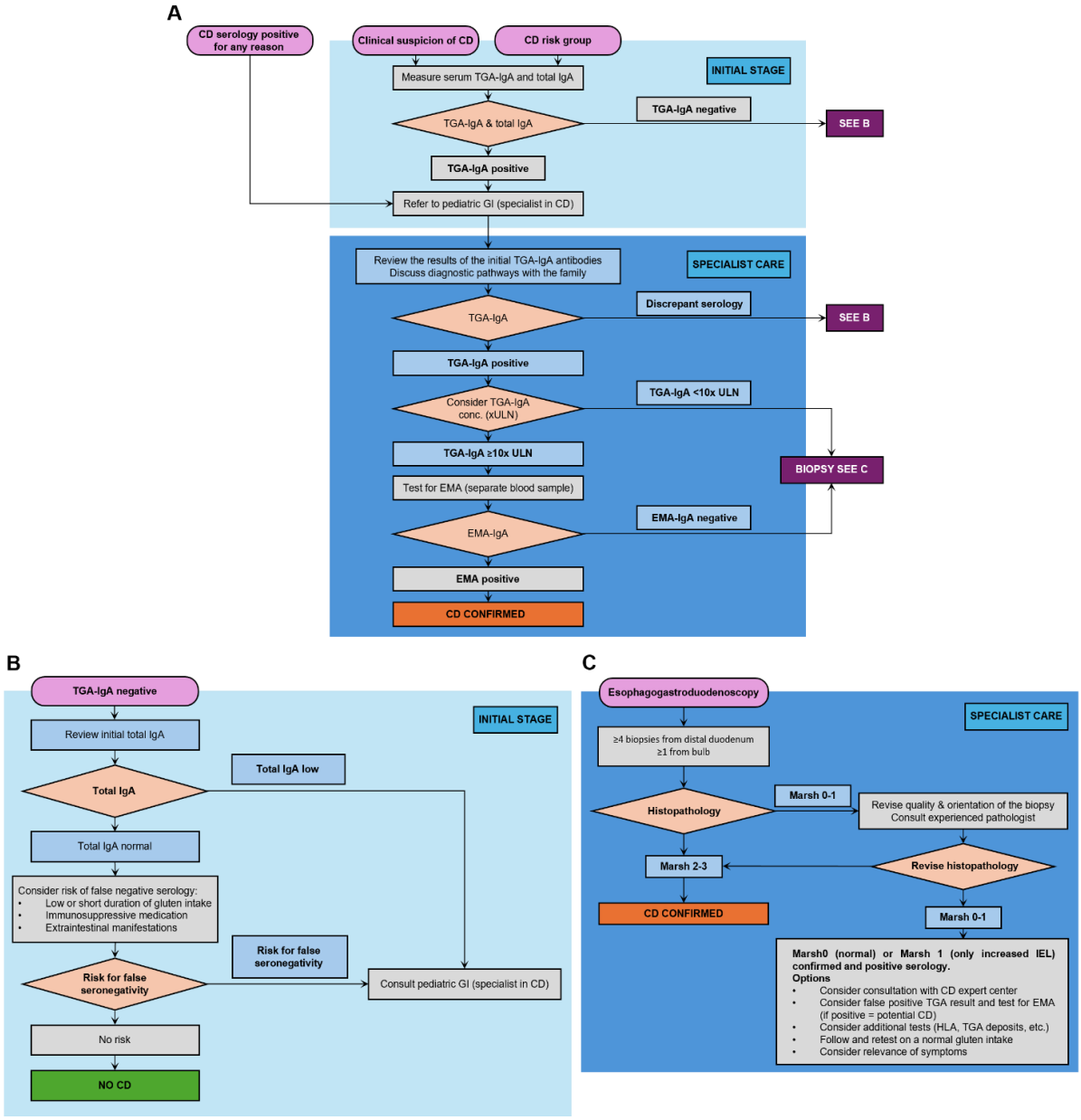

***Figure 8**: scheme for the diagnosis of CD following most recent ESPGHAN guidelines published in 2020. **A)** The diagnosis starts with the determination of anti-TG2 IgA titer: in case of a positive result, a concentration 10 times the upper limit of normal (ULN) and a positive result for the anti-EMA IgA, CD diagnosis is confirmed. **B)** If the patient results negative for the presence of anti-TG2 IgA, then the total IgA concentration is assessed: with a positive result various factors like short duration of gluten intake are taken in consideration to rule out the possibility of a false seronegative and the CD diagnosis is excluded, overwise with low total IgA it is recommended to consult a CD specialist. **C)** In case of a low anti-TG2 IgA titer or negative anti-EMA IgA result, it is necessary to analyze the intestinal biopsies from the patient and an evaluation of the damage on the Marsh-Oberhuber scale: a biopsy with a Marsh grade of 2 or 3 confirms CD diagnosis, on the other hand having a Marsh grade of 0 or 1 and positive serology opens different options, like consultation with a CD expert, the possibility of a false positive in previous testing or additional tests like HLA genotyping (modified image from [5].*

requires both positive serological result (in particular anti-TG2 IgA) and histological modifications from duodenal biopsies with a scoring of 3 on the Marsh-Oberhuber scale [74].

For pediatric patients, CD diagnosis can be formulated without an histological examination if the serological exam shows that the titer of anti-TG2 IgA are over 10 times the normal level and there is positivity to anti-EMA IgA: in this case, CD is diagnosed without an histological exam, avoiding to take a biopsy from the children, and independently from the presence of symptoms [5].

1.1.7 Treatment

To date, the only effective treatment for CD is the complete elimination of gluten from the diet and following a strict and **lifelong gluten-free diet** (GFD), removing the triggering cause of the disease. Despite not being a cure, following a GFD leads to the resolution of the intestinal and extraintestinal symptoms in a short period spanning from few weeks to some months for the majority of patients [22], [75]. This is confirmed by the negativization of CD specific antibodies like anti-TG2 and anti-EMA IgA, that decline rapidly after starting GFD implying a switch off of their production [54], and by the regeneration of intestinal villi, even if the complete remission can take up to even 2 years in adult patients or longer in older patients despite a strict adherence to GFD [76].

Even though adherence to GFD restores normal conditions in CD patients and prevents several complications characteristics of CD like malabsorption, it has also some **side-effects**. First of all, maintaining a lifelong strict GFD is difficult, especially in children and during adolescence, and has a negative impact on the quality of life, with possible psychological problems [2]. Moreover, despite being nutritionally safe, following a GFD can lead to insufficient intake of some nutrients, especially vitamins and minerals and gluten-free products contain more sugars and fats than their gluten counterparts and in case of certified deficiencies, it is appropriate to supplements GFD with the corresponding integrators [6], [7]. Lastly, gluten contamination is common due to involuntary gluten intake and cross-contamination between foods or even during production processes and even low amounts of gluten can chronic inflammation despite following a GFD [1], [7].

1.1.8 *In vitro* and *in vivo* models in celiac disease

To study the processes involved in CD pathogenesis, several *in vitro* and *in vivo* models have been used. These models need to replicate the signaling pathways and cellular processes that characterize the inflamed intestine of CD patients.

Most *in vitro* studies used cell lines model, in particular, **Caco-2 and HT29 cells**. These are colon-cancer derived cell lines able to form a polarized cell monolayer resembling the intestinal epithelial barrier when grown on a permeable membrane support. Caco-2 cells can also spontaneously differentiate resembling intestinal epithelial cells morphology and functions [77] developing a brush border mimicking typical characteristics of human small intestinal epithelium. On the other hand, HT29 cells cannot differentiate spontaneously in standard conditions, mimicking undifferentiated colon epithelial cells [78].

Despite being like mature intestinal epithelial cells, forming an epithelial barrier and responding to inflammatory stimuli, these cell lines **differ from the normal epithelium** for several reasons. First, there are inherent karyotypic abnormalities with chromosomal loss and amplification being cancer cell lines, resulting in important differences in gene and protein expression. For the same reason, HT29 and Caco-2 cells have several oncogenic mutations that could affect pathways and mechanisms of interest, like inflammatory ones. Moreover, these cell lines monolayers consist of an homogenous cell population, missing on the complexity and heterogeneity of the intestinal epithelium, therefore it is important to take account of the important differences between an *in vitro* and *in vivo* situation, and not misinterpret results obtained *in vitro* when translating them to an *in vivo* scenario [77], [78].

For what concern ***in vivo* models**, there have been various attempts to establish a good animal model, but it turned out to be troublesome. The first animal model was the **Irish setter**, in which if given a gluten containing diet as pups, they would develop IELs infiltration and partial villous atrophy, however this effects are independent of the dog MHC-II, therefore lacking the adaptive immune component characteristic of CD, possibly being more relevant for the role of the innate immune response in gluten sensitivity [79]. A similar problem was encountered in the CD model in **rhesus macaque**: despite showing villous atrophy and anti-tTG and anti-gliadin IgA and IgG antibodies when following a gluten containing diet, there is no remission after removing gluten from the diet, additionally, the association between this symptomatology and MHC-II has yet to be determined, so the role of the adaptive immune system is still unclear [80]. Mice have also been extensively used to establish a CD model thanks to the vast knowledge of their genetic manipulation and the availability of different

transgenic mice lines, and the intrinsic advantages of using mice instead of bigger animals. **Non-Obese Diabetic (NOD) mice** have a spontaneous sensitivity to gluten ingestion, showing an increase in IELs in the small intestine and shortening of villi: unfortunately, the antibody response to tTG was a peculiarity of the NOD strain rather than a response to gluten ingestion [81]. Another attempt was made by transferring activated T-cells from mice sensitized to gliadin to the **immunodeficient Rag1 knockout mice** on a gluten containing diet. These show in response IELs infiltration in intestinal tissues, crypt hyperplasia, villous atrophy and increased cytokines levels; this response demonstrated that CD4+ T cells are involved in gluten mediated intestinal damage, but this activity is dependent on the mouse MHC-II and not on the HLA-DQ2 or DQ8 genes [82]. To have a model that relays on these genes, various transgenic mice have been used: one initial approach was done with **HLA-DQ8 transgenic mice**. This transgenic strain develops an immune response after gluten sensibilization, showing a strong T cell proliferative response and increased levels of anti-gliadin antibodies. Moreover, this strain showed that, after injection of unmodified DQ8 binding gliadin peptides, there is a stronger response to the deamidated forms of the peptides, suggesting that in CD, initially there's an aberrant innate immune response to gliadin which activates tTG resulting in the simultaneous presence of native and deamidated gliadin peptides, accelerating the T cell response against them and leading to the enteropathy. However, this model has its limitations, above all there are no development of clinical symptoms or intestinal damage, which is typical in CD [83]. Other works evaluated the **role of IL-15 in CD**, systemically overexpressing it in DQ8 transgenic mice: this resulted in increased IELs when fed with gliadin after being kept on a GFD at levels comparable with the ones in CD patients, a phenotype absent in the strains only DQ8 transgenic or with only IL-15 overexpression: nonetheless DQ8 transgenic mice overexpressing IL-15 lack villous atrophy and crypts hyperplasia [84]. On the contrary, another group overexpressed IL-15 under an enterocyte specific promotor in mice, thus IL-15 is produced only in the small intestine; these mice show altered ratio between villous height and crypts like in CD, and an increased number of plasmacells with a corresponding increased production of anti-tTG IgA. However, this model lacked the gluten specific CD4+ T cell response present in CD patients [85].

1.1.8.1 The Gut-Ex-Vivo System to model celiac disease

A different mouse model that combine the complexity of an animal model with the accessibility of an *in vitro* system is the **Gut-Ex-Vivo Sistem** (GEVS), that uses **small**

intestine tissue sections from gluten-sensitive Balb/c mice to resemble CD symptomatology in the gut after quick gluten peptides exposure and then analyze the samples. The system is composed of a chamber in which the surgically removed small intestine is placed and connected to a paired input and output, allowing perfusion of the intestinal lumen with complete medium and treatment (Figure 9). The chamber is also filled with complete medium and supplemented with oxygenation and pH control by an air/O_2/CO_2 mix; the chamber is also kept at 37°C, allowing to keep the resected small intestine vital for several hours. When small intestines of gluten sensitive Balb/c mice are exposed to gliadin peptides in GEVS, they show **typical CD markers** like a down-regulation of CFTR and an up-regulation of TG2, additionally there's the production of pro-inflammatory cytokines like IL-15, an alteration of the intestinal barrier and villous damage/atrophy, indicating that GEVS can be used as an *ex vivo* model for CD, with the limitations of an *ex vivo* model [86].

The GEVS can be used to model inflammatory bowel diseases, like **ulcerative colitis (UC)**: indeed, intestines from Balb/c mice were cultivated in GEVS and here, were exposed to

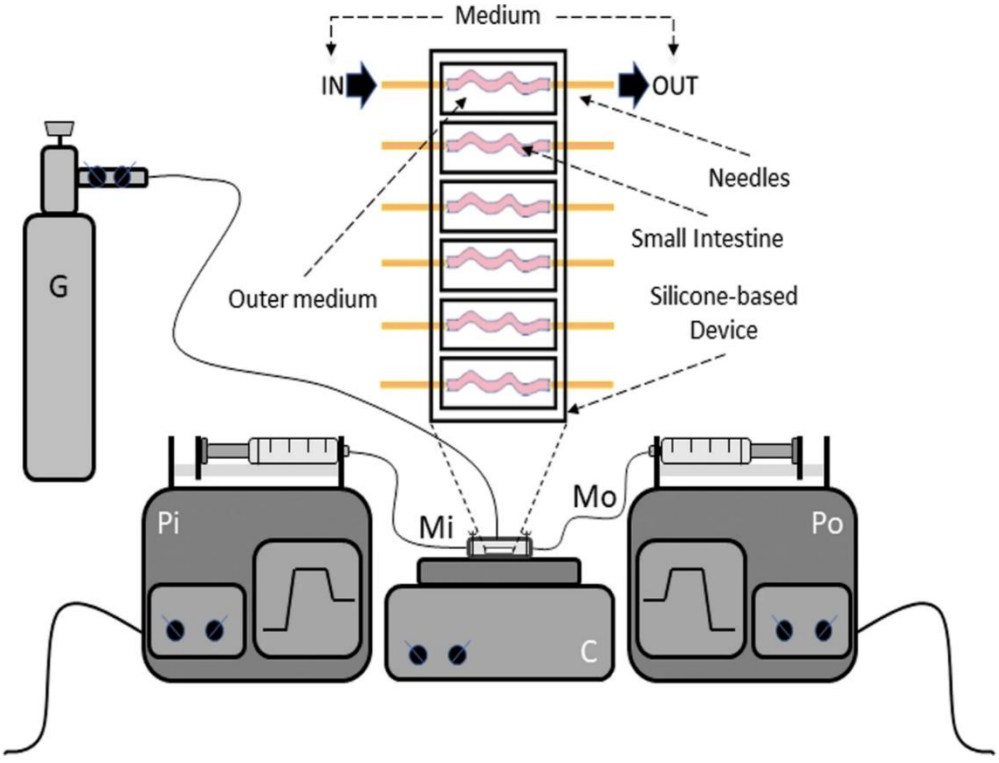

***Figure 9**: schematic representation and silicone-based device consisting of 6 independent chambers in which small intestines are inserted and connected to two needles allowing the flow of complete medium in the inner intestinal compartment (luminal flow). Each chamber is also filled with a complete medium, in which small intestines are immerged, to sustain the full viability of tissues. The circuit allowing the flow of the medium through each small intestine consists of two synchronized pumps, which inject (Pi) and suck (Po) the culture medium. The temperature is set to 37 °C and maintained by a heating plate; proper oxygenation is allowed by humidified air/O2/CO2 gas mixture blown into the device chamber. Pi infusing pump; Po sucking pump; Mi medium entering; Mo medium exit; G air/O2/CO2 cylinder [86].*

dinitrobenzene sulfonic acid (DNBS), a known inducer of intestinal inflammation especially to mimic UC, and all the main hallmarks of the disease were observed after a brief incubation time with DNBS; in particular the intestine showed damage of the epithelium and submucosa, increased TG2 expression, impairment of the intestinal permeability and a dose-dependent increase of pro-inflammatory cytokines together with the induction of ER stress [87]. With the same system, intestines from C57BL/6 mice were cultivated and exposed to DNBS, that mimic UC at high dosage *in vivo*, while here lower concentrations of DNBS were sufficient to induce the same effects observed in Balb/c mice guts. Therefore, both Balb/c and C57BL/6 mice intestines were exposed to DNBS to study UC, observing an up-regulation of the apoptosis and ferroptosis markers; interestingly, giving pro-biotics together with DNBS prevented all the damaging effects observed otherwise, suggesting their possible use in therapy [88].

Overall, these studies on CD and UC proved the versatility of GEVS to model inflammatory bowel diseases, reproducing reliably the pathologies and offering a more practical and ethical approach to animal modeling.

1.2 Organoids

The term “organoids” refers to a self-organized 3D structure, generated from stem cells, that mimics the functions, structure and biological complexity of an organ [89]. To support organoids development into a 3D structure, they are typically seeded and grown in biologically derived matrices like **matrigel**, which is a soluble and sterile extract of basement membrane proteins derived from Engelbreth-Holm-Swarm (EHS) tumor that forms a 3D gel at 37°C, supporting organoid morphogenesis and differentiation, mimicking the extracellular matrix. The main components of matrigel are laminin, collagen IV, entactin, perlecan and growth factors [90].

Compared to using 2D cultures, organoids have several **advantages**, indeed they resemble more closely the structure and functions of the organ of origin. Additionally, in the organoid is present a population of genetically stable and self-renewing stem cells able to generate differentiated cells present in the living tissue and allowing to expand the organoids in culture for long time [91]. On the other hand, when compared to *in vivo* animal models, organoids generated from human tissues better recapitulate specific disease and keep gene expression and mutations from the parental tissues, giving access to patient specificity studies for personalized medicine for drug testing and treatments. Moreover, organoids can

reduce the animal usage in research, are cheaper to generate and maintain, quicker to produce and easier to manipulate than animal models [89], [91], [92].

Despite these advantages, organoids have some **limitations**: first, although organoids show heterogeneity, they lack the microenvironment component present *in vivo*, limiting the study of some disease and their interaction with other cell types, like the immune cells during an immune response; the use of matrigel could interfere with specific signaling pathways or mechanisms of interest and since the organoids are enveloped in it with growth factors, this can disrupt or alter the natural morphogen gradient found in the tissues of origin. Matrigel makes organoids manipulation and passage more complex, influencing also the possibility to scale up the sample, compared to 2D cultures. Additionally, reagent cost for organoid generation, growth and maintenance is still high [93].

Given organoids disadvantages and the advantages, they have found several **applications in research** (Figure 10). Thanks to their ability to mimic their organ of origin maintaining patient specificity and the patient genetic background, organoids can be used as a model

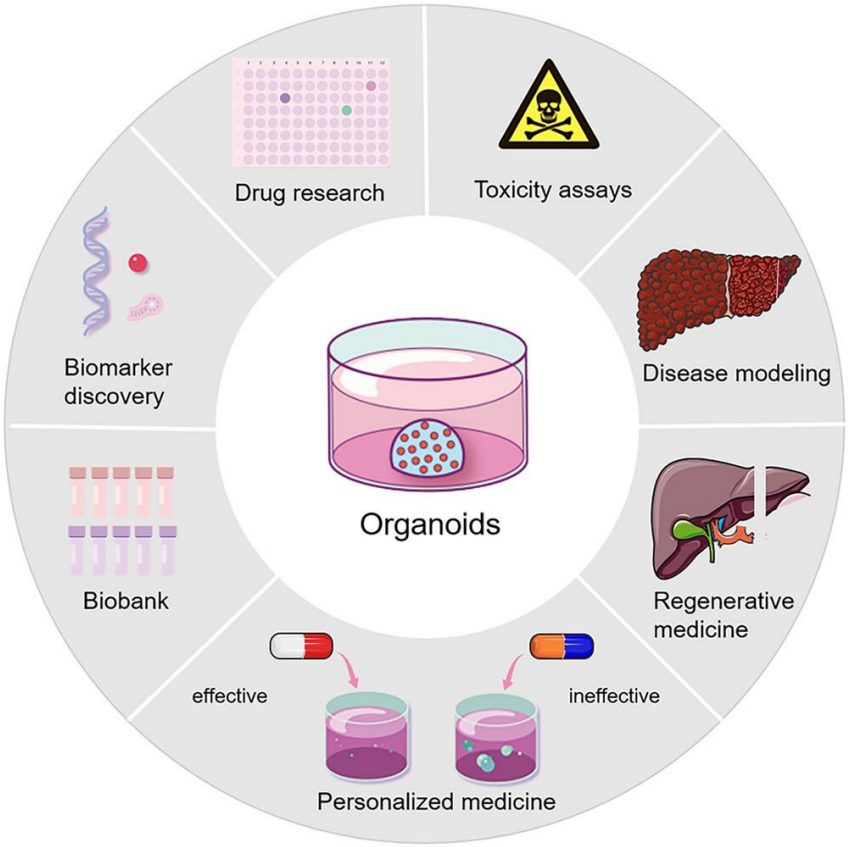

***Figure 10**: applications of organoids. Organoids have found application in many research sectors like disease modeling, drug studies to discover new effective drugs and to assess the toxicity of them or other molecules, discovery of new biomarkers, creation of disease-specific biobanks thanks to cryopreservation, development of personalized therapy and regenerative medicine as a source of patient-specific transplantable tissue [82].*

for genetic diseases and in drug testing, exploring the effectiveness of new drugs as well as their possible side effects like toxicity on liver, heart and kidneys for example [94]. Since organoids are suitable for long-term expansion, they allow the establishment of disease-derived organoids biobanks useful for omics analysis in precision medicine and for drug screening studies. Finally, organoids can be considered as a source of patient specific transplantable tissue in regenerative medicine, avoiding problems of limited tissue availability and the need for immunosuppressive treatments of traditional organ transplants[93], [95].

1.2.1 Human organoids generation

Human organoids can be obtained from **adult stem cells** (ASCs), which are resident stem cells present in adult tissues, or **pluripotent stem cells** (PSCs): this term refers to both **embryonic stem cells** (ESCs), obtained from the inner cell mass of a human blastocyst, and **induced pluripotent stem cells** (iPSCs) (Figure 11). iPSCs are obtained from a process of dedifferentiation of somatic cells, usually fibroblasts, in which the specific genes OCT4, KLF4, SOX2 and MYC are activated ending up transforming the cells into stem cells: then both ESCs and iPSCs are exposed to germ layers and tissue-specific patterning factors and are embedded in matrigel, to facilitate the formation of a 3D structure, where they are treated with differentiation factors to obtain the desired organoids [96].

Compared to PSC-derived organoids, **organoids obtained from ASCs** are directly produced from regenerative human adult tissues. ASCs are multipotent stem cells that keep

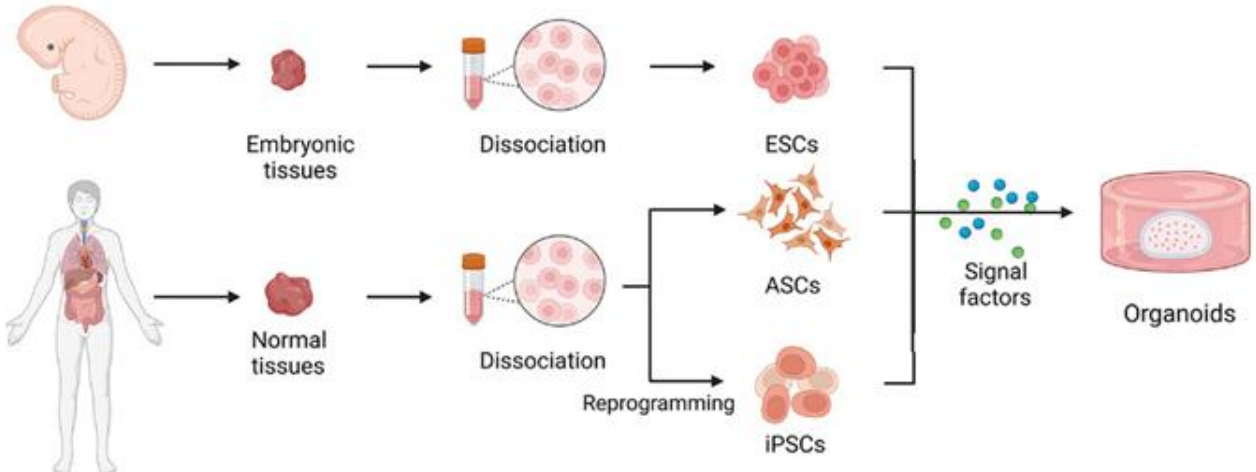

***Figure 11**: organoid generation. Organoids can be generated from ESCs, obtained from embryonic tissues; from ASCs isolated from adult tissues in which there are resident stem cells; from iPSCs obtained adult somatic cells fully differentiated that through a dedifferentiation are reprogrammed into the state of iPSCs (modified from [82]).*

their stemness throughout development to then continue to generate perpetually specialized differentiated cells for specific function and the specific tissue they are in. Based on the tissue of origin, ASCs can differentiate both in 2D and 3D structures *in vitro*, based on the combination of growth factors added: these structures are composed of polarized and specialized cell types resembling their tissue of origin [95]. Since there is no need to dedifferentiate ASCs, ASC-derived organoids can be generated directly from biopsies taken from the organ or tissue of interest, therefore their production is simpler and takes less time compared to PSC-derived organoids, showing also a maturity more like the adult tissue of origin. Moreover, they can be cultured for extended periods of time maintaining genetic stability. The downside of ASC-derived organoids is that the tissue needs to be accessible to take biopsies and there's the need for prior knowledge of tissue-specific culture conditions, while iPSCs once obtained from a patient, they can be used for the generation of multiple tissue models indefinitely [94].

On the other hand, **PSC-derived organoids** require a complex, time-consuming and specific step by step procedure to be generated, need also the understanding of the factors guiding germ layer formation and subsequent cells differentiation into specific cell types and when cells from PSCs reach a fully differentiated state they lose the ability to further expand. The pluripotency of PSCs generate complex and intricate organoids that can include the epithelial, mesenchymal and endothelial component, making them good models to investigate organogenesis and human development [94], [95].

1.2.2 Human intestinal organoids

Intestinal organoids are 3D structures derived from intestinal stem cells, characterized by the expression of the Leu-rich repeat-containing G protein-coupled receptor 5 (LGR5). These organoids resemble both the structure and cellular composition of the human intestinal epithelium and they are composed of a **closed-loop hollow lumen lined with a monolayer of intestinal epithelial cells**: initially they create a small cyst-like morphology that under the right signals and conditions grow into a budding-like morphology, corresponding to crypts domains in which intestinal stem cells reside, while the more differentiated cells are lined in the villous domains [97].

Intestinal organoids can be **generated from ASCs or PSCs**. ASC-derived intestinal organoids are obtained from isolated $LGR5^+$ intestinal epithelial stem cells from small intestinal or colonic crypts generating respectively enteroids or colonoids (Figure 12a) [98].

PSC-derived organoids are obtained by direct differentiation of either ESCs or iPSCs. Both ASC and PSC-derived organoids generate self-organizing 3D structures with self-renewal capabilities, but PSC-derived organoids require more expertise and resources given the presence of both epithelial and mesenchymal components, despite representing the intestine more faithfully (Figure 12b). Because of their complexity and the intense procedure to generate them, PSC-derived organoids generation is harder to standardize causing reproducibility problems, therefore the main source to produce intestinal organoids are patient-derived adult stem cells [97].

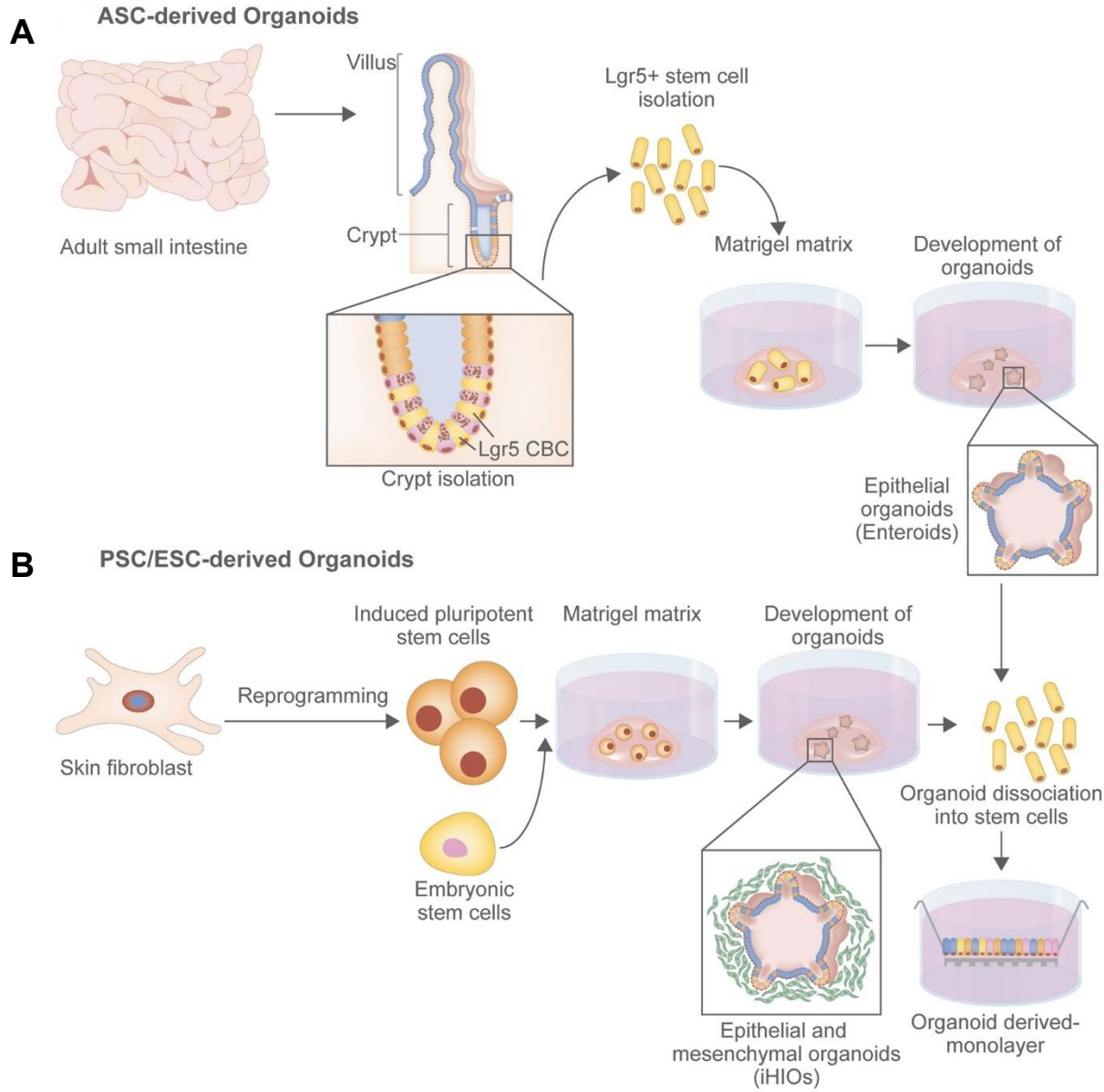

***Figure 12**: intestinal organoid generation. **A)** Intestinal organoids can be generated from ASCs present in the intestinal crypts and positive for Lgr5 marker, obtaining enteroids or colonoids based on the origin of the stem cells. **B)** Intestinal organoids can be generated also from ESCs or iPSCs obtained from the dedifferentiation and reprogramming of somatic cells. The intestinal organoids obtained from PSCs differ from the ASCs-derived one because of the presence of both the epithelial and the mesenchymal component, which is missing in ASCs-derived organoids. However, both can be dissociated to expand them or to obtain a 2D monolayer grown on permeable supports [88].*

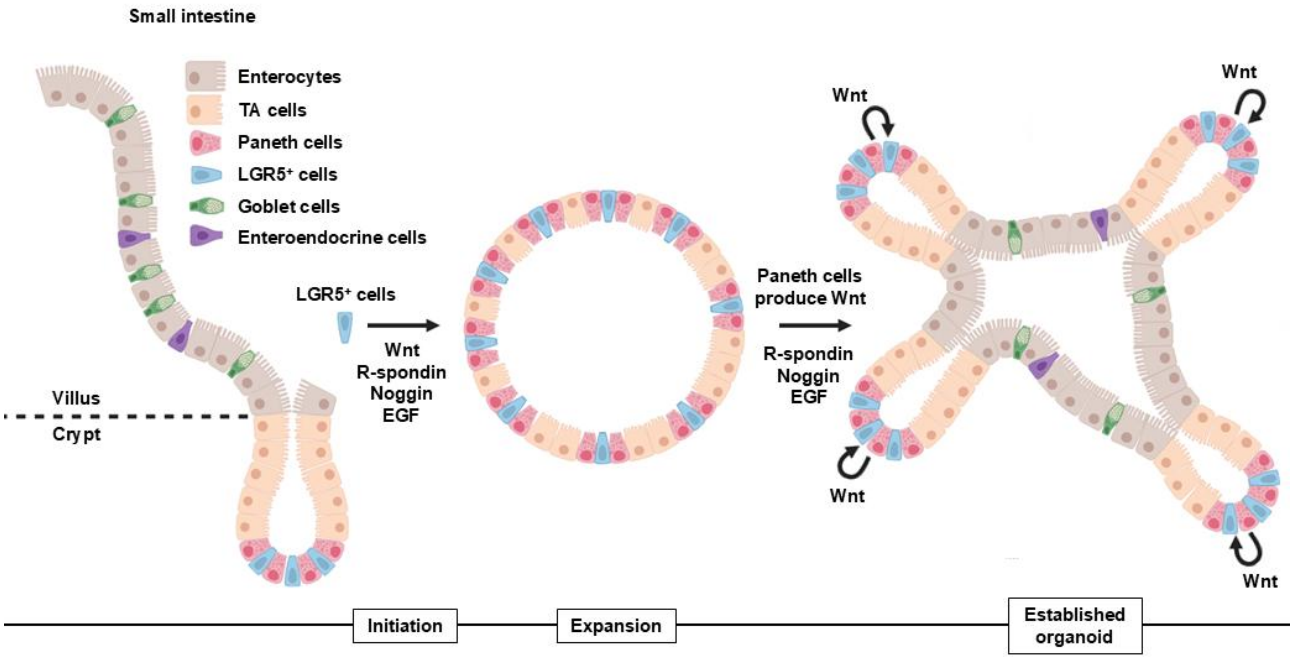

***Figure 13**: staminal and differentiated organoids cell composition. In the intestinal villous-crypt structure, Lgr5+ stem cells resides in the bottom of the crypt, while enterocytes compose most of the villous component. Staminal organoids are kept with factors that keep the staminal condition of the Lgr5+ stem cells and most of the organoid is composed of cell types found in the crypt, allowing the expansion of the organoids. After the removal of the staminal factors from the medium, the other components induce differentiation of the organoid, that assume a morphology that resembles the villous-crypt structure in the intestine and is constituted of mainly differentiated cells like enterocytes (modified from [110]).*

Independently from their origin, the **two essential components** to generate and grow organoids are an **extracellular support matrix and a culture medium**. The extracellular matrix, usually matrigel as substitute, is fundamental in offering structural support and providing biochemical signals necessary for adherence, growth and differentiation of stem cells, while the culture medium with its components supports the formation and development of organoids. These components must mimic the signaling pathways present in the crypt *in vivo*, more precisely in the stem cell niche, to sustain stem cell functionality and their expansion and differentiation into specific cell types: the key ingredients in the medium for culturing intestinal organoids are **Wnt-3a, epidermal growth factor, noggin and R-spondin 1**. These growth factors are incorporated following a temporal scheme, regulating the signaling pathway in the stem cell niche [99]. By withdrawing growth factors that support the stem cell state and adding components that induce the **differentiation process**, it is possible to differentiate intestinal stem organoids to the different cell lineage present along the crypt-villous axis in the small intestinal epithelium (Figure 13) [100].

Intestinal organoids have found several applications in research, being used in therapeutic studies, interactions between host and microbe, delivery of biomolecules, intestinal biology

and development, and using samples from healthy and diseased patients they helped in comprehending and further study the pathogenesis of various diseases like CD [101].

1.2.3 Culture methods of intestinal organoids

Intestinal organoids are closed in cyst-like 3D structures where the apical membrane faces inwards towards an internalized lumen, while the basolateral surface is associated with the extracellular matrix in which the organoids are embedded, therefore these organoids are called **basolateral-out organoids** (Figure 14A): this disposition limits the access to the inner apical-luminal surface of the epithelium, which represents the mucosal interface that typically interacts with the external environment in processes like nutrient absorption, interactions with gastrointestinal microbes and uptake of drugs or toxins, making this side of the organoid essential for various applications [102]. Moreover, when organoids are embedded in matrigel they are positioned at various depths, limiting uniform exposure to the media and the possibility to conduct real-time imaging efficiently, therefore some studies have proposed the culturing of intestinal organoids as a 2D monolayer.

2D organoid monolayers are generated from the 3D structures that have been dissociated into single cells, then plated onto permeable supports on which they grow forming a monolayer (Figure 14B): this culturing system has two characteristics: it maintains functional and phenotypical characteristics like 3D organoids and the intestinal epithelium, and it provides easier and independent access to both the apical and the basolateral sides of the

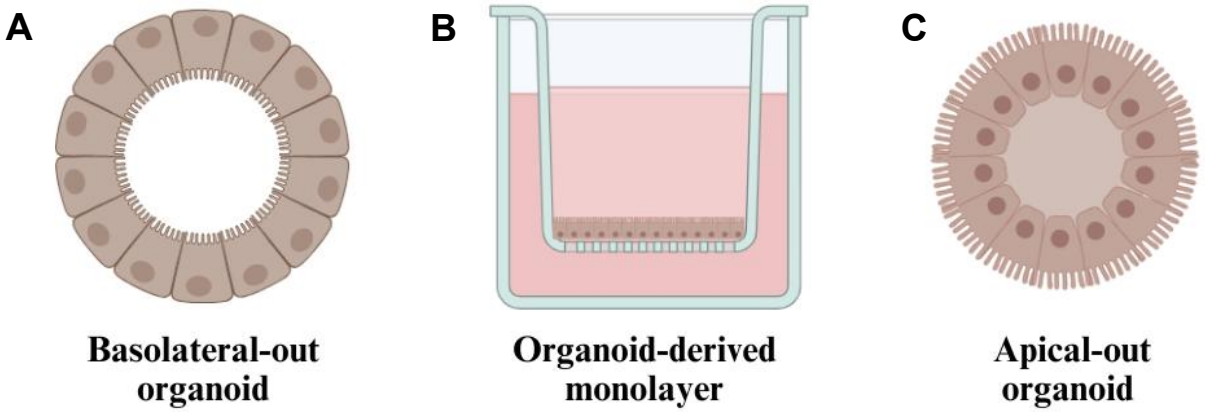

***Figure 14**: different approaches for culturing organoids. **A)** Basolateral-out organoids are embedded in matrigel, with the luminal surface of the cells facing inward while the basolateral side facing outward. **B)** 2D organoid-derived monolayers are obtained from the dissociation of organoids into single cells that are seeded on a permeable support, allowing the luminal apical surface of the cells to be exposed and accessible, and the basolateral side is associated to the surface of the insert. **C)** Apical-out organoids are obtained by removing matrigel and culturing organoids in suspension, this allows the spontaneous reversion of their polarity, exposing the apical surface of the cells outward, while the basolateral side is facing inward (created with BioRender.com).*

intestinal epithelium since the apical side is facing outward while the basolateral is associated with the support [103]. This organization enables more control on experimental parameters, since each side can be exposed to the desired treatment uniformly and transcytosis or diffusion from either side can be assessed since each compartment can be sampled independently. However, there are also some limitations in this system, like the time-consuming procedure to obtain cell confluency and the difficulty of expansion with the conventional methods of resuspension and passaging [102].

There's another technique that gives access to the apical side of the epithelia cells in the organoids that is the **inversion of the enteroid polarity**, generating **apical-out organoids** from basolateral-out organoids embedded in matrigel (Figure 14C). When basolateral-out organoids are separated from matrigel and kept in suspension culture, they spontaneously reverse their polarity in a few days, exposing the apical surface outward. The elimination of matrigel avoids the diffusion limitations present with basolateral-out organoids and allows to perform interaction studies between several targets and the apical surface of the organoids. However, this technique has some limitations too, since apical-out organoids have a slower proliferation and a faster differentiation time, additionally they make live-imaging more difficult given their freedom to float in the suspension medium [102].

1.3. Endoplasmic reticulum and ER stress

The endoplasmic reticulum (ER) is the largest organelle in the cell and is a major site of protein synthesis, transport and folding through various chaperone proteins and enzymes, lipid and steroid synthesis, carbohydrate metabolism and calcium storage [104]. ER consists of **reticular and tubular structures** that span across the cell, and it is constituted by two main domains (Figure 15): the **smooth ER**, without ribosome attachment and involved in lipid synthesis, metabolism functions and calcium storage; the **rough ER**, with ribosome attachment and is responsible for the synthesis and transport of secretory, transmembrane and cytosolic proteins [105].

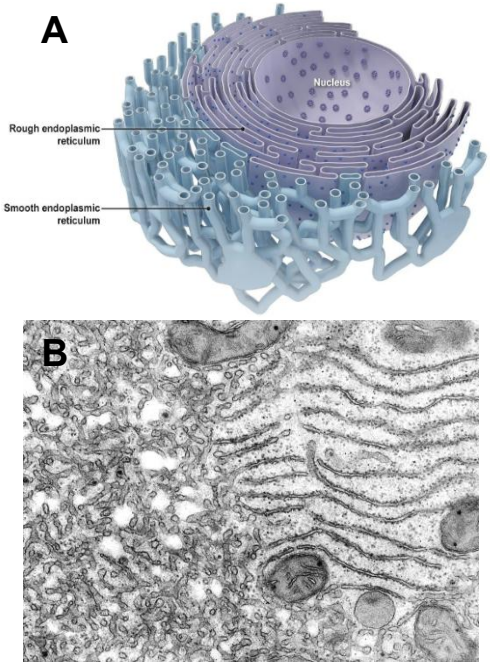

***Figure 15**: **A)** Schematic representation of ER [106]. **B)** Electron microscopy photo with smooth ER on the left side and rough ER on the right side [107].*

1.3.1 ER functions

One important role of ER is the **synthesis of membrane lipid**, which occurs in the ER compartment in close juxtaposition to the Golgi apparatus called ER-Golgi intermediate compartment (ERGIC), constituting an area rich in tubules and vesicles. Once lipids are mobilized to the ERGIC, they are **distributed throughout the cell** through organelle contacts or secretory vesicles [104]. More precisely, the Golgi apparatus is composed of several flattened and fenestrated cisternae, aligned in parallel forming a stack, which is compartmentalized in *cis*, *medial* and *trans* compartments, ending with a tubular, branching and reticulating compartment named *trans*-Golgi network : the *cis*-Golgi is the closest compartment to the ERGIC, lipids are transported here from the ERGIC and their movement continues through the Golgi apparatus to the *trans*-Golgi network from which they travel through vesicles to their destination [104], [106].

Another fundamental function of the ER is to **synthesize secreted and transmembrane proteins, as well as part of the cytosolic proteins**. Translation of secretory and

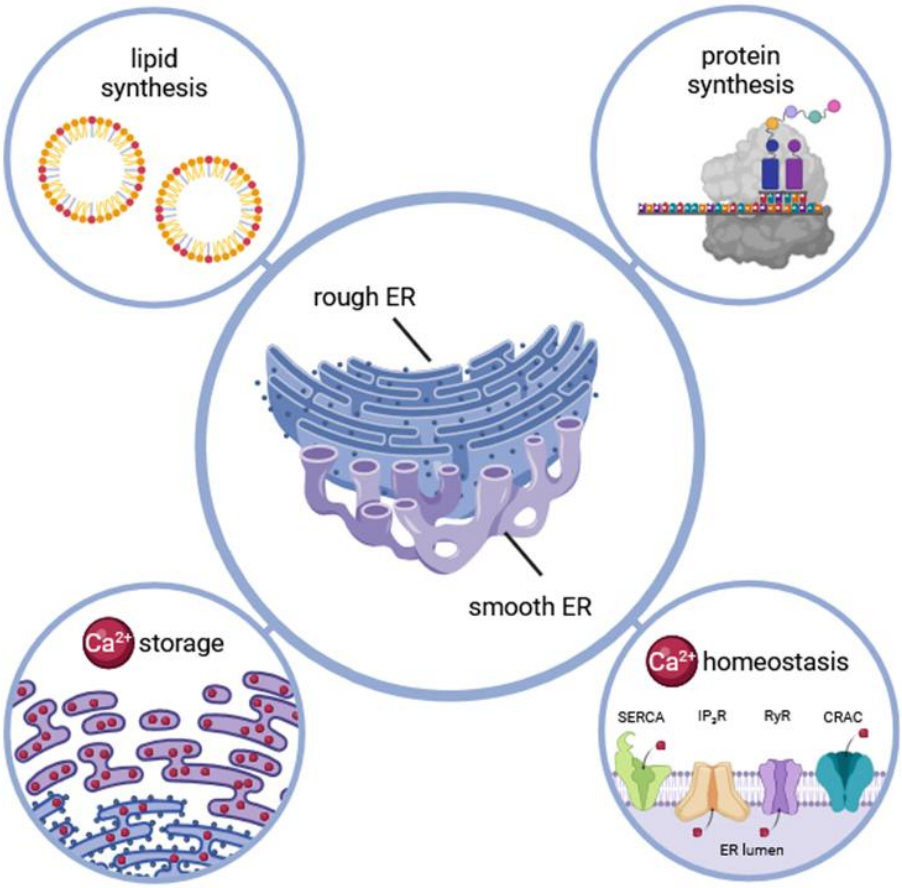

***Figure 16**: ER main functions. ER consists of the rough ER with ribosomes and smooth ER and a central role in the metabolism of the cell, since it is responsible for lipid synthesis and transportation to the Golgi apparatus, the synthesis of the majority of the proteins of the cells and starting the transport to their final location, and it is one the most important storage of Ca^{2+}, regulating its homeostasis thanks to multiple channels, allowing calcium movements both in and out of ER (created with BioRender.com).*

transmembrane proteins starts in the cytosol, then the mRNA-ribosome complex is recruited to the ER membrane through a signal sequence present in the N-terminal of the nascent protein recognized by a specific protein, the signal recognition particle (SRP). Translation then continues and the polypeptide co-translationally enters the ER through the translocon: if the protein is destined to be a transmembrane protein, it shifts to become anchored in the phospholipid bilayer, if the protein is destined to be secreted or to stay in a specific organelle within the cell, it is translocated into the ER lumen. Here the protein is folded and modified, then travels to the Golgi apparatus where it is transported to its destination [104], [107].

Other than synthesis processes, ER is involved in Ca^{2+} homeostasis being a **major store of intracellular Ca^{2+}**. The ER contains several calcium channels both for release and uptake of calcium: inositol 1,4,5-triphosphate (IP_3) receptor (IP_3R) and ryanodine receptor (RyR) are responsible for releasing Ca^{2+}. The first responds to the release of IP_3 upon G protein-coupled receptor (GPCR) activation, while the latter responds to an increased Ca^{2+} concentration. Sarcoendoplasmic reticular Ca^{2+} ATPase (SERCA) on the other hand can pump calcium back into the ER lumen, replenishing the Ca^{2+} stored in response to calcium leakage from the ER into the cytoplasm. Instead, in case of a rapid depletion of ER stores of Ca^{2+} in response to intracellular signals like IP_3, a mechanism to uptake extracellular calcium is activated through the assembly of Ca^{2+} release-activated channels (CRAC), pumping Ca^{2+} directly into the ER lumen.

Calcium homeostasis is important and finely regulated since it is a widespread signaling molecule involved in several processes like localization, function and association of proteins, either with other proteins, molecules, organelles o nucleic acids [104], [108]. Its dysregulation can contribute to several diseases, and it shows to be involved in CD too since anti-TG2 antibodies can mobilize Ca^{2+} from intracellular stores, both ER and mitochondria, by interaction with cell-surface TG2, inducing a rapid increase in intracellular Ca^{2+} concentration. This could influence various pathways given the widespread role of Ca^{2+} as a signaling molecule, like TG2 externalization or the activation of intracellular TG2, which is kept inactive by low Ca^{2+} concentration inside the cell under normal conditions. Since TG2 has several proteins as its substrates, it can lead to alteration of different signaling pathways like inflammatory ones. Moreover, its crosslinking activity can further link gliadin peptides to TG2 and other proteins enhancing the autoimmune aspect of CD [109].

1.3.2 ER stress and the unfolded protein response

Even with many proteins and complexes to control that proteins synthesized fold properly, a fraction of these do not reach their functional form and are misfolded or aggregated. These proteins can remain in the ER or can enter the **ER-associated degradation (ERAD) pathway** mediated by the proteasome [110]. Multiple events can lead to an accumulation of misfolded proteins, like inhibition of N-glycosylation and alteration of Ca^{2+} concentration in the ER, an increased protein synthesis, ATP depletion, osmotic stress, viral infection and increased temperature. If the misfolded proteins exceed the threshold, ER can't maintain its homeostasis and it enters a condition known as ER stress, that activates several signals and pathways leading to specific gene transcription, a process collectively called the **unfolded protein response (UPR)**. ER stress is often transitory and UPR can appropriately control this state returning to normal conditions: however, if ER stress is prolonged, there are major implications in protein synthesis, affecting other cell functions and resulting in premature apoptosis [111].

UPR activates mainly **three ER stress sensors** (Figure 17): inositol-requiring enzyme 1 α (IRE1α), protein kinase R-like endoplasmic reticulum kinase (PERK) and activating transcription factor 6 (ATF6). These are transmembrane proteins with three domains: a domain in the ER lumen that senses misfolded proteins, a transmembrane domain and a cytoplasmic domain that transmit the signals starting the pathways leading to transcription in the nucleus [112]. In normal conditions, these three sensors bind to the molecular chaperone-binding immunoglobulin (BiP) in the ER lumen, this binding blocks UPR signaling. When ER stress condition is reached, BiP is isolated by misfolded proteins, allowing the three sensors to become active by homodimerization, autophosphorylation and cleavage processes, thus starting the three UPR branches [113].

IRE1α is an ER resident type I transmembrane protein (N-terminal in the ER lumen, C-terminal in the cytosol and a cleaved signal peptide) which cytoplasmic domain has two enzymatic activities: a serine/threonine kinase activity and a ribonucleic acid endonuclease activity. When IRE1α can dimerize after BiP is bound by misfolded proteins, it activates itself through autophosphorylation thanks to its protein kinase activity; its ribonucleic acid endonuclease activity then splices an unconventional intron from X-box binding protein 1 (XBP1) mRNA generating the functionally active protein XBP1s. The latter is transferred into the nucleus where it promotes the transcription of UPR target genes, including chaperones and protein folding enzymes, ER and Golgi components and the ERAD pathway, thus

promoting ER lipid synthesis, protein folding and membrane expansion to reduce ER stress [114], [115]. The activation of IRE1α mediates also the decay of mRNA, also known as regulated IRE1-dependent decay (RIDD), reducing the load of protein-folding of the ER [107].

PERK is also an ER resident type I transmembrane protein, the N-terminal in the ER lumen is important for dimerization and the association with BiP, while the C-terminal in the cytoplasm has a serine/threonine protein kinase domain. When during ER stress BiP is bound by misfolded proteins, PERK is activated by autophosphorylation and dimerization:

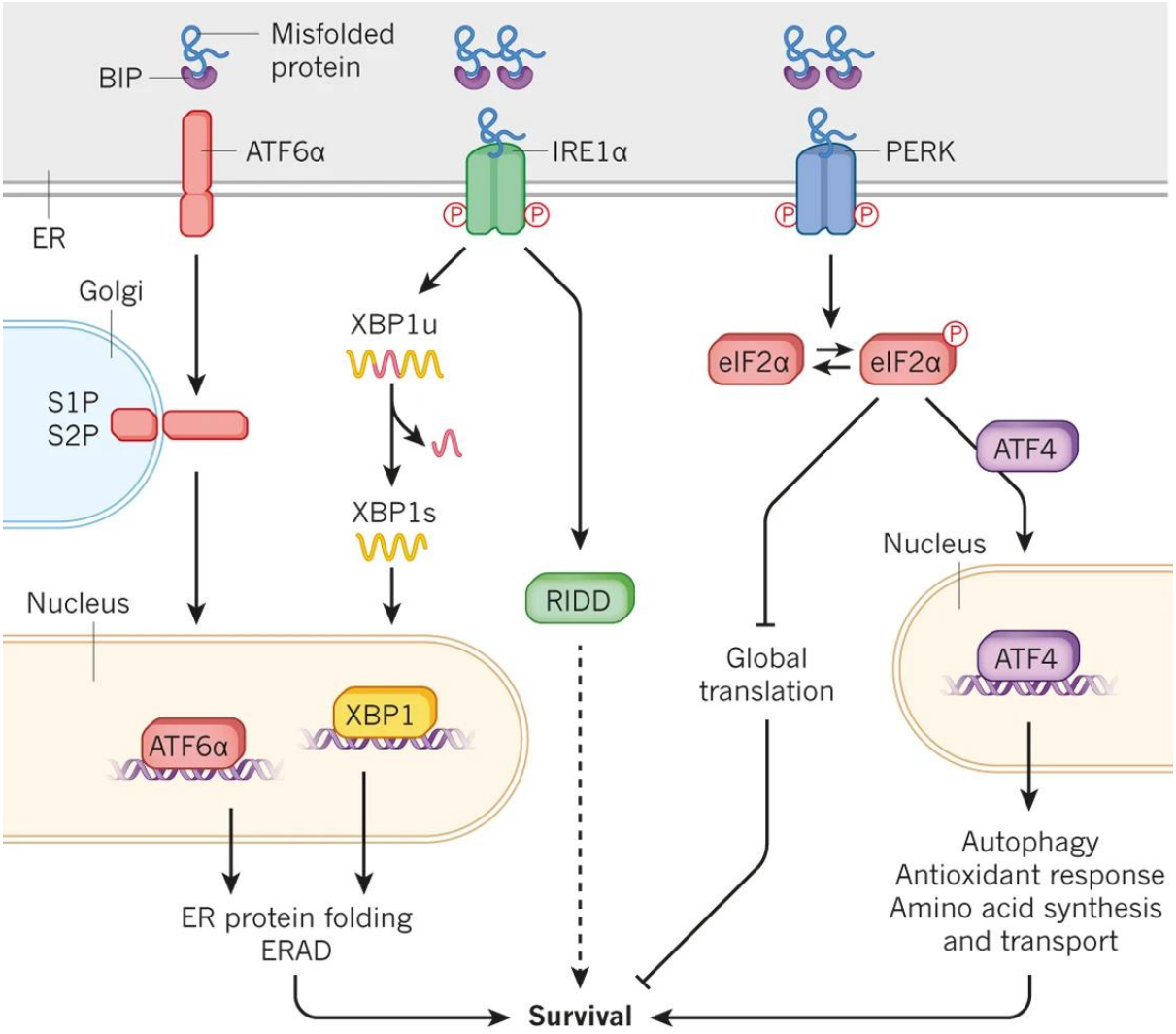

***Figure 17**: UPR pathways. During ER stress, BiP binds to the accumulation of misfolded proteins, allowing the activation of the three main pathways of UPR: IRE1α is activated through heterodimerization and autophosphorylation, its endonuclease activity splices an unconventional intron of XBP! mRNA generating the functionally active form of XBP1 called XBP1s, which translocate in the nucleus to promote UPR genes transcription. IRE1α mediates also mRNA decay (RIDD) to alleviate the load on ER. PERK is also activated through heterodimerization and autophosphorylation; active PERK phosphorylates eIF2α decreasing its activity and consequently decreasing mRNA translation, although contemporaneously increasing the translation of specific mRNA like ATF4, a transcription factor that translocates in the nucleus promoting UPR genes transcription and other genes to alleviate ER stress. ATF6 after being separated from BiP is translocated to the Golgi apparatus where the cytoplasmic domain is cleaved, that becomes active and can translocate to the nucleus promoting UPR genes translation (modified from [96]).*

its kinase activity phosphorylates both itself and the translation initiation factor eukaryotic initiation factor 2 α (eIF2α). Phosphorylation of eIF2α decrease its activity, consequently decreasing mRNA translation, but it also causes mRNA with short open reading frames in the 5' untranslated region to be preferentially translated, like activating transcription factor 4 (ATF4) mRNA. Additionally, PERK phosphorylation leads to the separation of nuclear factor-erythroid 2-related factor 2 (NRF2) from Kelch-like ECH-associated protein 1 (KEAP1), NRF2 then translocate to the nucleus and promotes ATF4 expression [105], [116]. ATF4 is a key transcriptional regulator activated in response to various stress signals like ER stress; it targets genes involved in protein folding, autophagy and apoptosis, amino acid metabolism and homeostasis of ROS. Among these genes there are also C/EBP-homologous protein (CHOP) and growth arrest and DNA damage-inducible 34 (GADD34). CHOP is another transcription factor upregulated by ATF4 expression that activates genes to restore the ER balance, including XBP1 and chaperones, as well as proapoptotic genes; GADD34 is regulatory subunit of protein phosphatase 1 catalytic subunit gamma (PP1C), which dephosphorylate eIF2α, counteracting PERK and showing the importance of the balance in PERK signaling at the eIF2α phosphorylation level, protective at modest levels of signaling but can contribute to cell death pathways. Finally, activated PERK interferes also with the assembly of the 5'-cap on mRNA, thus directly inhibiting mRNA translation and protein synthesis, reducing the stress load on ER [115], [117].

ATF6 is an ER resident type II transmembrane protein (N-terminal in the cytosol, C-terminal in the ER lumen and the signal peptide is not cleaved) has transcription factor domain at the N-terminal in the cytoplasmic domain. In ER stress conditions, the ER luminal domain is separated from BiP and ATF6 then is translocated to the Golgi apparatus: here, site-1 and site-2 proteases (S1P and S2P) cleave ATF6, removing the luminal and the transmembrane domain. The now free N-terminal cytoplasmic domain is translocated to the nucleus where it activates UPR target genes like BiP, chaperones and folding enzymes, promoting ER expansion and folding [118].

To sum up, **UPR has three main effects** on the cell in response to ER stress: **decreasing translation, restoring protein folding and degradation of the misfolded proteins via ERAD**. The inhibition of translation induced by PERK tries to limit further misfolding while allowing the synthesis of protein products of UPR genes. Additionally, the dimension of ER can be increased by UPR, increasing the capacity to correctly fold proteins and degrade the misfolded ones. However, in case of prolonged ER stress, UPR interacts with the apoptosis

pathway, inducing it via the intrinsic pathway, moving the balance towards proapoptotic signals and promoting premature apoptosis via the intrinsic pathway. An important role in this process is the activation of CHOP, that modulates anti- and proapoptotic proteins. UPR is also connected with autophagy, a process that surround intracellular debris and organelles with a membrane fusing them with lysosomes to facilitate degradation, since misfolded proteins aggregates that can't be removed by ERAD are redirected to autophagy to eliminate them [111], [113].

2. AIMS

CD is an **autoimmune enteropathy** caused by the ingestion of gluten and it is one of the most diffused chronic diseases worldwide, having an overall average prevalence of 1%. CD affects patients of at all ages, manifesting itself in the early years of childhood or even during adulthood, with a variety of intestinal and/or extraintestinal symptoms. To date, there is still **no cure for CD**, and the only available therapy is a lifelong strict GFD, that despite leading to a total remission of the symptoms, have several physical and psychological side effect.

Its pathogenesis is multifactorial, comprehending a genetic component and an autoimmune one that have been extensively studied over the years, but still can't fully explain CD mechanisms, meaning that other components must be present and have an important role in the insurgence of this disease. Among these, the **effect of gluten peptides on the enterocytes is still unclear** and could possibly play an important role in the damage mechanism of the intestinal epithelium.

In literature there is evidence that gluten peptides can induce inflammation and mucosal damage at the intestinal level, together with the release of inflammatory cytokines and the production of ROS. Additionally, gluten peptides can **mobilize Ca^{2+}** from intracellular stores, leading to TG2 activation, an essential enzyme in modifying gluten peptides enhancing their immunogenicity, and **ER stress**.

Given the importance of TG2 in CD and the detection of ER stress in the enterocytes, which is a condition present in widespread diseases like diabetes, neurodegenerative disorders and several cancer types [119], and as such there are drugs used in therapy and under clinical trials [120], it could be an improvement in the understanding the pathogenesis of CD and a step closer to find an alternative treatment to GFD.

With this objective in mind, in this PhD thesis we aimed to **verify ER stress activation in our available models**: first in a cellular model using the CaCo-2 cell line, then an animal model with the intestines from Balb/c mice cultured in GEVS thanks to the collaboration with Prof. Corazzari's research group at the University of Eastern Piedmont, Novara (Italy), and finally in CD patients' intestinal biopsies to confirm the involvement of ER stress in CD.

However, to investigate more in depth ER stress in CD, we needed **a more accessible human CD model** rather than cell lines and mouse model.

For this purpose, in collaboration with Dr. De Leo's research group at Burlo Garofolo Pediatric Institute, Trieste (Italy), we aim to establish protocols for the generation, and culturing of **patients' derived intestinal organoids** that recapitulate the variability found between patients and can function as a human *in vitro* CD model.

The organoid model is chosen because of its ability to self-organize in structures like the organ of origin, maintaining its core functions and the genetic characteristics of the parental tissue while being a better *in vitro* system than cell lines, since the latter can't mimic organ complexity and can't maintain patients' specificity. Moreover, most cell lines, deriving from tumor tissues, have genetic alterations that, despite being necessary to be cultured indefinitely, negatively influence how well they can recapitulate a specific tissue. On the other hand, organoids cultures while being a good replica of the tissue of origin, maintain also the advantages of a 2D culture, self-renewal capability (although limited), the possibility to be expanded, easily accessible for various treatments and manipulations, therefore having less limitations than using an animal model, being more ethical too.

After establishing functioning protocols for organoids generation, culturing, inversion and differentiation to mimic closely the intestine in the human organism, we want to **evaluate the induction of ER stress in CD patients' derived organoids upon PTG stimulation**, confronting them with control patients' derived organoids, attempting to investigate the mechanisms and pathways that connect PTG and ER stress in the context of the enterocyte.

3. MATERIALS AND METHODS

3.1 Pepsin-trypsin-gliadin (PTG) preparation

A pepsin and trypsin resistant gliadin (PTG) was prepared. Each 50g of gliadin from wheat (Sigma) was dissolved in 500mL 0,2N HCl for 2h at 37°C with 1g pepsin (Sigma). The resultant peptic digest was further digested by addition of 1g trypsin (Sigma), after pH adjusted to 7,4 using 2M NaOH. The solution was stirred vigorously at 37°C for 4h, boiled to inactivate enzymes for 30', lyophilized and then stored at -20°C until used. PTG was freshly suspended in sterile PBS to a final concentration of 100mg/mL.

3.2 Cell culturing and treatments

Caco-2 cells were maintained in DMEM (Merk) supplemented with 10% FBS (EuroClone), 2mM glutamine (Merck), and 1% penicillin/streptomycin (Merck). Cells were treated with PTG at a final concentration of 1mg/mL alone or in combination with 4-phenylbutyric acid (4PBA) (Santa Cruz) at a final concentration of 5μM for 9h or left untreated.

3.3 Mouse intestine culturing and treatments

Experiments with small intestine from Balb/c mice cultured in GEVS were done in collaboration with Corazzari's research group at University of Eastern Piedmont (Novara, Italy).

Small intestine from 13 days old Balb/c mice, feed with a GFD for at least three generations were freshly resected and cultivated in a silicone based GEVS (as previously described in *1.1.8.1 Introduction - The Gut-Ex-Vivo System to model CD*).

All procedures were approved by the local Ethics Committee for Animal Welfare (DB064.N.TMC) and conformed to the European Community regulations for animal use in research (2010/63 UE).

Each intestine was infused with serum-free tissue culture medium (IMDM), supplemented with 20% KnockOut serum replacement (Gibco), 2% B-27 and 1% of N-2 supplements (Gibco), 1% L-glutamine, 1% NEAA (Gibco), 1% HEPES (EuroClone) and stimulated with

PTG at a final concentration of 2,5mg/mL and thapsigargin (TPSG) (Merck) 5µg/mL, both alone or in combination with 4-phenylbutyric acid (4PBA) (Merk) at a final concentration of 3µM for 16h or left untreated.

3.4 Patients' biopsies

Duodenal biopsies were obtained from pediatric patients (<18 years old) at Maggiore della Carità University Hospital (Novara, Italy) via upper gastrointestinal endoscopy. Parents or guardians and patients, where appropriate, provided written informed consent, and the local ethics committee (Comitato Etico Interaziendale Novara, CE 402/23) approved the study protocol.

Endoscopies were performed, according to current ESPGHAN guidelines [121], to confirm the suspicion of CD in patients with anti-TG2 IgA antibodies levels lower than 10 times the ULN, or in the case of total IgA deficiency, or when a biopsy-sparing diagnosis was refused by the patient's family, even if in the presence of diagnostic elevation of anti-TG2 IgA above 10 times the ULN. If the histologic examination confirmed the suspicion of CD (Marsh grade 2 or higher), the patient is diagnosed with CD. As control subjects, pediatric patients undergoing diagnosis (gastritis, eosinophilic esophagitis, etc.) were enrolled. The samples were frozen at -80°C immediately after resection and stored until analysis.

3.5 Quantitative PCR (qPCR) for cellular, mice intestine and patients' biopsies experiments

TRIzol reagent (Thermo Fisher Scientific) was used to extract total RNA, then ExcelRT™ Reverse Transcription Kit (Smobio) was used to produce cDNA by using 2µg of RNA. ExcelTaq™ 2XFastQ-PCR Master Mix (Smobio) was used to produce fluorescently labeled PCR products. Primer sequences are reported in Table 1. Mouse GAPDH or human L34 were used as reference.

3.6 Organoids

Organoid culturing was done at Pediatric Institute Burlo Garofolo (Trieste, Italy) in collaboration with Dr. De Leo's research group.

Species	Gene	Forward primer sequence Reverse primer sequence
Mouse	TG2	F: AAGAGCGAAGGGACATACT
		R: TGAGCACAGACCCATCTT
	CLDN2	F: CCTCGCTGGCTTGTATTATC
		R: AAAGACTCCACCCACTACA
	ATF4	F: GTTTAGAGCTAGGCAGTGAAG
		R: CCTTTACACATGGAGGGATTAG
	ATF6	F: GATGGTGACAACCAGAAAGA
		R: TGGAGGTGGAGGCATATAA
	XBP1s	F: AGTCCGCAGCAGGTG
		R: GGTCCAACTTGTCCAGAATG
	GAPDH	F: TTCAACGGCACAGTCAAG
		R: CCAGTAGACTCCACGACATA
Human	hTG2	F: CACCCACACCTACAAATACC
		R: CAAAGTCACTGCCCATGT
	CLDN2	F: TTCCCTGTTCTCCCTGATAG
		R: TGGTAGGCATCGTAGTAGTT
	ATF4	F: CCCGGAGAAGGCATCCTC
		R: GTGGCCAAGCACTTCAAACC
	ATF6	F: TTTGCTGTCTCAGCCTACTGTGGT
		R: TCCATTCACTGGGCTATTCGCTGA
	Xbp1(s)	F: AGAGAAAACTCATGGCCTTGTAGTTG
		R: CATTCCCCTTGGCTTCCG
	L34	F: GTCCCGAACCCCTGGTAATAGA
		R: GGCCCTGCTGACATGTTTCTT

Table 1: *primer sequences used in qPCR for CaCo-2, GEVS and patients' biopsies gene expression analysis.*

Intestinal organoids were generated from LGR5+ stem cells from duodenal biopsies, obtained from pediatric patients (<18 years old) at IRCCS Burlo Garofolo Pediatric Institute (Trieste, Italy) via upper gastrointestinal endoscopy with the approval of the ethics committee and after obtaining the written informed consent of the parents.

Endoscopies were performed, according to current ESPGHAN guidelines [121], to confirm the suspicion of CD in patients with anti-TG2 IgA antibodies levels lower than 10 times the ULN, or in the case of total IgA deficiency. If the histologic examination confirmed the suspicion of CD (Marsh grade 2 or higher), the patient is diagnosed with CD. As control

subjects, pediatric patients undergoing diagnosis (gastritis, eosinophilic esophagitis, etc.) were enrolled. The samples were used for organoids generation immediately after resection.

3.6.1 Organoids' media compositions

Below are reported the compositions of the media used to culture organoids and during different protocols to work with organoids:

- **Staminal medium** was prepared including factors for the growth of intestinal cells and to maintain stemness. In Table 2, there are reported medium components and their final concentration.
- **Differentiation medium** was prepared to induce differentiation of staminal organoids into enterocytes and other intestinal cell types. Differentiation medium contains the

Components	Manufacturing company	Final concentration
Advanced DMEM/F-12	Gibco	50%
Wnt	Conditioned medium produced from *in vitro* culturing of L-Wnt-3A cell line, CRL-2647, ATCC	50%
HEPES	Gibco	10mM
GlutaMAX	Gibco	1X
N-2 Supplement	Gibco	1X
Nicotinamide	Sigma	10mM
B-27 Supplement	Gibco	1X
N-Acetyl-L-Cysteine	Sigma	1mM
Normocin	InvivoGen	100µg/mL
Gastrin I human	Sigma	1µg/mL
Recombinant Human Noggin	PeproTech	100ng/mL
Human EGF Recombinant Protein	Gibco	50ng/mL
SB202190	Sigma	10µM
Recombinant Human R-Spondin 1 Protein	Sino Biological	530ng/mL
Galunisertib (LY2157299)	Selleck Chemicals	500nM
Prostaglandin-E2	Sigma	100nM

Table 2: *staminal medium composition with relative components and final concentrations.*

same components of the staminal medium without the reagents responsible for maintaining stemness; in Table 3, there are reported components and their final concentration.

Components	Manufacturing company	Final concentration
Advanced DMEM/F-12	Gibco	100%
HEPES	Gibco	10mM
GlutaMAX	Gibco	1X
N-2 Supplement	Gibco	1X
B-27 Supplement	Gibco	1X
N-Acetyl-L-Cysteine	Sigma	1mM
Normocin	InvivoGen	100µg/mL
Gastrin I human	Sigma	1µg/mL
Recombinant Human Noggin	PeproTech	100ng/mL
Human EGF Recombinant Protein	Gibco	50ng/mL
Recombinant Human R-Spondin 1 Protein	Sino Biological	530ng/mL
Galunisertib (LY2157299)	Selleck Chemicals	500nM

Table 3: *differentiation medium composition with relative components and final concentrations.*

- **Washing medium** was prepared to be used during washing steps when working with the organoids. It contains essential components and nutrients to avoid excessive stress on the cells when left in the washing medium. In Table 4, there are reported components and their final concentration.

Components	Manufacturing company	Final concentration
Advanced DMEM/F-12	Gibco	100%
HEPES	Gibco	10mM
GlutaMAX	Gibco	1X
FBS	Gibco	5%

Table 4: *washing medium composition with relative components and final concentrations.*

- **Differentiation washing medium** was prepared to do the washing steps during the differentiation protocol of organoids embedded in matrigel. In Table 5, there are reported components and their final concentration.

Components	Manufacturing company	Final concentration
Advanced DMEM/F-12	Gibco	100%
HEPES	Gibco	10mM
GlutaMAX	Gibco	1X
N-2 Supplement	Gibco	1X
B-27 Supplement	Gibco	1X

Table 5: *differentiation washing medium composition with relative components and final concentrations.*

3.6.2 Organoid generation

Intestinal organoids were generated from 3 or 4 intestinal biopsies from the distal duodenum via upper gastrointestinal endoscopy for each patient: from these, intestinal crypts were isolated and cultured, forming intestinal organoids through the following protocol.

Biopsies were washed 2 times with cold PBS (EuroClone) and incubated under rotation in 10mL of PBS supplemented with 2,5µg/mL Amphotericin B (Gibco), 0,5mg/mL Normocin (Invivogen) and 0,5mg/mL Gentamicin (Gibco) for 15-20' at room temperature. Then, the antibiotic solution was removed, and biopsies were washed with cold PBS and incubated in PBS with 8mM EDTA (Invitrogen) and 0,5mM DTT (Sigma-Aldrich) under rotation for 45' at 4°C.

After the incubation, the EDTA/DTT solution was removed, and biopsies were washed with cold PBS: then, new cold PBS was added and biopsies were shaken vigorously to release the intestinal crypts into the PBS, which was collected, adding FBS to it at 5% final concentration. This step to collect intestinal crypts was repeated 3 to 4 times with new cold PBS each time.

The collected samples were centrifugated at 200G for 3' at 4°C, then supernatant was removed, and each pellet was gently resuspended in 1mL of washing medium that were combined in a single sample, which was centrifugated at 200G for 4' at 4°C. Supernatant was removed and pellet was resuspended in 1mL of washing medium and transferred into

an 1,5mL eppendorf tube, to make intestinal crypts resuspension in matrigel easier, and centrifugated at 200G for 4' at 4°C.

Supernatant was removed and pellet was resuspended in liquid matrigel (Corning), 22µL per drop of matrigel (numbers of drops varied based on pellet dimension) and seeded in a pre-warmed 48-well plate. The plate was incubated for 10-20' at 37°C (p_{CO2}=5%) to allow matrigel solidification, after which 250µL/well of staminal medium is added. Medium was changed every 2 days.

3.6.3 Protocols to work with organoids

Below are reported protocols used to work with the organoids generated from patients' biopsies: in particular, protocols for organoid passage, organoid inversion and organoid differentiation are described.

3.6.3.1 Organoid passage

Organoid passage is performed to expand an organoid culture, disrupting staminal organoids into single staminal cells that can generate new organoids, increasing their number. It is usually performed 2-3 days after crypt seeding or 7 days after previous organoid passage. An organoid culture can be kept for a maximum of 14 days before passage, after which organoid passage must be done to change the matrigel in which organoids are embedded. To do organoid passage, the next protocol was followed.

Old medium was removed from wells with organoids in matrigel drops, which were washed with cold PBS. Then, 300µL of cold Cell Recovery solution (Corning) was added to each well and matrigel drops containing the organoids were collected in a 15mL Falcon tube and incubated in agitation for 30' at 4°C to facilitate matrigel dissolvement,

After the incubation, 5mL of washing medium was added to the sample and centrifugated at 400G for 3' at 4°C. Supernatant was removed and the pellet was resuspended in trypsin solution (Sigma-Aldrich). The organoid suspension in trypsin solution was incubated 2' at 37°C and then mechanical disaggregation through pipetting of the organoids followed: this step was repeated one more time, after which trypsin activity was stopped by adding 5mL of washing medium.

Disaggregated organoids were centrifugated at 800G for 4' at 4°C, supernatant was discarded, and the pellet was resuspended in matrigel complemented with Y27632 inhibitor

of Rho-associated coiled protein kinase (ROCK) (LifeTechnologies) at 10μM final concentration. Single cells resuspension in matrigel were seeded in pre-warmed 48-well plate as 22μL matrigel drops and incubated for 10-20' at 37°C (p_{CO2}=5%) to allow matrigel solidification, after which 250μL/well of staminal medium complemented with 10μM Y27632 is added. Medium was changed after 2 days with new staminal medium without Y27632, and then every 2 days.

3.6.3.2 Organoid inversion

Organoid inversion is performed to invert organoid's polarity, from basal-out when they are embedded in matrigel, to apical-out to bring the apical side of the cells on the outside; this was done with the following protocol.

Old medium was removed and wells with organoids in matrigel drops were washed with cold PBS, then 300μL of Cell Recovery solution was added to each well and matrigel drops with organoids were collected in a 15mL Falcon tube. An additional 1mL of Cell Recovery solution was added to the sample, followed by incubation for 1h at 4°C in agitation to facilitate matrigel dissolvement.

After the incubation, the sample was filled with washing medium up to 10-12mL and centrifugated at 300G for 3' at 4°C. The supernatant was removed, and the pellet was resuspended in 5mL of washing medium, followed by centrifugation at 300G for 3' at 4°C.

The supernatant was removed, and the pellet was resuspended in culturing medium. The organoid suspension was distributed in a 24-well plate for cell suspension, adding 700μL of the organoid suspension in each well and incubated at 37°C (p_{CO2}=5%). The medium was changed every 2 days.

The resulting pellet from the last centrifuge can be resuspended both in staminal and differentiation medium, depending on the desired condition for the organoids, organoids inversion did not show to be affected by medium composition.

When inverted, the organoids contained in a single matrigel drop in a well of a 48-well plate were distributed in 2 wells of a 24-well suspension plate, in a ratio of 1:2 to avoid overcrowding in the well.

3.6.3.3 Organoid differentiation

Organoid differentiation is performed to differentiate staminal organoids into the different cell types present in the gut. Differentiated organoids lose their stemness and can't be expanded anymore, additionally, they can be kept in culture approximately for 14 days, after which they die, since they lack renewal capacity.

Organoid differentiation can be performed both on basal-out organoids in matrigel and apical-out organoids during the inversion protocol. Differentiation of basal-out organoids was done with the following protocol.

Staminal medium was removed from wells with organoids in matrigel drops and differentiation washing medium was added to each well, incubating for 2-3' at 37°C after which it is removed: this washing step was repeated 3 times. After the last washing step, 250µL/well of differentiation medium was added.

After 2 days, medium was changed with new differentiation medium, and after 4 days medium was changed with differentiation medium without R-spondin 1. On day 5, organoids were differentiated and used for experiments.

Differentiation of apical-out organoids during the inversion protocol was performed by separating the organoids from matrigel following the protocol for organoids inversion described in *3.6.3.2 Material and methods - Organoid inversion*. At the end of the procedure, the pellet composed of isolated organoids was resuspended in differentiation medium and seeded in a 24-well suspension plate adding 700µL/well of the organoid suspension.

Medium was changed after 2 days with new differentiation medium, and after 4 days medium was changed with differentiation medium without R-spondin 1. On day 5, organoids were differentiated and used for experiments.

3.6.4 Organoid hematoxylin and eosin staining

Organoids were collected in Cell Recovery solution as described in *3.6.3.1 Material and methods – Organoid passage* and centrifugated at 300G for 1' at 4°C, supernatant was removed, and they were washed with cold PBS, followed by centrifugation at 300G for 1' at 4°C. The resulting pellets were resuspended in 300µL of paraformaldehyde fixative solution and incubated overnight at 4°C.

The next day, fixed samples were centrifugated at 300G for 1' at 4°C, supernatant was removed, and they were washed with cold PBS, followed by centrifugation at 300G for 1' at 4°C and resuspended in PBS until analysis.

Then, organoids were fixed in 10% v/v buffered formalin and paraffin embedded; 4µm-thick sections were de-waxed with two changes of xylene, 10 min each. Slides were then transferred to 100% alcohol, for two changes, 10 min each, and once through 95 and 70% alcohol respectively, for 5 min each, after which they were rinsed in de-ionized water, twice for 3 min each. The antigen unmasking technique was performed with Novocastra Epitope Retrieval Solutions pH9 EDTA-based buffer in thermostatic bath at 98°C for 30 min. Sections were brought to room temperature and washed in PBS. Subsequently, the neutralization of the endogenous peroxidase with 3% v/v H_2O_2 and Fc blocking by a specific protein block (Novocastra, Leica Biosystems) were performed. Finally slides were stained with hematoxylin and eosin.

3.6.5 Bioinformatic analysis

AllPrep DNA/RNA Mini Kit (QIAGEN) was used to extract total RNA from organoids, following manufacturer's protocol. 1µg of RNA with an RNA integrity number (RIN) above 7 from each sample was sequenced using the transcriptome sequencing service at Macrogen Inc. (Seoul, South Korea), obtaining raw FastQ data.

FastQC program was used with default settings to check the quality of FastQ data from RNA sequencing. FastQ sequencing data for each sample was compacted into a single file using MultiQC tool with default settings, allowing comparison between samples.

Tool STAR (Spliced Transcripts Alignment to a Reference) was used, after the quality control of samples' data, to map reads from RNA sequencing to a human reference genome (version hg38), allowing the identification and genomic localization of each read. Default settings were used in this analysis, adding the "--guantMode GeneQuant" parameter to quantify the number of reads for each gene used to perform a principal component analysis (PCA); gene annotations were downloaded from gencode in gtf format.

Differentially expressed genes between samples were identified with DESeq2 software, confronting the obtained transcriptomic data, resulting in a list of differentially expressed genes between the different conditions of the samples.

3.6.6 qPCR for differentiation genes

To confirm differential gene expressions from bioinformatic analysis, AllPrep DNA/RNA Mini Kit (QIAGEN) was used to extract total RNA from organoids, following manufacturer's protocol. 200ng of RNA for each sample were retrotranscribed to cDNA using SensiFAST cDNA Synthesis kit (Meridian BIOSCIENCE), following manufacturer's protocol. iTaq Universal SYBR Green Supermix was used to produce fluorescently labeled PCR products, following manufacturer's protocol. Primer sequences are reported in Table 6 Human GAPDH was used as reference.

Gene	Forward primer sequence Reverse primer sequence
Lgr5	F: GGACGACCTTCATAAGAAAGATGC
	R: CTGCTATGGTCCACACTCCA
SI	F: TCCAGCTACTACTCGTGTGAC
	R: CCCTCTGTTGGGAATTGTTCTG
MUC2	F: GCTGCTATGTCGAGGACAC
	R: CCATCCTGGGTCTGGTTAAGA
LYZ	F: GGTTACAACACACGAGCTACAAAC
	R: AGTTACACTCCACAACCTTGAACA
CHGA	F: TGTCCTGGCTCTTCTGCTCTG
	R: GTTCATCTCCTCGGAGTGTCTC
GAPDH	F: GACATCAAGAAGGTGGTGAAGC
	R: GTGGTCGTTGAGGGCAATG

Table 6: *primer sequences used in qPCR for differential expression of the differentiation genes in staminal and differentiated organoids.*

3.6.7 Immunofluorescence for polarity reversal

Basal-out and apical-out staminal organoids, and basal-out and apical-out differentiated organoids were collected to verify polarity inversion through immunofluorescence. The collected samples were centrifugated at 300G for 1' at 4°C, supernatant was removed, and they were washed with cold PBS, followed by centrifugation at 300G for 1' at 4°C. The resulting pellets were resuspended in 300µL of paraformaldehyde fixative solution and incubated overnight at 4°C.

The next day, fixed samples were centrifugated at 300G for 1' at 4°C, supernatant was removed, and they were washed with cold PBS, followed by centrifugation at 300G for 1' at 4°C. Each pellet was resuspended in 100µL of antibody staining solution (BSA 3% and Triton X-100 1% diluted in PBS) with Alexa Fluor™ 594 phalloidin (Invitrogen) (used dilution 1:800) and Hoechst 33342 (Thermo Fisher) (final concentration of 0,5µg/mL), and samples were incubated for 1h at room temperature.

Then, samples were centrifugated at 300G for 1' at 4°C, supernatant was removed, followed by a washing in cold PBS, after which samples were centrifugated at 300G for 1' at 4°C. Supernatant was removed, and pellets were resuspended in cold PBS, ready to be visualized.

Organoids were observed with the confocal microscopy ZEISS LSM 900, acquiring images every 4µm along the z-axis of the organoid, constructing z-stack images of multiple organoids for each sample. ZEN 3.10 software was used to handle images acquisition and visualization, while images analysis and reconstruction was performed with Fiji-ImageJ image processing package.

3.6.8 Organoids stimulation

Intestinal organoids were generated from duodenal biopsies following the protocol described in *3.6.2 Materials and methods - Organoid generation* and cultured in staminal medium. After expansion of each patient's derived organoid line, staminal organoids were inverted to reverse their polarity and differentiated to obtain apical-out differentiated organoids following respectively protocols described in *3.6.3.2 Materials and methods - Organoid inversion* and *3.6.3.3 Materials and methods - Organoid differentiation*.

Apical-out differentiated organoids were stimulated in differentiation medium without R-spondin 1 with PTG at a final concentration of 1mg/mL for 1h and 8h or left untreated.

3.6.9 qPCR for treated organoids

TRIzol reagent (Invitrogen) was used to extract total RNA from apical-out differentiated organoids following manufacturer's protocol. Then, 400ng of RNA for each sample were retrotranscribed to cDNA using Xpert cDNA Synthesis Supermix (GRISP), following manufacturer's protocol. PowerUp™ SYBR Green Master Mix (Applied Biosystems) was

used to perform qPCR with the produced cDNA, following manufacturer's protocol. Primer sequences are reported in Table 1. Human L34 was used as reference.

3.7 Statistical analysis

All experiments were performed in triplicate and statistical analysis was performed using GraphPad_Prism_8. Frequency distribution analysis were done setting a bin center of 40. The student t-test or ANOVA was used to determine statistical significance. A p-value equal to or less than 0,05 was considered significant.

4. RESULTS AND DISCUSSION

As described in literature, CD pathogenesis comprehends an immune component, consisting of an inflammatory immune response against unmodified and modified gliadin peptides in the intestine: this response damages the intestinal tissues leading to typical CD symptoms. Even though CD immune components have been extensively studied, it is not the only responsible of CD since several attempts have been made to replicate the pathology in animal models focusing on this aspect and the role of HLA-DQ2/8 characteristics of CD but resulting in no complete model that can fully recapitulate all the aspects of the disease. Therefore, there are **other factors involved in CD damaging mechanisms** independent of the immune system and that are direct consequences of the interaction of gliadin peptides with the organism.

Several effects of gliadin have been described at the cellular level, among these there is the induction of Ca^{2+} movements from the intracellular stores, causing ER stress and TG2 activation. If these pathways are active at the intestinal epithelium level, gliadin peptides could directly participate in intestinal damage since prolonged ER stress induces apoptosis in the affected cells. Moreover, TG2 activation would help to increase the amount of enzymatically active TG2 in the intestine able to modify gliadin peptides, generating new immunogenic molecules and making the activation of the immune system easier.

For these reasons, this PhD thesis investigates more specifically the **effects of gliadin peptides at the intestinal epithelial cells level using several models to verify ER stress and CD markers activation** in this cell type, attempting to deepen the role of ER stress in CD pathogenesis and allowing to increase the knowledge on the mechanism present in CD.

First, we evaluated **ER stress** induction by gliadin peptides **in the intestinal epithelial cell line** CaCo-2 and **in an *ex vivo* animal model** using Balb/c mice small intestine cultivated in GEVS, investigating the presence of ER stress also **in patients' biopsies**.

After confirming the presence of ER stress in these models, wanting to study it in a human model that could maintain the complexity of intestinal tissue and could give us the accessibility of an *in vitro* model, **we developed protocols to generate and grow organoids** from both control and CD patients' intestinal biopsies.

Finally, with our organoids set up, we **stimulated organoids** from control and CD patients **with gliadin peptides** to evaluate ER stress levels in our model.

4.1 ER stress activation by PTG in CaCo-2 cell line

The induction of ER stress by gliadin peptides was evaluated initially in the intestinal **cell line CaCo-2** together with expression of CD markers.

The cells were left untreated (CTRL) or treated with a digestion of gliadin with pepsin and trypsin to obtain gliadin peptides (peptic-tryptic gliadin digest, PTG) (1mg/mL) for 9h. Then, UPR activation was verified by the expression of ATF4, ATF6 and Xbp1(s) through qPCR.

The data presented in Figure 18 show a statistically significant **activation in response to PTG for all three UPR activation pathways** when compared to the untreated sample. Together with the activation of UPR pathways, a statistically significant increase in TG2 and CLDN2 has been observed; both are CD markers that show high levels in CD patients.

Statistically significant **increased levels of hTG2 and CLDN2** were also observed in response to PTG, indicating that CaCo-2 cell line, when stimulated with gliadin peptides,

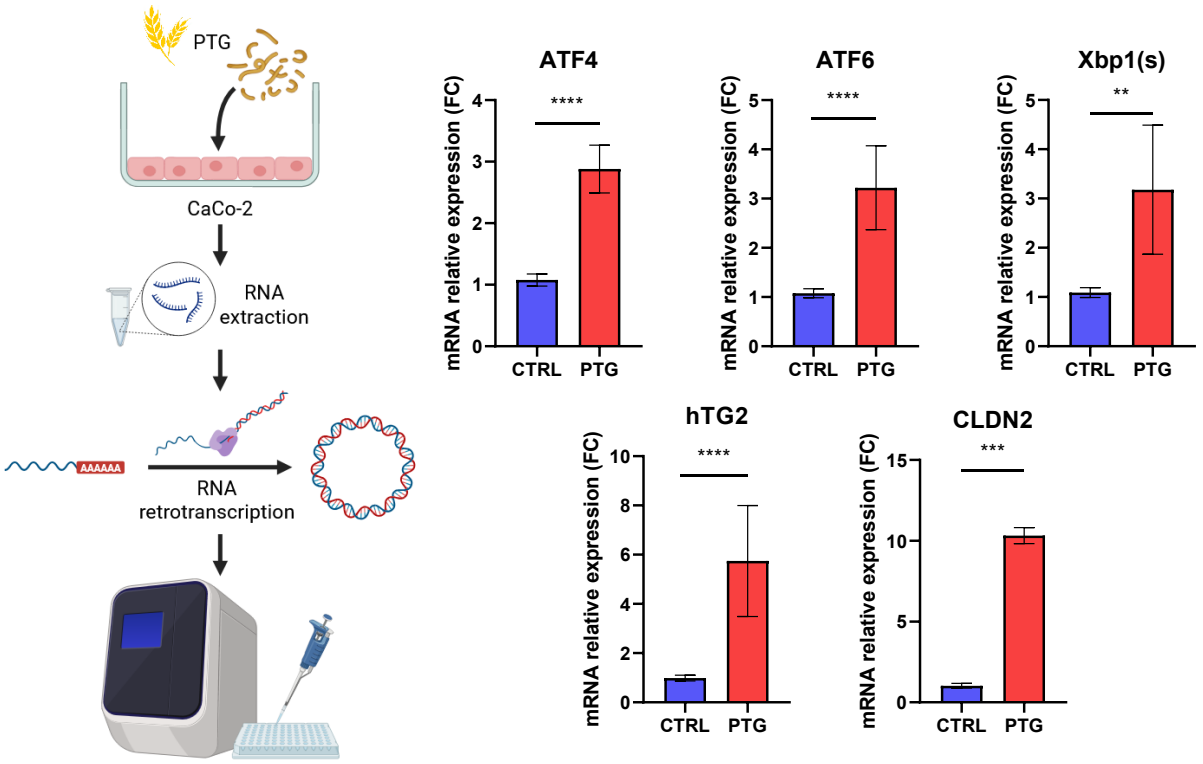

Figure 18: *CaCo-2 were exposed to PTG (1mg/mL) or left untreated (CTRL) for 9h, ER stress induction by PTG was evaluated through qPCR by the expression of ER stress markers ATF4, ATF6 and Xbp1(s). CD markers hTG2 and CLDN2 was also evaluated by qPCR. Histograms represent mean ± s.d.; *p<0,05, **p<0.01. ***p<0.001. ****p<0.0001.*

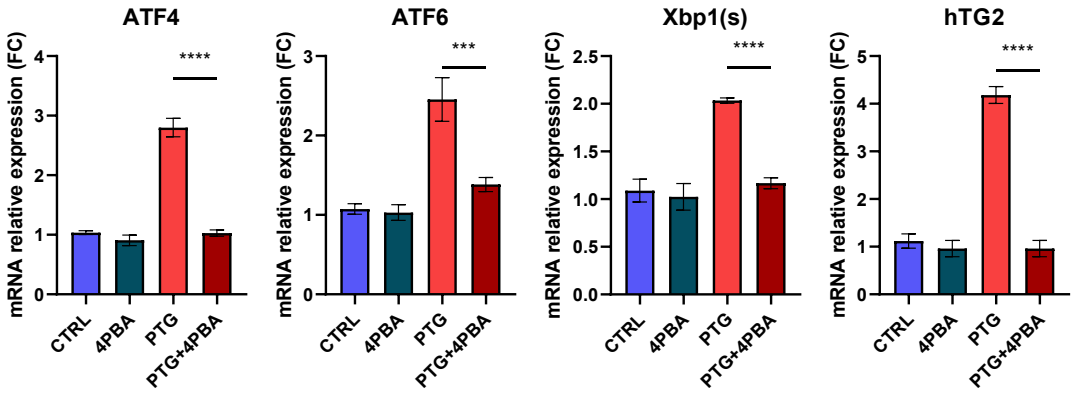

Figure 19: *CaCo-2 were stimulated with PTG (1mg/mL) alone or in combination with 4PBA (5μM) for 9h or left untreated (CTRL), ER stress induction by PTG was evaluated through qPCR by the expression of ER stress markers ATF4, ATF6 and Xbp1(s). The expression of hTG2 was also evaluated in all tested conditions by qPCR. Histograms represent mean ± s.d.; *p<0,05, **p<0,01, ***p<0,001, ****p<0,0001.*

mimic the CD phenotype recapitulating important hallmarks of its pathogenesis, like hTG2 increased expression and loosening of cell junctions.

To confirm that the increased expression of ATF4, ATF6 and Xbp1(s) are a result of ER stress induced by PTG, we treated CaCo-2 cells with PTG as described above, alone or in **combination with 4-phenylbutyric acid (4PBA)** (5μM), a chemical chaperone able to inhibit ER stress. As shown in Figure 19, the administration of 4PBA together with PTG statistically significantly inhibited all UPR pathways, that otherwise have increased levels in response to PTG. Therefore, 4PBA was able to inhibit ER stress induced by PTG stimulation, as indicated by the expressions of ATF4, ATF6 and Xbp1(s) that are comparable to the control samples, confirming **the relationship between gliadin peptides and ER stress**.

Interestingly, **4PBA inhibited in a significant way also hTG2** expression in response to PTG, suggesting that its regulation depends not directly on gliadin peptides stimulation, but it's connected to the response to ER stress, otherwise even when inhibiting it we would have observed increased hTG2 expression levels.

.

4.2 ER stress activation by PTG in an *ex vivo* model of celiac disease

After observing UPR activation upon PTG stimulation in a cellular model, to confirm this result in a more complex and reliable model, in collaboration with Corazzar's research group at University of Eastern Piedmont, Novara (Italy) **small intestines from Balb/c mice cultivated in GEVS** have been used as an *ex vivo* CD animal model. With this model, UPR

activation and CD markers in response to PTG stimulation have been assessed, additionally, to investigate if CD markers expression is influenced directly by PTG or is upstream to ER stress induction, a stimulation with thapsigargin (TPSG), an ER stress inductor, has been done in parallel to PTG.

Small intestines from mice on GFD are cultivated in GEVS and treated with PTG (2,5mg/mL) or TPSG (5µg/mL) for 16h or left untreated. The expression levels of ATF4, ATF6 and Xbp1(s) as markers of UPR activation and TG2 and CLDN2 as CD markers are determined by qPCR upon RNA extraction and retrotranscription.

The data in Figure 20 shows a statistically significant increase in the expression of all three of the ER stress markers ATF4, ATF6 and Xbp1(s), and of the CD markers TG2 and CLDN2 when stimulated with PTG, in accordance with what was observed in the CaCo-2 cell line model. Therefore, **PTG can induce ER stress and the expression of CD markers in Balb/c mice**. Considering TPSG stimulation, there is ER stress induction and activation of the three UPR pathways as expected, but interestingly there is also a statistically significant increase in both TG2 and CLDN2 compared to the untreated sample. Since TPSG is a well-known specific ER stress activator, these results indicate that **TG2 and CLDN2 increased expression are a downstream consequence of ER stress and UPR**, which therefore

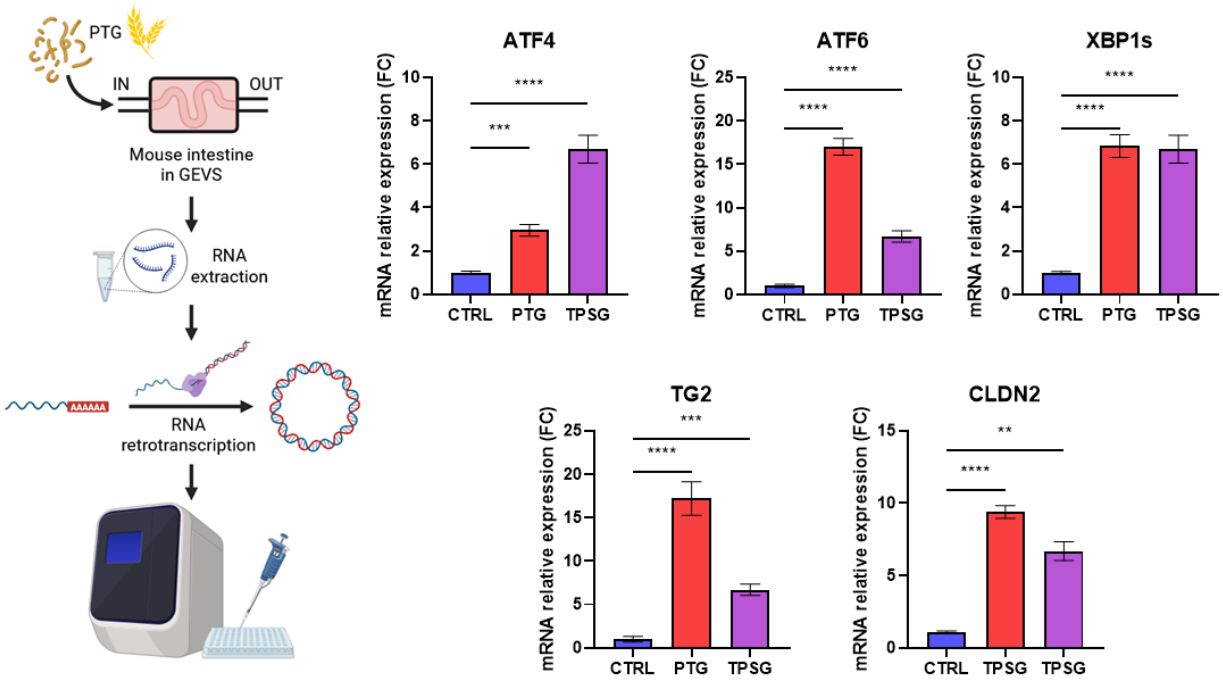

Figure 20: *gluten sensible mice's guts cultivated in GEVS were treated with PTG (2,5mg/mL), TPSG (5µg/mL) or left untreated (CTRL) for 16h. Gene expression of ER stress markers ATF4, aTF6 and Xbp1(s) in response to PTG stimulation was evaluated by qPCR; TPSG stimulation was used as a positive control for ER stress induction and to investigate if CD markers hTG2 and CLDN2 would increase as a consequence of it. Histograms represent mean ± s.d.; *p<0,05, **p<0,01, ***p<0,001, ****p<0,0001.*

could be considered a possible novel mechanism involved in CD pathogenesis, contributing to intestinal epithelial damage and increased levels of TG2 and its active form, as well as interfering with intestinal permeability.

To confirm these results, as done for CaCo-2 cells experiments, we also treated small intestines from Balb/c mice with PTG and TG both alone or in combination with **4PBA** (3µM) or left untreated for 16h. The results in figure 21 show a statistically significant inhibition of all UPR pathways when 4PBA is given with TPSG, as expected, but also with PTG, confirming that ATF4, ATF6 and Xbp1(s) increased expressions observed with PTG stimulation depend on the induction of ER stress by it. A similar inhibition is present for TG2 and CLDN2 expressions when treated with 4PBA and PTG or TPSG: since inhibiting ER stress keeps TG2 and CLDN2 levels like those of the control samples, we confirm that **TG2 and CLDN2 increased expressions** observed with the TPSG and PTG treatments are a **consequence of the induction of ER stress**.

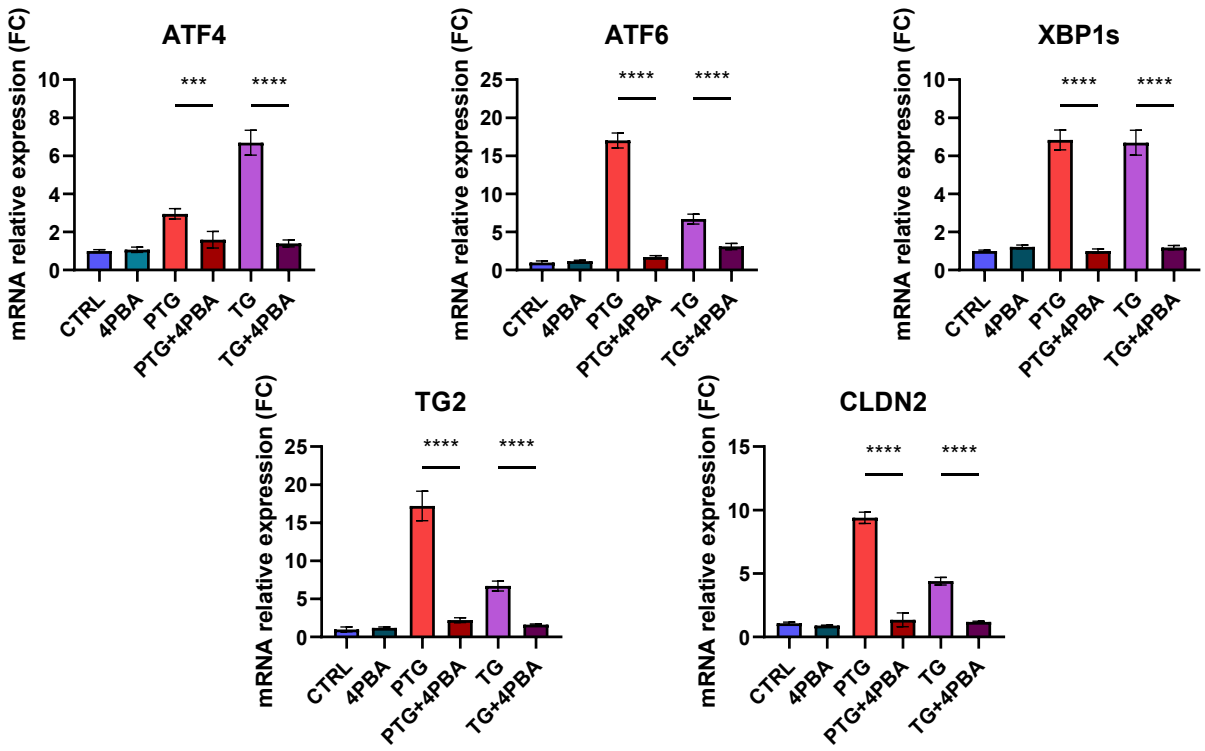

Figure 21: *gluten sensible mice's guts cultivated in GEVS were treated with PTG (2,5mg/mL), TPSG (5µg/mL) alone or in combination with 4PBA (3µM) or left untreated (CTRL) for 16h. Gene expression of ER stress markers ATF4, aTF6 and Xbp1(s) in response to PTG stimulation was evaluated by qPCR; TPSG stimulation was used as a positive control for ER stress induction and to investigate if CD markers hTG2 and CLDN2 would increase as a consequence of it, while 4PBA was used to inhibit ER stress and confirm that the increased expressions observed depend on it. Histograms represent mean ± s.d.; *p<0,05, **p<0,01, ***p<0,001, ****p<0,0001.*

4.3 ER stress activation in patients' biopsies

After the results in the cellular and animal model showed ER stress activation upon PTG stimulation, this hypothesis was investigated in the human organism, to check if there is any evidence of the involvement of ER stress in CD patients. To do so, **duodenal intestinal biopsies from pediatric patients** (<18 years) enrolled at Maggiore della Carità University Hospital (Novara, Italy) have been used: the biopsies have been taken via upper gastrointestinal endoscopy from 8 control patients affected by other intestinal pathologies not correlated with CD and 9 CD patients.

RNA is extracted from the biopsies, retrotranscribed and analyzed with qPCR to check the expression of CD markers hTG2 and CLDN2 and ER stress markers ATF4, ATF6 and Xbp1(s).

From the data in Figure 22, there is a statistically significant **increase in CD patients of hTG2 as expected and of CLDN2**, showing increased intestinal permeability typical of active CD. There is also a statistically significant increase in CD patients of all three of the ER stress markers compared to control patients. This confirms the **presence of ER stress in the intestinal tissues of CD patients with an ongoing CD**, contributing with its signaling to damaging intestinal tissue. Moreover, the presence of ER stress in CD patients could be

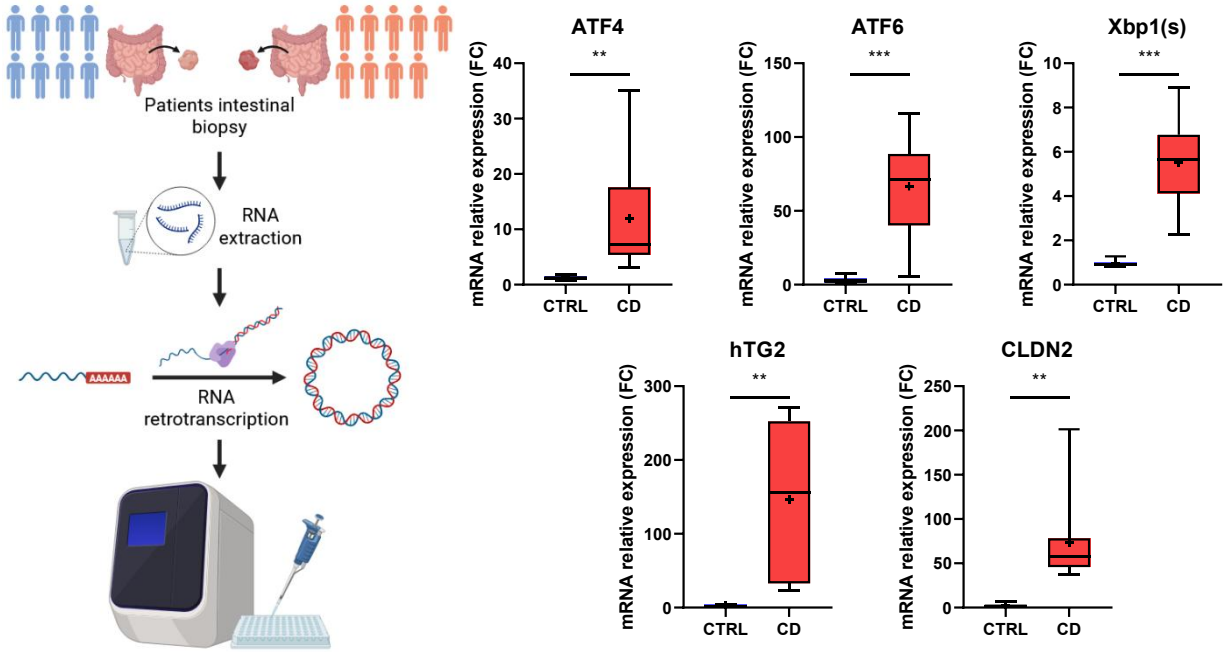

Figure 22: *intestinal biopsies from 8 control patients (CTRL) and 9 CD patients were collected and analyzed by qPCR to evaluate the level of ER stress through ER stress markers ATF4, ATF6 and Xbp1(s). CD markers hTG2 and CLDN2 was also evaluated as a confirmatory data. Box plots represent 25th and 75th percentile with minimum and maximum values, line shows median while + shows mean; *p<0,05, **p<0,01, ***p<0,001, ****p<0,0001.*

used as an additional marker for CD diagnosis, especially in patients with an uncertain diagnosis after serological testing.

4.4 Organoids development

To study more precisely how ER stress is involved in CD there is the need for a model as close as possible to the human organism and the pathological conditions of CD; for this reason, we developed a **patient's derived organoid model generated from duodenal intestinal biopsies**. This has several advantages compared to the CaCo-2 cellular model and the gluten sensitive mouse model, being a human model with duodenal intestinal epithelial cells and other cell types found in the intestinal epithelium; moreover, working *in vitro*, it is easier to manipulate and to regulate direct stimulations and timing.

4.4.1 Enrolled patients' characteristics

CD pediatric patients and control patients have been enrolled at IRCCS Burlo Garofolo Pediatric Institute in Trieste (IT) for the generation of organoids from duodenal intestinal biopsies; control patients are children affected by gastrointestinal pathologies non correlated to CD. Through gastroendoscopy, **duodenal biopsies** are collected from the patients to be analyzed and two or three biopsies of these are used for the isolation of the intestinal crypts and patients derived organoids generation.

A total of 54 organoid cultures from different patients have been generated and used to set up our patient derived organoid model; among these, in Table 7 are reported the data from the **7 control patients and 6 CD patients** which organoid cultures have been specifically used to verify ER stress activation in response to PTG stimulation. The data shown are:

- **Gender**. There is a prevalence of male patients in the control group and an equal representation in the CD group.
- **Age**. The mean age of control patients is close to the one of CD patients and it is near the middle of the pediatric age range (0-18 years), with the youngest patients being 4,5 and 6 years old while the oldest being 16 and 18 years old.
- The **final diagnosis** for both control and CD patients after laboratory analysis.
- **IgA αTG2 titer and its cut-off**. A titer under the 7 U/mL is not considered at risk for a possible CD diagnosis and as expected, the mean titer for control patients is 2 U/mL since all, expect one who lacks other symptoms of CD, have negative or low IgA

αTG2 titer. On the other hand, CD mean titer is 15 U/mL, with all patients showing high antibody titer except for two patients, one of which is diagnosed as seronegative CD.

- **Presence of αEMA antibodies**. All control patients are negative for this antibody while all CD patients are positive, except for the one who is diagnosed as seronegative CD.
- **HLA typing**. While all CD patients carry either the HLA-DQ2 or DQ8 variant as expected, these variants are found in most of the control patients, with only one carrying the HLA-DQ7/DR5 variant.
- **Classification of the collected biopsies**, if available, for the pathology. Interestingly, all CD patients presented with a grade M3 intestinal damage at least on the Marsh-Oberhuber scale, having villous atrophy, crypts hyperplasia and IELs increased counts, confirming the CD diagnosis for all CD patients.

Samples ID	Gender	Age	Disease		Laboratory results					
			Diagnosis Final, General cathegory	Diagnosis, Final, specific cathegory	IgA Anti-TG2 Ab value (IgG for IgA deficiency)	IgA Anti-TG2 Ab Unit of measure	IgA Anti-TG2 Ab cut-off	EMA 1=positive; 0=negative; .=unknown	HLA	Classification Celiac=Marsh, IBD=Paris EGID: 1=positive, 0=remission(EOS/HPF) Other: 0=normal/1=abnormal
2321	M	18	EGID	EC	2	U/ml	<7	0	DQ2	1
2482	M	6	Other	Gastro-esophageal Reflux	neg	U/ml	<7	0	DQ2	-
2627	M	12	Other	Functional Abdominal Pain	0,1	U/ml	<7	0	DQ7DR5	M1
2644	F	18	Other	Cycling Vomiting Syndrome	0,7	U/ml	<7	0	DQ2	0
2672	M	13	IBD	Chron Disease	6,1	U/ml	<7	0	DQ2	-
2674	M	12	Other	Abdominal pain	0,3	U/ml	<7	0	DQ2	0
2678	M	13	EGID	EE	0	U/ml	<7	0	DQ2	1
MEAN		13			2	U/ml	<7			
2680	F	9	Celiac	Seronegative	6	U/ml	<7	0	DQ8	M3b;M3c
2390	M	4	Celiac	Classical	25	U/ml	<7	1	DQ2	M3b
2396	F	11	Celiac	Classical	13	U/mL	<7	1	DQ2	M3c
2452	M	5	Celiac	Classical	26	U/ml	<7	1	DQ2/DQ8	M3b
2531	F	16	Celiac	Classical	15	U/ml	<7	1	DQ2	M3
2594	M	9	Celiac	Classical	5,8	U/ml	<7	1	DQ2	M3a
MEAN		9			15	U/ml	<7			

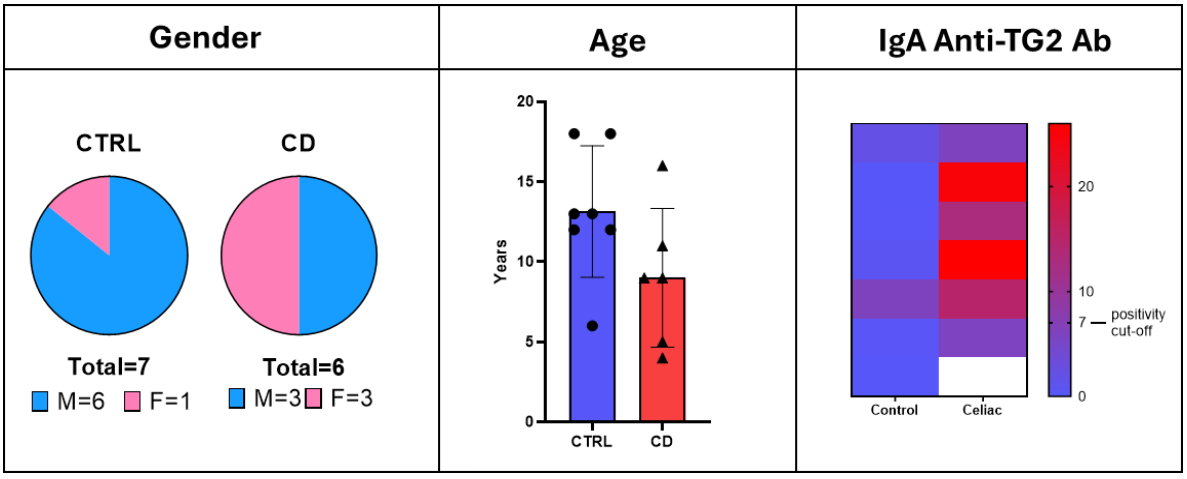

Table 7: *general characteristics and diagnostic information from 7 control patients and 6 CD patients. Here are collected gender and age of all patients and the final diagnosis of each patient after serological testing, genotyping and biopsy analysis with their respective results.*

4.4.2 Organoids culture establishment

In literature, organoids generation starts with stem cells that can be either adult stem cells (ASCs) if present in the tissue of interest, or pluripotent stem cells (PSCs), both embryonal and induced through a complex de-differentiation process. For the generation of intestinal organoids, stem cells in the intestinal crypts, characterized by the expression of LGR5, can be used. After their isolation, they are seeded in matrigel with the necessary growth factors where they generate intestinal epithelial organoids. If iPSCs were used, intestinal organoids with epithelial and mesenchymal components could be obtained, but the process of doing so is more complex and time consuming, therefore in this project we decide to use **intestinal crypts and their stem cells obtained from duodenal biopsies to generate organoids**.

4.4.2.1 Intestinal crypts isolation

The **isolation protocol** (represented in Figure 23) starts with incubating the duodenal biopsies with antibiotics and antifungal to clean the tissue from microorganisms found in the intestine, and trypsin and EDTA to loosen intercellular connections between epithelial cells: then, intestinal crypts are collected with a series of mechanical agitations and centrifuges. Once isolated, they are included in matrigel drops (Figure 24) and grown in staminal medium containing growth factors to maintain the stemness of organoids. The factors we decide to use for this purpose are:

- **Wnt**: its signaling pathway is present in the intestinal crypt and maintains the stemness of the resident stem cells and promotes their proliferation.
- **Nicotinamide (NICO):** it supports the survival and long-term expansion of intestinal stem cells by inhibiting certain kinases like Rho-associated coiled protein kinase (ROCK), which prevents cell death.
- **SB202190**: it inhibits p38, suppressing secretory cell differentiation and by doing so, it prevents intestinal stem cells from differentiating into them.
- **R-spondin 1 (R-SPO1):** it is an agonist of LGR5, enhancing its signaling which consequently potentiate Wnt pathway [122], [123].
- **Prostaglandin E2 (PG-E2):** it acts as an activator of Wnt signaling, helping to maintain stemness.

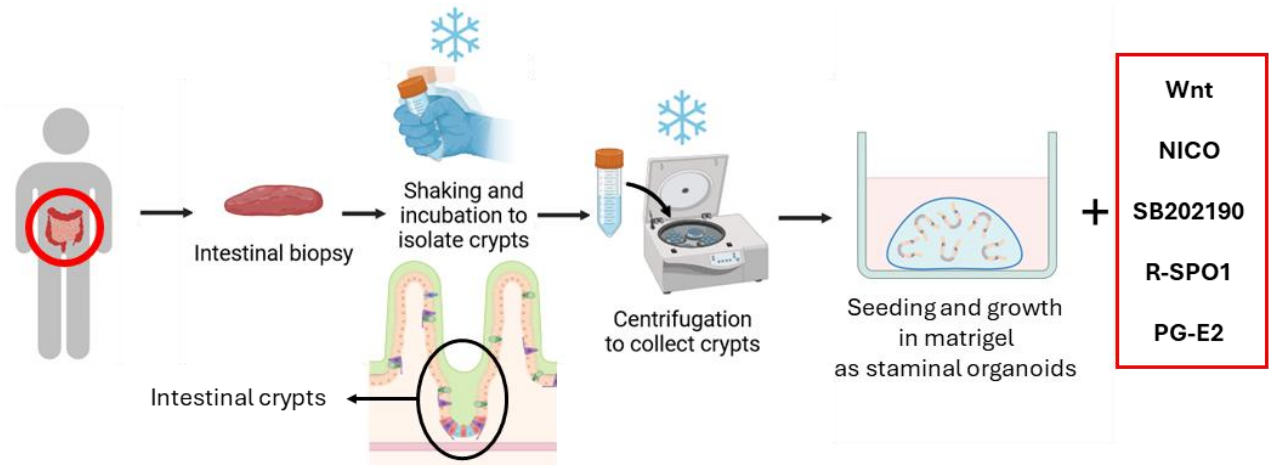

Figure 23: *schematic organoid generation protocol from intestinal biopsies with most important steps and staminal factor added to the medium to maintain stemness (Wnt, Nicotinamide (NICO), SB202190, R-spondin 1 (R-SPO1), prostaglandin-E2 (PG-E2)).*

The isolated crypts, like the ones in Figure 24, generally maintain their **U structure** after the isolation protocol, even if some of them can break, opening due to the mechanical agitation during the process, though this doesn't reduce their organoid generation capacity: after approximately 1 week of culturing in staminal medium, intestinal crypts generates staminal organoids that can be expanded through organoids passage.

On the background, several debris are present, being included in matrigel with the crypts: these debris come from the mechanical agitation of the biopsies, being collected during the centrifuges to pull down crypts and then included in matrigel with them. These debris don't interfere with organoid generation and aren't a potential risk for contamination since the biopsies have already been treated with antibiotics; debris will be progressively eliminated during the following passages to expand the organoid culture.

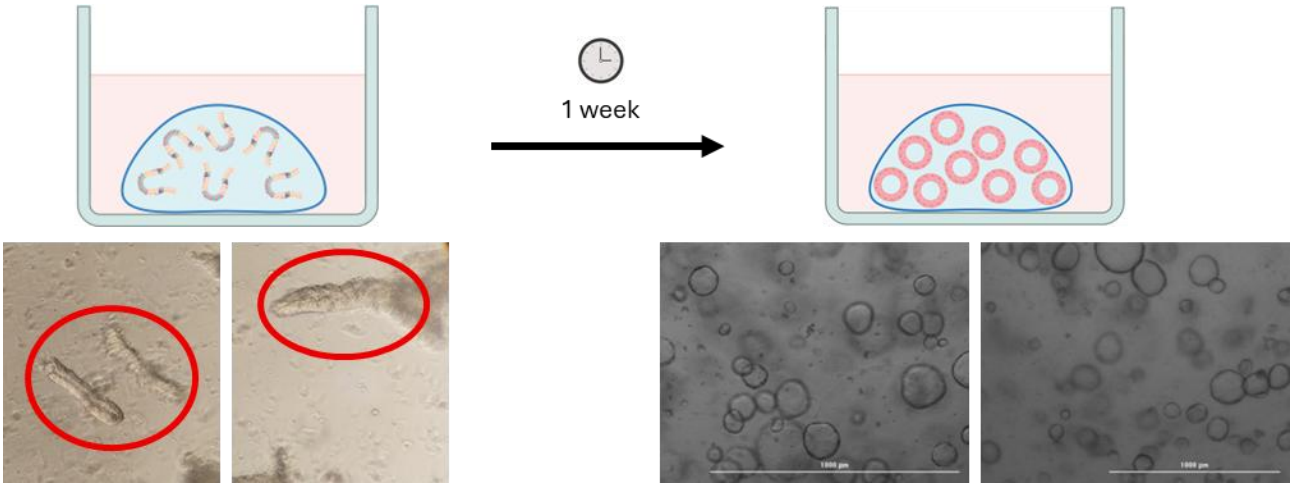

Figure24: *isolated intestinal crypts from duodenal biopsies seeded in matrigel (circled in red) generate new organoids after approximately 1 week of culturing in staminal medium. Organoids images taken with optical microscope (magnification 2,5X, scale bar 1000µm).*

The **organoids obtained are patient-specific** and are maintained **in staminal condition** to allow their culturing and expansion. Staminal organoid cultures are shown in Figure 24 after 6/7 days from the inclusion of crypts in matrigel: intestinal stem cells have proliferated organizing in **spheric structures** of different dimensions and with a **hollow inside**. When organoids in a single matrigel drop reach confluence, that should be interpreted as "crowding" of the matrigel due to an increase in organoids dimension and number, they are passed with a protocol similar to cellular passage, with which organoids are expanded and matrigel is changed to avoid it losing its properties as an ECM substitute, indeed organoid passage is done after 14 days of culturing at maximum to change matrigel.

4.4.2.2 Organoids passage

Organoid passage protocol (represented in Figure 25) starts with the isolation of the organoids from matrigel, which is dissolved and diluted during a washing step; then organoids are broken down into single cells thanks to an incubation with a trypsin and EDTA solution to loosen intercellular connection and pipetting, obtaining a single cell solution that is composed mainly of intestinal stem cells. These are included in matrigel drops and cultured in staminal medium, forming new organoids (Figure 26): when stem cells are plated after organoid passage, we added Y27632, an inhibitor of ROCK, to the matrigel and culture medium to prevent cell death by loss of contact.

During our experiments, we kept track of each time every organoid culture from different patients was passed until we couldn't expand that specific organoid culture anymore or at a maximum of the 30th passage. By doing so, we can have a record of the survival rate of our organoid cultures, obtaining the graph shown in Figure 27: **50% of our organoid cultures reached the 12th passage**, while 25% was able to reach the 20th passage and only 9% was

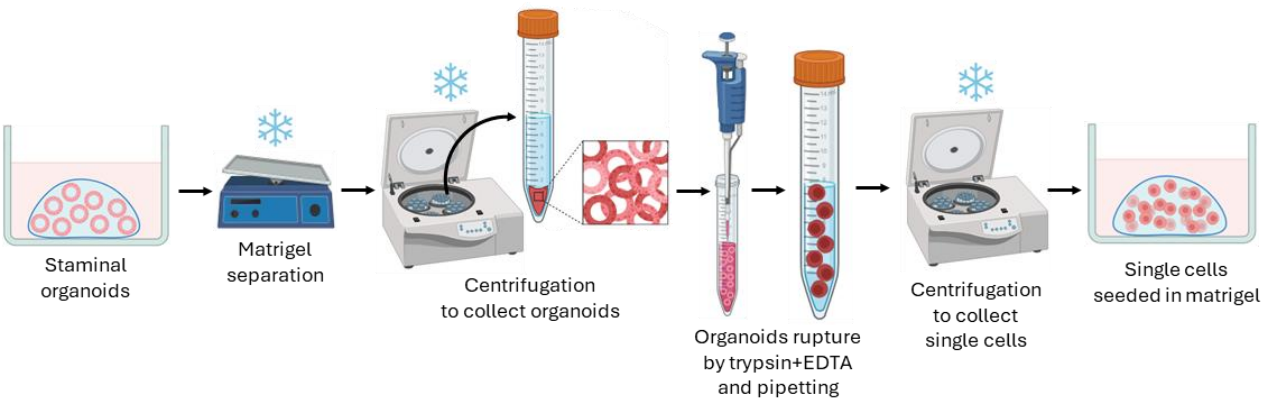

Figure 25: *schematic representation of organoid passage protocol for organoids expansion with most important steps for breaking down organoids and obtain single staminal cells.*

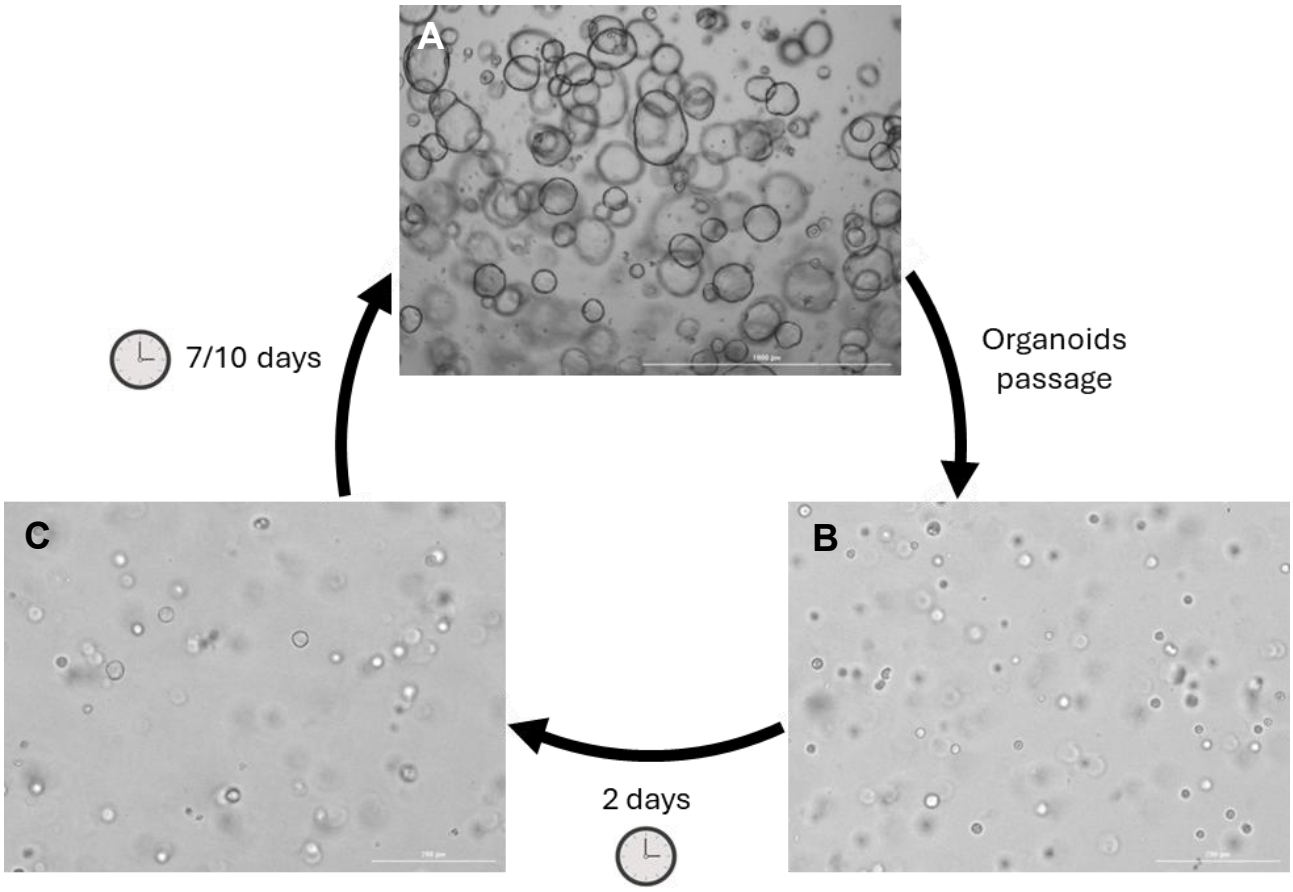

Figure 26: *organoids expansion cycle.* ***A)*** *Staminal organoids culture at confluency are ready to be expanded through organoids passage.* ***B)*** *After organoids passage, the obtained single staminal cells are included in matrigel and growth in staminal medium.* ***C)*** *After a couple of days, single cells have replicated forming new organoids that will grow throughout the days till reaching confluency again in 7/10 days. Images taken with optical microscope (magnification 2,5X, scale bar 1000µm for Figure 26A; magnification 10X, scale bar 200µm for Figures 26B-C).*

expanded till the 30th passage. Most of our organoid culture was expanded up to the 8th/9th passage, after which we observed an initial wave of extensive death in our organoid cultures at the 10th passage, followed by a gradual decline in mortality until the 24th passage, after which a second wave of cell death occurred among the few remaining viable organoids.

There is **high variability in the viability** of the different cultures, which is independent from the passage protocol being standardized throughout all organoid passages, and we suppose it depends on the patient of origin, since they retain their genetic background. Other external factors may have an impact on the stress sustained by the cells during passage, like environmental conditions and user-dependent variability during organoid breakdown with trypsin and EDTA solution, which is the most delicate step.

However, the ability to expand our organoid cultures for several times after their generation was sufficient to have enough organoids to carry out our experiments.

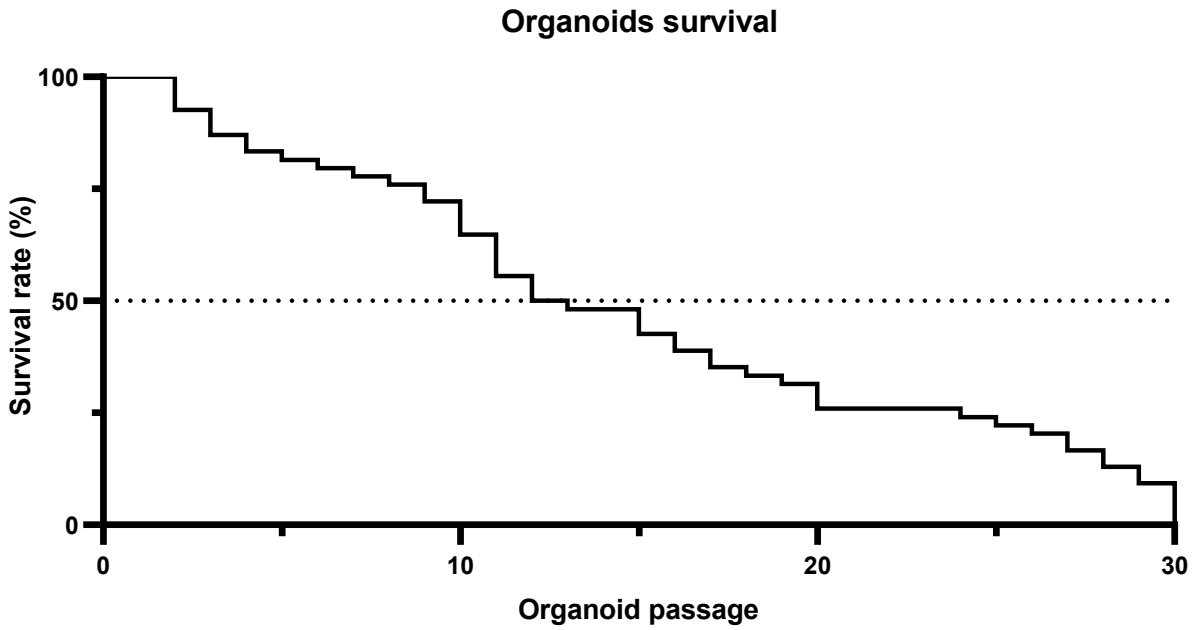

Figure 27: *each time an organoid culture is passed has been recorded until we couldn't expand it anymore or till the 30th passage. The last passage reached by each organoid culture was used to obtain our data on their viability, counting how many organoid cultures reached each passage number.*

4.4.3 Organoids characterization

Intestinal staminal organoids included in matrigel (Figure 28A-B-C) organize themself as a **hollow sphere, with an outer dark border** visible at the optical microscope corresponding to a layer of mostly intestinal stem cells. This 3D closed structure is formed thanks to the support given by matrigel, acting as a substitute for the extracellular matrix. Organoids appear transparent when they are alive, while when they die, they become opaque and dark as shown in the background of Figure 28C; this happens more frequently after long culturing periods and when the matrigel is highly crowded with organoids, so especially before organoids passage. Little debris can be spotted inside the matrigel drop together with the organoids; usually these are single cells or little organoids fragments from previous passage's dissociation that weren't able to generate a new organoid since, even if most cells in a staminal organoid are stem cells, some don't maintain their stemness and can't proliferate.

Staining staminal organoids with hematoxylin and eosin (Figure 28D-E-F) we confirm their spheric architecture with cells organized in an external border and a hollow inside: moreover, we can appreciate that this **border is mainly composed of a single cell layer**, as seen by the visible purple nuclei.

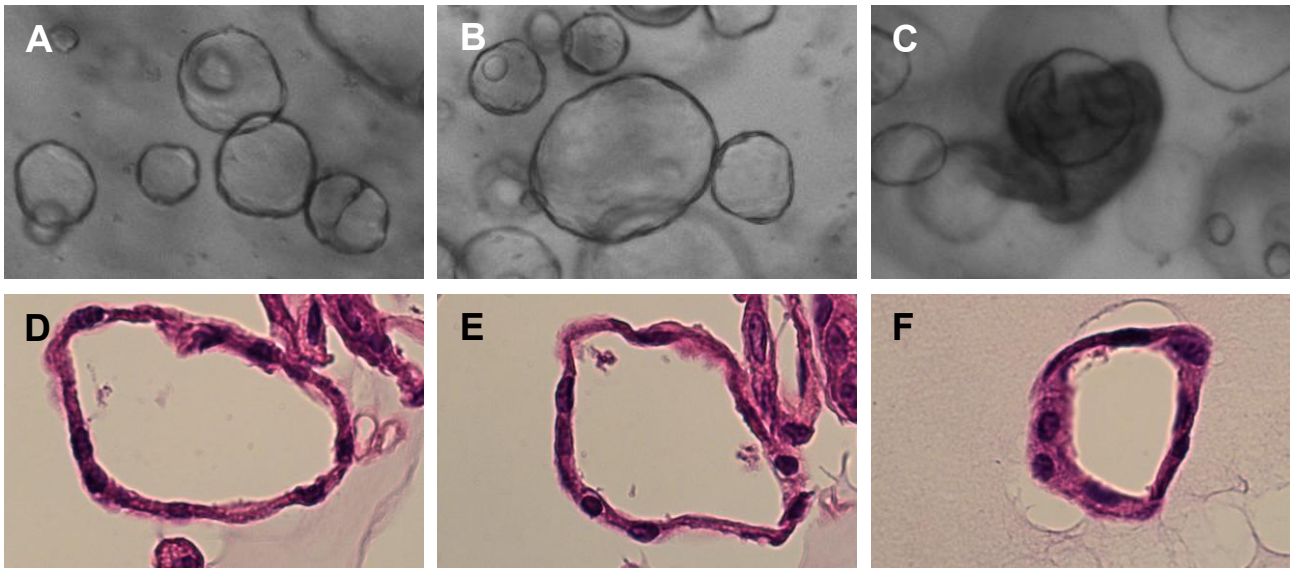

Figure 28: *staminal organoids.* ***A-B-C)*** *Staminal organoids embedded in matrigel appear as transparent spheres with a hollow inside and a dark outer border. On the background of Figure 28C there is a dead organoid, that appears opaque and dark. Images taken with optical microscope (magnification 2,5X).* ***D-E-F)*** *Staminal organoids stained with hematoxylin and eosin show the same spheric structure with a hollow inside; the nuclei coloration in purple highlights that the cell border of the organoids is composed of a single cell layer. Images taken with optical microscope (magnification 40X).*

4.4.3.1 General characteristics

Observing organoids from a single culture, they have different dimensions and constitute a **heterogeneous population**: all have the same architecture but in the same matrigel there is a big gap between the smallest and the biggest organoids observable. To evaluate more in depth this characteristic, we have taken images of six different organoids cultures after 7 days from their last passage (Figure 29A-B-C-D-E-F), and with ImageJ we measured the diameter of every organoid identifiable in the matrigel drops; then, all the measurements collected have been analyzed with Prism for **frequency distribution of the diameter**.

From this analysis we obtain an average **mean diameter of 134,7 ± 70,4µm** from the data of all the organoids cultures and the graph of the diameter average frequency distribution is shown in Figure 29G: the values have a wide range, spanning from the smallest diameter measured of 14,7µm to the biggest one of 520,574µm. The 25% percentile is at 82,4µm and the 75% percentile is at 175,7µm, therefore half of our measured organoids are enclosed between these values. Moreover, looking at the 75% percentile, the diameters over this value are spread in a wider range than th\e ones below the 25% percentile, meaning that, considering the maximum and minimum diameters measured, **organoids tend to grow to a size closer to small organoids** than to larger ones, indeed very big organoids, although being easily spotted, are rarer than the small ones. A possible reason for the formation of these big organoids could be the fusion of two or more small organoids short after organoid

passage, or the proximity of multiple stem cells in matrigel that forms an organoid with a higher replication rate.

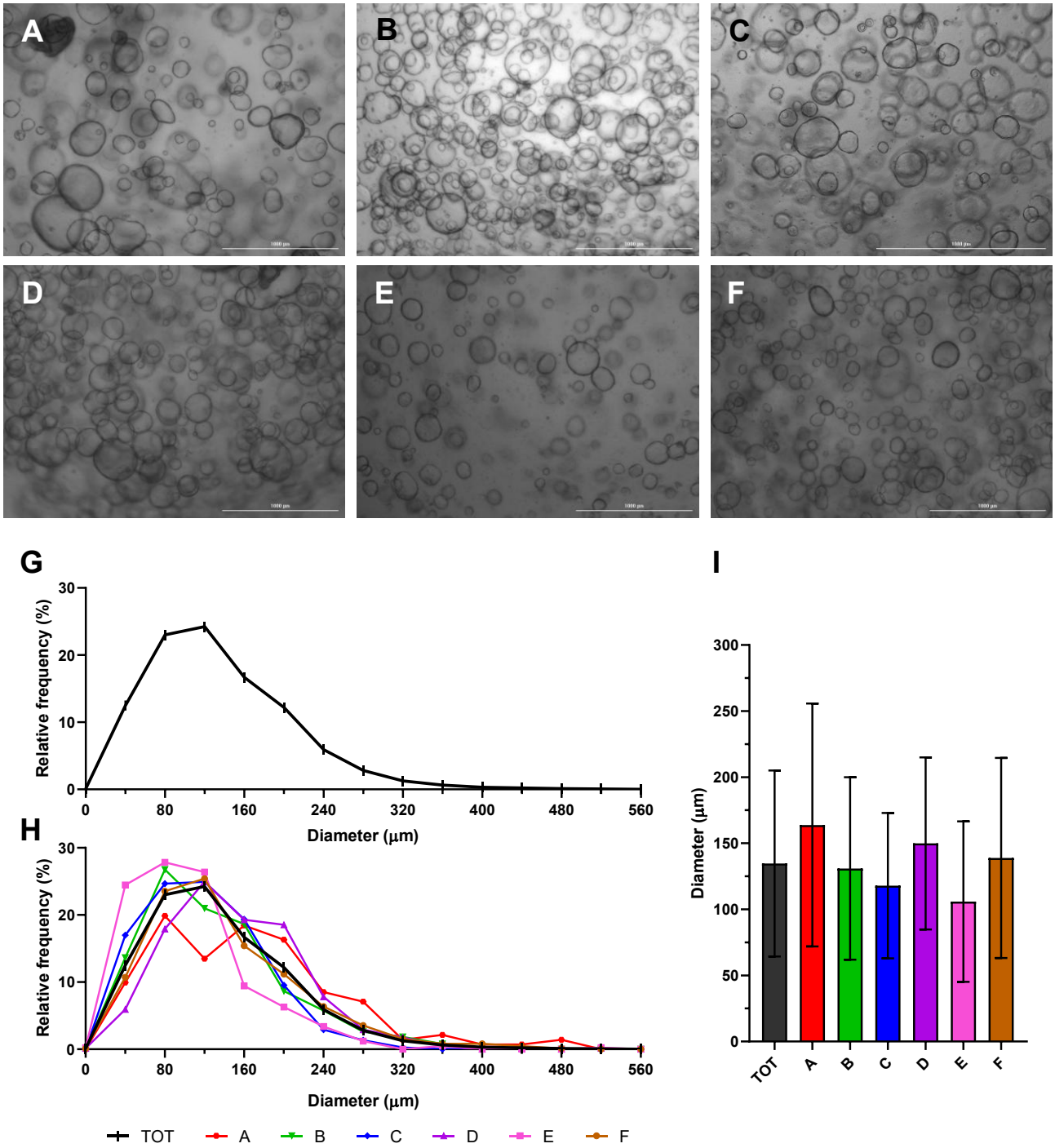

***Figure 29**: organoids diameter frequency distribution. **A-B-C-D-E-F)** Staminal organoids embedded in matrigel from different organoid cultures generated from different patients; each organoid culture is identified by the letter of its respective image. Imagen taken with optical microscope (magnification 2,5X, scale bar 1000µm). **G)** Diameter average frequency distribution of all organoids with bin center set at 40: diameter frequency is measured with the percentage of values enclosed in intervals of 40µm starting from 0. **H)** Diameter frequency distribution for each organoid culture (A, B, C, D, E and F) compared to the diameter average frequency distribution (TOT). **I)** Histogram with the mean diameter value for each organoid culture (A, B, C, D, E and F) compared to the average mean diameter (TOT). Histogram represent mean ± s.d.*

With our data on organoids diameter, we also tried to analyze the **frequency distribution dividing our measurements for the organoid cultures**, i.e. for the patient of origin, to see if the genetic background has an influence on the size of the organoids. For each organoid culture we analyzed the respective data for frequency distribution with a bin center of 40, like done previously for all our data, and obtained a graph for each one of them (Figure 29H), that were compared to the average frequency distribution (shown previously in Figure29G and reported in Figure 29H as TOT). From this comparison, there is no overall difference between single organoid cultures and the average one, observing only little deviations. However, some organoid cultures, namely A in red and E in pink, diverted more prominently from the average frequency distribution, with distinct curve peaks; we then plotted the mean ± s.d. values for each organoid culture (Figure 29I) and here we confirm that organoid cultures A and E have respectively the highest (163,8±91,9µm)and lowest (105,9±60,7µm) mean values.

So, although it is possible that the **genetic background** of the patient of origin influences the size of the organoids generated, given the distinct frequency distribution of organoid culture A and E, overall, it **does not affect heavily organoids size**, which therefore depends on the culturing condition.

4.4.4 Organoids inversion and differentiation protocols

In the human organism, ingested food is mainly digested in the stomach and the intestine, where it is broken down in its components and nutrients are absorbed: in the gut, the main protagonist of this process are enterocytes which turn their apical surface with microvilli towards the intestinal lumen to interact and absorb food components.

On the contrary, staminal organoids embedded in matrigel are polarized thanks to the support given by matrigel assuming the role of the extracellular matrix, and with which, for this reason, they interact through their basal side, while the apical side is facing the inner cavity, ideally corresponding to the intestinal lumen: therefore, these organoids are called basal-out. Because of their organization and cellular composition, **basal-out staminal organoids** can’t be used to mimic the interaction of gluten peptides with the apical side of differentiated intestinal epithelial cells, and they need to be turned inside out, to expose the apical side of their cells, and differentiate.

4.4.4.1 Organoid inversion protocol

To **expose the apical side** of organoids' cells, according to the literature, there are two approaches:

- **Rupture of the organoids** and plating of single cells on a permeable membrane inside wells, allowing cells to polarize and forming a 2D layer with the apical side facing up.
- **Spontaneously invert the organoids** by separating them from the support given by matrigel and growing them in suspension. Doing so they invert their polarity, exposing out the apical side and obtaining apical-out organoids.

We decided to use the second approach since it is easier and quicker than the first one and it only involves separating the organoids from matrigel that is washed away, then the collected organoids are resuspended in growth medium and after culturing for 24h they have spontaneously inverted their polarity (Figure 30A).

An **apical-out organoid** is shown in Figure 30B: after the inversion protocol, it keeps its spheric form, with a dark border and transparent interior. Unlike basal-out organoids, the inner cavity is no longer visible, and the cell layer appears thicker. The inversion protocol is a delicate procedure, while small organoids tend to remain intact, bigger ones easily rupture due to pipetting and centrifugation performed during the process; indeed, together with the apical-out organoids are visible on the background small debris and organoids fragments.

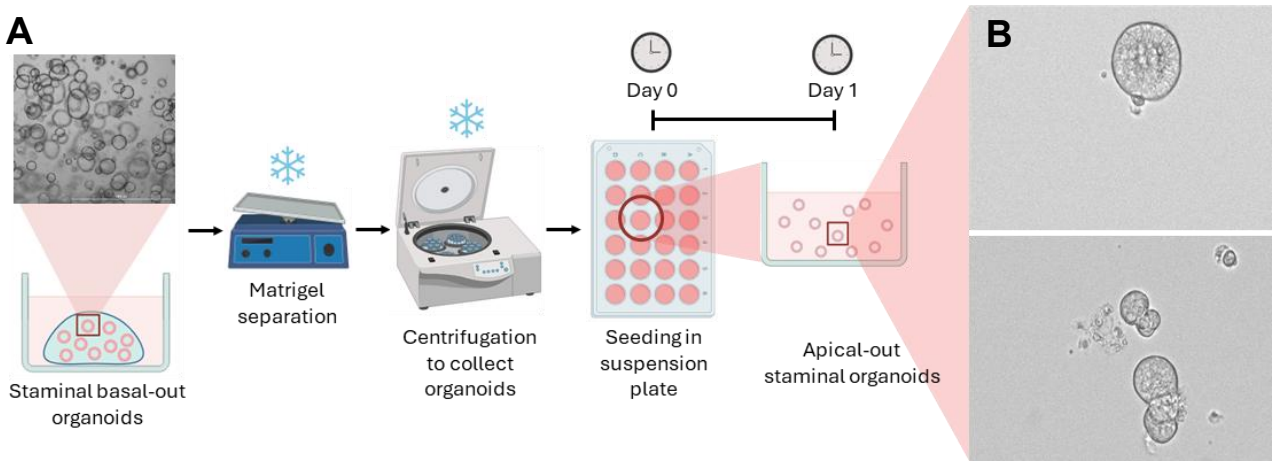

Figure 30: *organoids inversion.* ***A)*** *Schematic organoids inversion protocol with the most important steps to invert the polarity of basal-out organoids embedded in matrigel.* ***B)*** *Apical-out staminal organoids in a suspension plate after 24h from being inverted; images taken with optical microscope (magnification 10X, scale bar 200µm).*

4.4.4.2 Organoid differentiation protocol

Apical-out organoids are still composed mostly of intestinal stem cells, so there is the need to differentiate them obtaining organoids made for the most part by enterocytes, mimicking the intestinal tissue composition.

The **differentiation process** is performed by growing them in a differentiation medium and last 5 days: we prepared this medium by removing all the staminal factors we previously included in the preparation of the staminal medium for intestinal organoids (Wnt, NICO, SB202190, and PG-E2), and after 4 days of culturing another differentiation medium without R-SPO1 is used for organoid culturing, to completely shut down LGR5 signaling and therefore also Wnt signaling and stemness maintenance. On day 5 organoids are fully differentiated and can be kept in culture in this last medium usually for up to 14 days, because having lost their stem cell component they can't proliferate anymore and will eventually die. This differentiation protocol, represented in Figure 31A, differentiates especially enterocytes having decided to focus more on this cell type which constitutes most of the intestinal epithelium, we decide to exclude factors important for the differentiation of other cell types like Paneth cells that need N-[N-(3,5-difluorophenacetyl)-l-alanyl]-s-phenylglycinet-butylester (DAPT), an inhibitor of secretases and of Notch pathway [124].

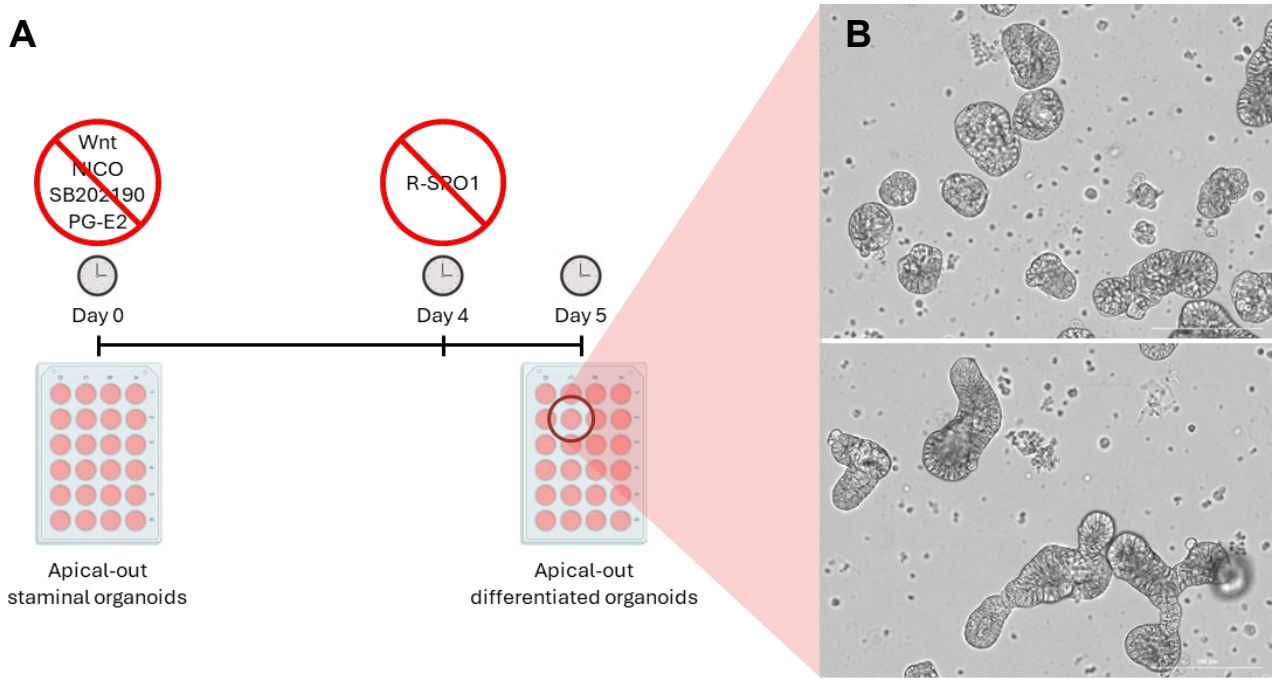

Figure 31: *organoids differentiation.* ***A)*** *Schematic organoids differentiation protocol, staminal factors removed during medium preparation are listed above the corresponding timepoint when they are removed.* ***B)*** *Apical-out differentiated organoids after the 5th day of differentiation, staminal organoids were inverted and then differentiated by changing the medium from the staminal to the differentiated one; images taken with optical microscopy (magnification 10X, scale bar 200μm).*

Differentiated apical-out organoids (Figure 31B) appear darker and more deformed compared to staminal organoids; despite keeping some sort of spherical structure in general, there is a variety of forms across the population, especially in bigger organoids which assume completely different 3D structure, maybe trying to organize a villous/crypt architecture. Even in differentiated apical-out organoids an internal cavity can't be identified.

4.4.5 Organoid differentiation verification

Staining differentiated organoids with hematoxylin and eosin (Figure 32D-E-F) and confronting them with staminal organoids (Figure 32A-B-C), we observed **phenotypical differences in their structure and cellular organization**, mainly elongated cells constituting a thicker organoid border compared to staminal organoids, which is constituted of more than one cell layer in some regions; furthermore, along the cell surface delimiting the internal cavity appears irregular with some formations that mimic structures similar to intestinal villi.

So, to verify that our differentiation protocol is effectively differentiating staminal intestinal cells into the different intestinal cell types we initially performed a **principal component analysis (PCA)** confronting staminal organoids with their respective differentiated counterparts to evaluate how far apart they are from a transcriptional point of view.

Then, through **gene expression analysis** we investigated the expression levels of the **differentiation markers** for the different intestinal cell types in the staminal and differentiated samples, confirming our bioinformatics analysis with **qPCR**.

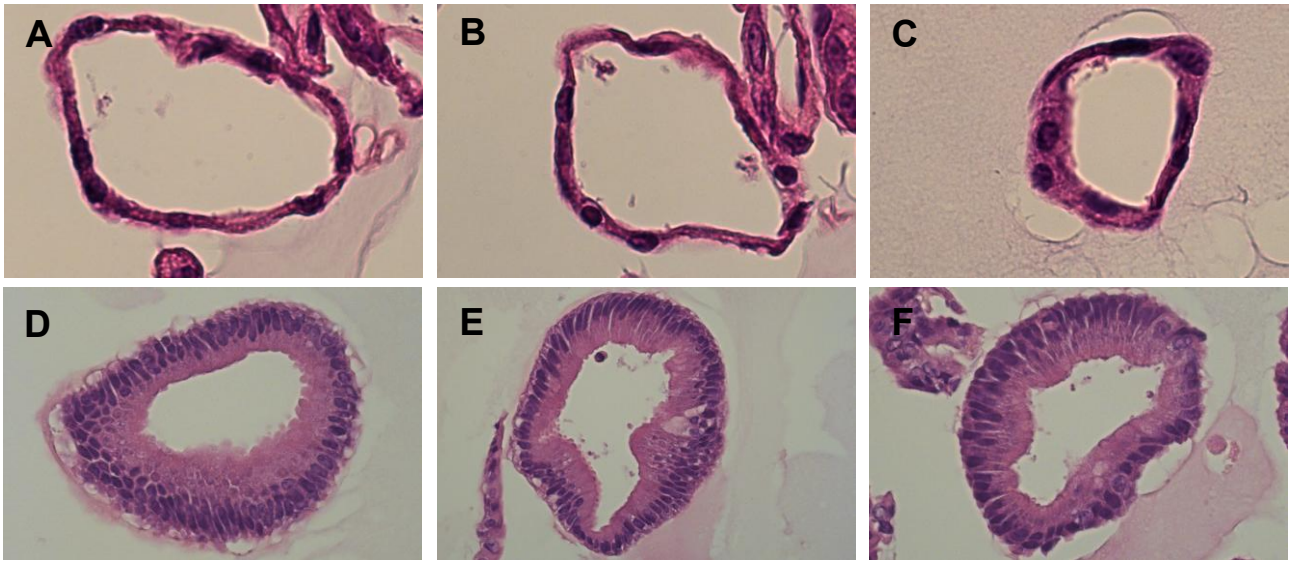

***Figure 32: h**ematoxylin and eosin staining of organoids **A-B-C)** Hematoxylin and eosin staining of basal-out staminal organoids **D-E-F)** Hematoxylin and eosin staining of basal-out differentiated organoids. Images taken with optical microscope (magnification 40X).*

4.4.5.1 PCA of staminal and differentiated organoids

We performed a principal component analysis (PCA) to verify staminal organoids differentiation: a PCA is a statistical technique that analyses different samples and all their associated data in different combinations, each of one is unique and express how much variance there is among samples: the two combinations of data resulting in the highest variance are PC1 and PC2, that can be used to graph the analyzed samples based on the highest variances among them.

To do this analysis, we used organoids from 4 control and 3 CD patients, which have been generated and expanded. Then for each patient, a fraction of the staminal organoid is lysed to obtain the staminal sample, and another fraction is differentiated; at the end of the differentiation protocol, the differentiated organoids are lysed to obtain the differentiated sample. RNA is extracted and sequenced from each sample at Macrogen Inc. (Seoul, South Corea), then sequencing data are aligned to a reference human genome (Figure 33A). Lastly, gene reads are counted with the tool STAR.

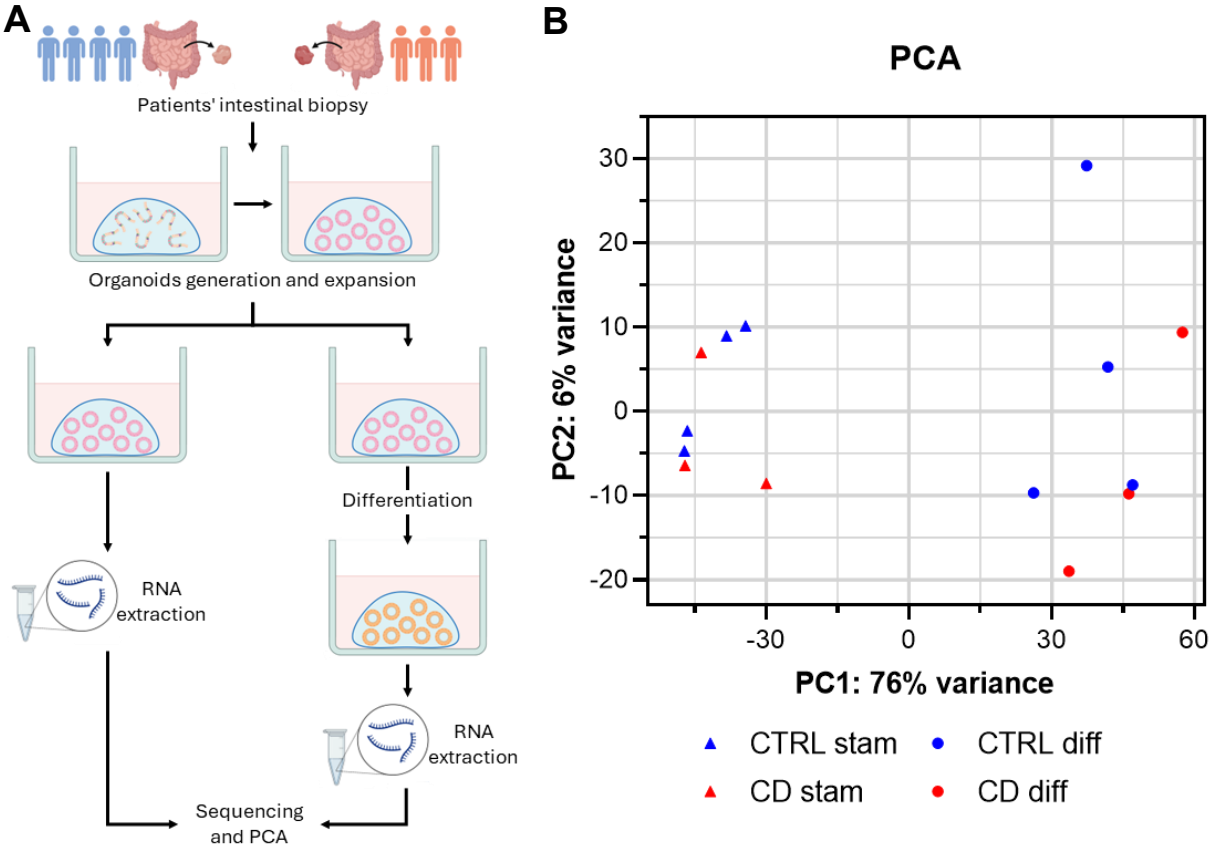

Figure 33: *Organoid differentiation verification by PCA.* ***A)*** *Schematic experimental workflow: organoids from 4 control patients (CTRL) and 3 CD patients were generated from intestinal biopsies; they were expanded, and then staminal organoids were collected obtaining the staminal sample, while a fraction of them were differentiated before being collected obtaining the differentiated sample. These were sequenced and sequencing used to perform PCA.* ***B)*** *PCA, plotting of PC1 variance and PC2 variance, to obtain a dispersion of the different samples based on the PCs with higher variances.*

Gene reads counts are used to do a PCA and with the PC1 and PC2 obtained the graph in Figure 33B is generated. PC1 represents a variance between samples of 76% and they are distributed along PC1 in two groups, on the left the staminal samples (represented by triangles) and on the right the differentiated ones (represented by circles); there is no clear separation between control and CD samples. PC2 on the other hand represents a lower variance of 6% and there is no evident separation between staminal and differentiated samples, or control and CD samples either.

Since PC1 and PC2 show the highest variance across PCs, and PC2 variance being so low, **most variability between samples is represented in PC1 where staminal organoids are clearly separated from differentiated ones**, making differentiation the most important factor in gene expression differences. Interestingly, there is no separation between control and celiac patients, this doesn't mean there are no differentially expressed genes between the two groups, but that patient's disease doesn't influence the overall expression profile of the organoids: this also means that independently from the belonging to one of the two groups, the organoids are generated and differentiated with the same efficiency and that the patient's disease does not show to heavily influence our protocols, which is really important to establish a solid and reproducible model on which to test different stimuli.

4.4.5.2 Gene expression analysis and qPCR of staminal and differentiated organoids

From PCA we confirmed high diversity between staminal and differentiated samples. Since the most impactful condition for this difference is the differentiation process, using the gene expression data collected, we can evaluate the **expression levels of genes involved in stemness and differentiation** using DeSeq2 software to analyze the data. Gene expression analysis results were then validated through qPCR.

The expression of the following genes has been checked:

- **LGR5**, as an intestinal stem cell marker.
- **Sucrase-isomaltase (SI)**, a marker of enterocytes.
- **Mucin-2 (MUC2)**, a marker for Goblet cells.
- **Lysozyme (LYZ)**, a marker for Paneth cells.
- **Chromogranin A (CHGA)**, as an enteroendocrine cells marker.

LGR5 is a marker of **intestinal stem cells**, being expressed specifically on their surface [125]: this is confirmed by gene expression analysis (Figure 34A) that shows a higher statically significant expression of LGR5 in the staminal samples compared to the differentiated ones, confirming the stemness of the staminal organoids and the loss of it after differentiation, explaining also why differentiated organoids die after long time in culturing. This data is confirmed in qPCR too (Figure 34A).

Enterocytes compose most of the intestinal epithelium and their purpose is to increase the surface being able to absorb nutrients coming from the digestion process while minimizing the occupied space. They are characterized by the expression of SI [126], which in our differentiated samples has a statistically significant higher expression than the staminal ones from the gene expression analysis (Figure 34B), result confirmed also by qPCR data (Figure 34B). The increase in SI levels and the decrease of LGR5 after differentiation indicates that the differentiation protocol induces the differentiation of intestinal stem cells in enterocytes.

The differentiation protocol used induces especially the differentiation in enterocytes, but despite being the most abundant cell type composing the intestinal epithelium, it is not the only one, and intestinal stem cells can differentiate in other cell types too, so we evaluated the presence of Goblet cells, enteroendocrine cells and Paneth cells with the expression level of their respective markers.

Goblet cells are responsible for the production of mucus to lubricate the internal surface of the intestine, making the passage of nutrients easier [127]. These cells are characterized by the expression of MUC2 gene, which in our gene expression analysis (Figure 34C) shows a statistically significant increased expression in differentiated samples compared to staminal ones, therefore stem cells were able to differentiate and form a population of Goblet cells within the differentiated organoid. This result is confirmed by qPCR too (Figure 34C).

Paneth cells produce enzymes like lysozymes, that are secreted in the intestinal lumen and constitute the first defense against bacteria and infections [128]. Their presence is detected by the expression of the gene LYZ, which from gene expression analysis doesn’t show major differences between staminal and differentiated samples (Figure 34D). A similar result is obtained through qPCR; the relative expression of the gene indicates similar levels between staminal and differentiated organoids (Figure 34D). So, the differentiation protocol doesn’t induce Paneth cells differentiation, but this was expected since DAPT is absent.

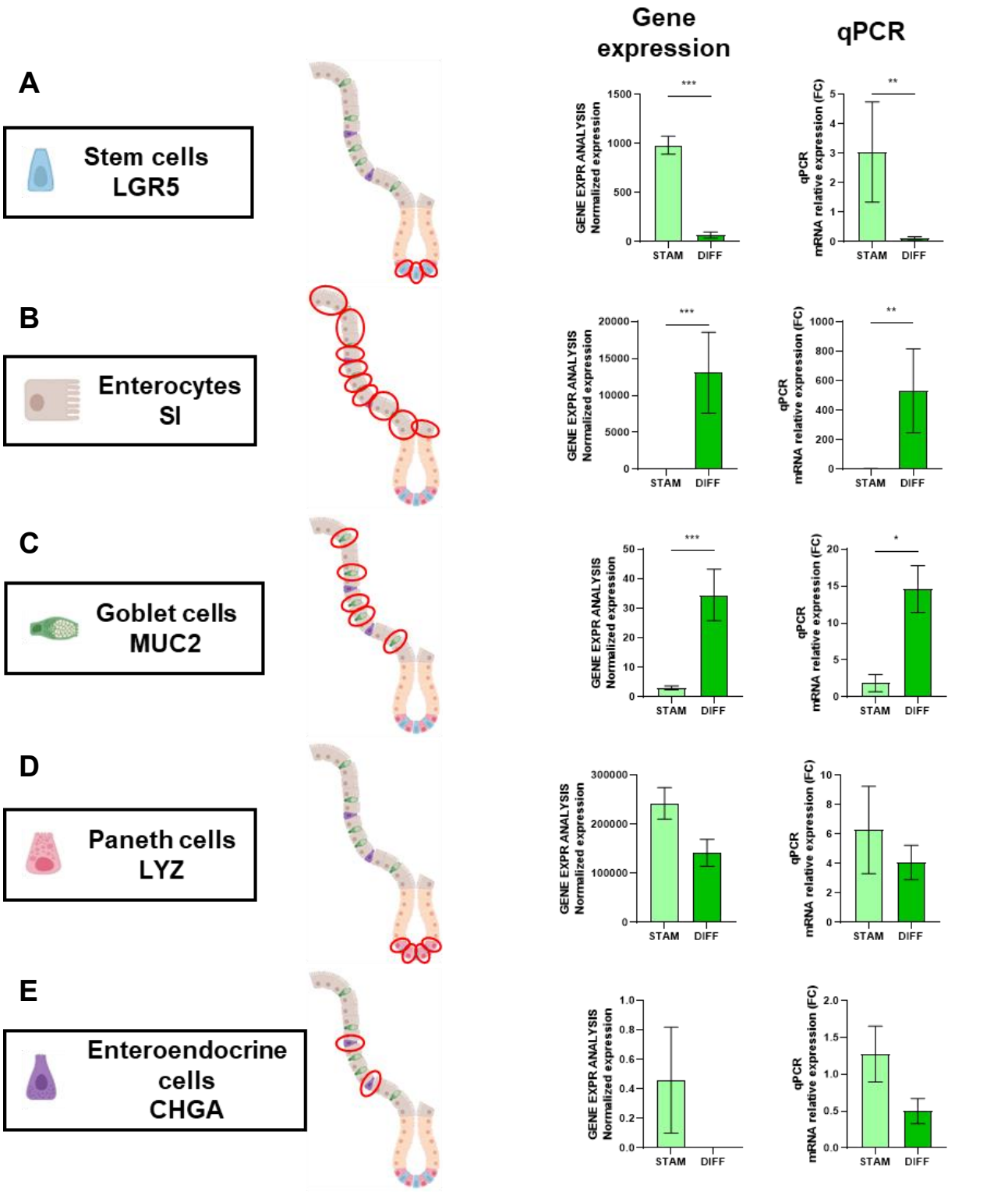

Figure 34: *gene expression analysis to verify differentiation of various cell types. Using sequencing data from the staminal and the respective differentiated counterpart of the 7 patients analyzed in PCA , gene expression analysis was performed confronting staminal organoids versus differentiated ones: these data were then confirmed by qPCR analysis of staminal organoids and their differentiated counterparts from 6 different patients. Staminal cell presence was evaluated by Lgr5 gene expression* ***A)****, enterocytes presence by SI gene expression* ***B)****, Goblet cells presence by MUC2 gene expression* ***C)****, Paneth cells presence by LYZ gene expression* ***D)*** *and enteroendocrine cells presence by CHGA gene expression* ***E)****. Histograms represent mean ± SEM; *p<0,05, **p<0,01, ***p<0,001, ****p<0,0001.*

Lastly, **enteroendocrine cells** secrete serotonin and cholecystokinin in the intestine, constituting a small population in the gastrointestinal mucosa [129]. They are characterized by the expression of CHGA, which has low expression in both staminal and differentiated organoids based on gene expression analysis, not showing any expression differences across the two groups (Figure 34E), in accordance with the low representation of this cell type in the intestinal epithelium. The qPCR analysis confirmed the low level of this gene in both staminal and differentiated organoids given the poor signal observed, indicating that CHGA is a rare transcript with low expression. The analysis of these data resulted in a higher relative expression of CHGA in the staminal organoids compared to the differentiated ones (Figure 34E), but due to the poor signal registered in qPCR for CHGA, this consideration is not reliable.

These differences in gene expression are observed between staminal and differentiated organoids without considering organoids' belonging to the control or the CD group. So, to investigate if this influences differentiation, we performed a **gene expression analysis** between staminal and differentiated organoids **dividing control and CD organoids** into separate groups.

Inside the control and CD group, gene expression differences between staminal and differentiated organoids are the same observed when analyzing the organoids as one whole group (control plus CD organoids), so there is higher expression of LGR5 in staminal organoids, higher expression of SI and MUC2 in the differentiated ones, and no differences in LYZ expression between staminal and differentiated organoids (Figure 35). CHGA was not analyzed due to its low expression.

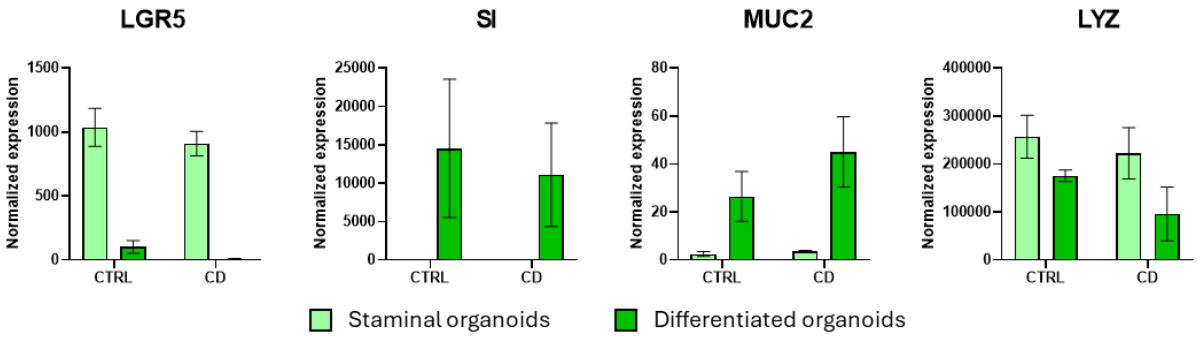

Figure 35: *gene expression analysis to investigate differences in differentiations between control and CD patients' derived organoids. Using sequencing data from the staminal and the respective differentiated counterparts of the 7 patients analyzed in PCA, gene expression analysis was performed confronting staminal organoids versus differentiated ones dividing them between control and CD organoids, to assess the presence of staminal cells, enterocytes, Goblet cells and Paneth cells checking the expression of their markers, Lgr5, SI, MUC2 and LYZ respectively inside the control and CD group. Histograms represent mean ± SEM.*

Interestingly, comparing control staminal organoids and CD staminal organoids for LGR5 expression, there is no difference between them, and same results are obtained comparing control differentiated organoids with CD differentiated organoids for SI, MUC2 and LYZ expression, indicating that **patient's disease has a negligible influence in the stemness and differentiation process** of their derived organoids, confirming the result obtained from PCA in which organoids are separated between staminal and differentiated ones, not by their pathologies.

4.4.6 Organoid inversion verification

After confirming that the differentiation protocol is working, we need to verify the functioning of the **inversion protocol**.

To do so, a highly proliferative staminal organoid line has been chosen to have a high number of organoids for the experiment. Once the organoids form a big enough spherical structure, we generated 4 samples to have all the possible conditions in which we can have our organoids through our differentiation and inversion protocols: these samples are then fixed in paraformaldehyde to be conserved (Figure 36).

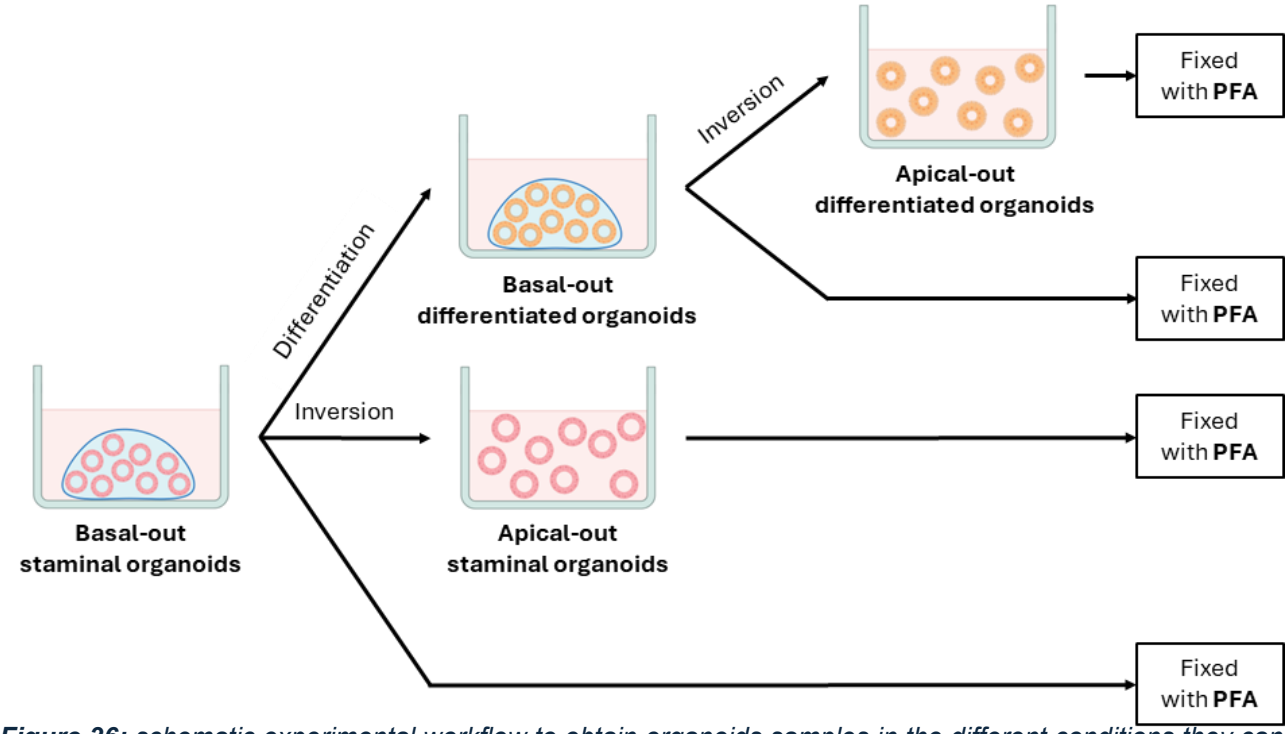

Figure 36: *schematic experimental workflow to obtain organoids samples in the different conditions they can be used. Starting from a staminal organoid culture, the basal-out staminal organoid sample was immediately obtained. A fraction of these organoids was inverted to obtain the apical-out staminal organoids while another fraction was differentiated. After complete differentiation the basal-out differentiated organoid sample is obtained while a fraction was inverted to obtain the apical-out differentiated organoid sample.*

After this procedure the following samples are obtained:

- **Basal-out staminal organoids**.
- **Apical-out staminal organoids**.
- **Basal-out differentiated organoids**.
- **Apical-out differentiated organoids**.

All these samples are stained in immunofluorescence using DAPI to visualize nuclei in blue, and phalloidin to visualize β-actin filaments in red, that are concentrated in higher quantities on the apical surface, allowing its identification [130]. For each sample, images of several organoids have been taken with confocal microscopy, creating a Z-stack of the organoid.

Looking at the staminal samples, in Figure 37A1-A2 there are 4 sections from the z-stack of two **basal-out staminal organoids**: in both, it is clearly shown that actin filaments in red form a ring on the inside of nuclei, which mark the organoid border constituted mainly of a one cell layer. Basal-out staminal organoids generally appear as a well-defined round sphere, here the actin filaments outline the inner cavity of the staminal organoid placing the apical surface of the cells on the inside. In Figure 37B1-B2 there are 4 sections from the z-stack of two **apical-out staminal organoids** in which actin filaments are on the outside while the nuclei are on the inside of the organoid, the exact opposite of the basal-out staminal organoid; these organoids are generally spherical with an inner cavity and mainly with a one cell layer border too. Thanks to actin visualization it is confirmed that the apical surface is now on the outside while the basal side is facing the inner cavity, therefore our inversion protocol worked as intended.

Looking at the differentiated organoids, in Figure 38A1-A2 there are 4 sections from the z-stack of two **basal-out differentiated organoids**; like in the basal-out staminal organoids, the actin filaments in red outline an inner ring delimiting the inner cavity while the nuclei are on the outer border. Even the differentiated organoids have generally a spherical structure with well-defined inner cavity, mainly delimited by a single cell border; unlike their staminal counterpart, the apical surface appears more jagged, showing big indentations too thanks to the differentiation of the cells in enterocytes that form complex structures like microvilli on their apical surface and try to organize themselves in the villous-crypt intestinal architecture, despite not being able to accomplishing it probably because of the small dimensions of the organoids. In Figure 38B1-B2 there are 4 sections from the z-stack of two **apical-out differentiated organoids**, and, in this case too, nuclei are defining an inner border and the

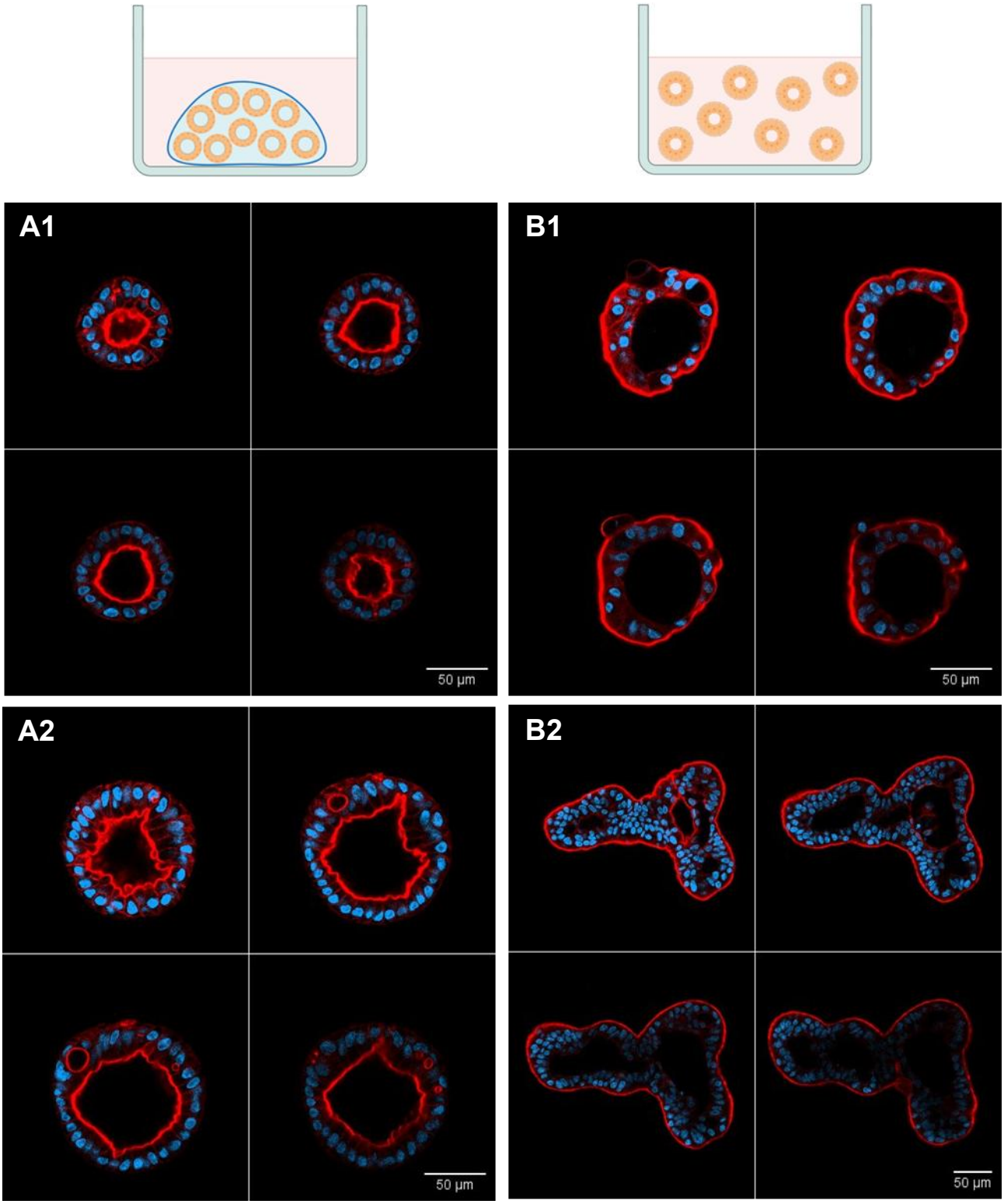

Figure 38: *basal-out differentiated organoids and apical-out differentiated organoids were stained in immunofluorescence with DAPI and phalloidin to see nuclei in blue and actin filaments in red respectively. Here are shown 4 sections from the z-stacks of basal-out differentiated organoids (**A1** and **A2**) and 4 stacks from the z-stacks of apical-out differentiated organoids (**B1** and **B2**); images taken with confocal microscopy (magnification 40X, scale bar 50µm).*

internal cavity while the actin filaments are concentrated on the outside outlining the apical surface, confirming that even for differentiated organoids our inversion protocol is working.

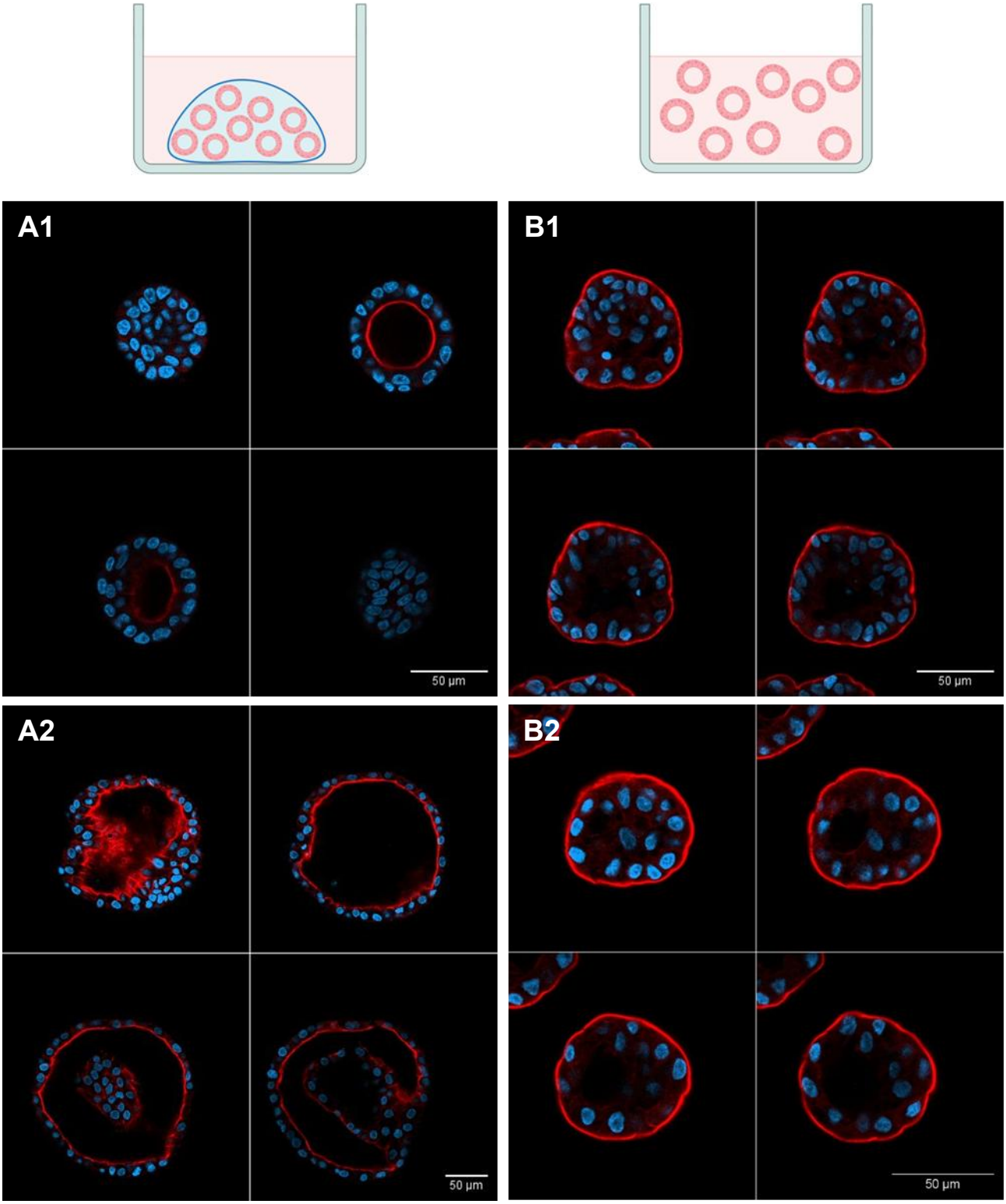

Figure 37: *basal-out staminal organoids and apical-out staminal organoids were stained in immunofluorescence with DAPI and phalloidin to see nuclei in blue and actin filaments in red respectively. Here are shown 4 sections from the z-stacks of basal-out staminal organoids (**A1** and **A2**) and 4 stacks from the z-stacks of apical-out staminal organoids (**B1** and **B2**); images taken with confocal microscopy (magnification 40X, scale bar 50µm).*

In contrast with their staminal counterparts, apical-out differentiated organoids present a more jagged apical surface and cells protruding outwards; moreover, they organize more frequently in more irregular structures compared to the spherical one of basal-out organoids

and apical-out staminal organoids, probably because of the combined effects of the loss of the support given by matrigel and the differentiation process with the structural changes it brings to the cell organization.

4.5 ER stress activation by PTG in a patients' derived organoid model

Once we have set up the differentiation and the inversion protocols, we generated organoids for the 7 control and 6 CD patients enrolled from duodenal biopsies and expanded them under staminal conditions. Once obtained enough organoids, we inverted and differentiated them to obtain **apical-out differentiated organoids**, as the organoid set up most close to the physiological conditions in the intestine where the encounter between gliadin peptides and enterocytes happens.

Then we treated apical-out differentiated organoids with PTG (1mg/mL) for 1h and 8h or left untreated. At the end of the incubation, samples are collected and lysed to extract RNA, which is retrotranscribed and analyzed through qPCR to evaluate gene expression of **hTG2 as a CD marker and ATF4, ATF6 and Xbp1(s) as marker of ER stress** and UPR activation (Figure 39A).

The qPCR data obtained from each control and CD patient have been normalized on their respective untreated samples to see the responsiveness of each patient to PTG stimulation, so independently from the starting amount of mRNA of the target gene in the untreated sample, we are able to evaluate how it changes in response to PTG in each patient. With these measurements, we obtained the mean response to PTG for control and CD patients for each gene (Figure 39B). As expected, in control patients there is no increased expression of hTG2 since they are affected by diseases non-related to CD: similarly, there is no increased expression of either of the three ER stress markers ATF4, ATF6 or Xbp1(s) at both timepoints, showing expression levels close to that of the untreated samples. On the contrary, CD patients show increased expression of hTG2 after 8h from PTG stimulation as expected, even though after 1h its expression is like in the untreated samples; likewise, ATF4, ATF6 and Xbp1(s) have expression levels close to the untreated samples after 1h but show slightly increased expressions after 8h of incubation with PTG.

The two timepoints of 1h and 8h allow the evaluation of the reaction time to PTG stimulation, since there are practically no changes after the first hour of incubation, but **every gene**

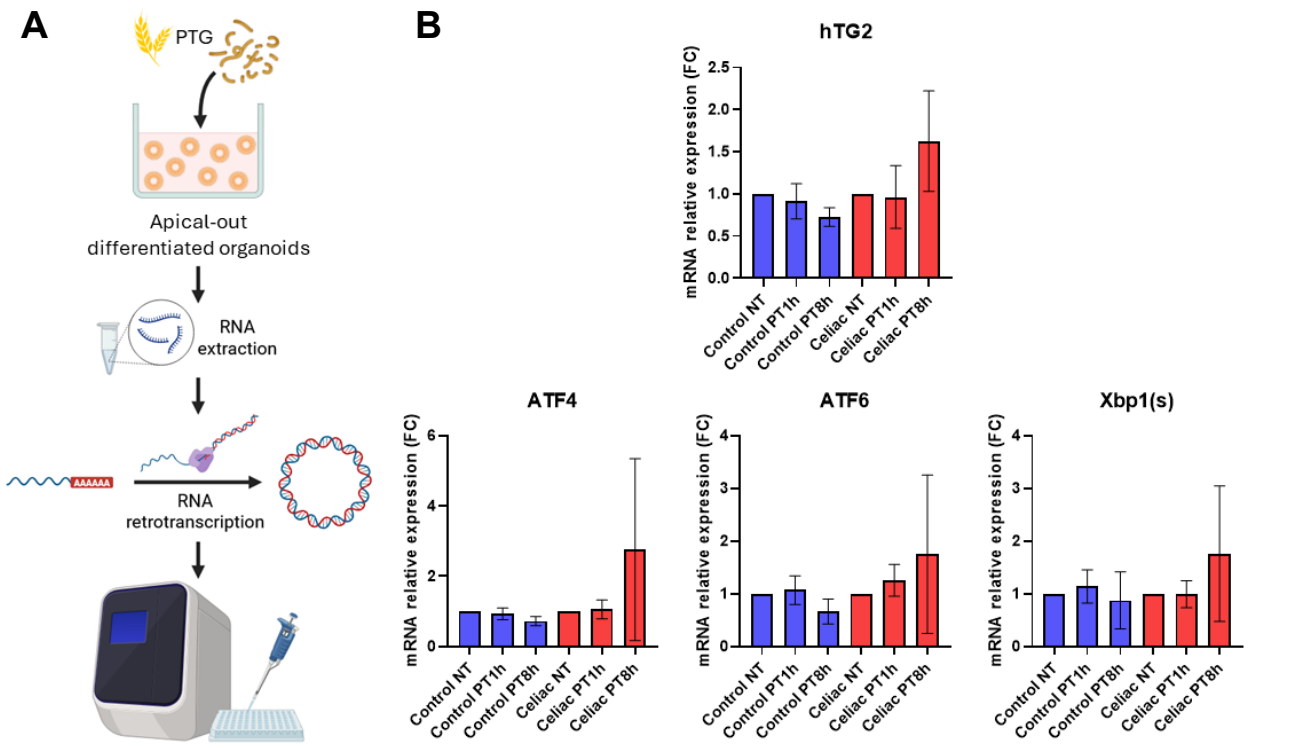

Figure 39: *ER stress induction by PTG in control and CD organoids.* ***A)*** *Schematic experimental workflow: organoids from 7 control patients and 6 CD patients have been inverted and differentiated, then they were stimulated with PTG for 1h and 8h or left untreated (NT). Then samples were collected and lysed to extract RNA, which is retrotranscribed and analyzed in qPCR.* ***B)*** *Data from qPCR for ER stress markers (ATF4, ATF6 and Xbp1(s)) expression and hTG2 expression as a CD marker; for each gene, treated samples of the control and CD groups have been normalized on their respective NT sample to evaluate their sensibility to PTG stimulation. Histograms represent mean ± s.d.*

shows increased expression after 8h, it is possible that PTG stimulation starts a response in the cells that requires time to start a detectable signal using these marker genes. Since there is the indication of a slight induction of ER stress by PTG, it is possible that it requires time to reach stress levels that activate UPR and consequently the increased expression of ATF4, ATF6 and Xbp1(s), explaining why their expression levels are higher after 8h and not after 1h. There is still no clear information on how PTG can directly interact with the cell and start its downstream signaling, since to date no receptor has been identified with confidence. From literature there are evidence of PTG inducing Ca^{2+} mobilization and inducing ER stress [25], [26] in CaCo-2 cell line and in CD-derived fibroblast, suggesting the possible activation of ER stress in CD, but still this is the first time there is an indication of **UPR activation in an enterocyte-like model**, in accordance with our preliminary results in CaCo-2, GEVS models and patient's biopsies. Moreover, the higher expression of hTG2 in the CD organoid model confirms that this model can recapitulate some key aspects of CD symptomatology, since it is **specific to CD organoids** and the increased expression is absent in the control ones.

The specific induction of ER stress in CD patients could be another factor involved in the pathogenic mechanisms of this disease that still aren't fully clear, especially when looking at the direct effects of gliadin peptides to enterocytes. From literature gliadin peptides have shown mainly to increase enterocytes susceptibility to inflammatory stimuli or to increase the inflammatory condition in the intestine; identifying ER stress as a new mechanism induced in these cells in CD patients could **associate gliadin peptides action to a direct damaging mechanism**, rather than being only associated with making enterocytes more susceptible to other damaging factors like the immune system. Indeed, a prolonged condition of ER stress leads to cell death, and in a context of still undiagnosed CD there is a continuous introduction of gluten that would cause an uninterrupted ER stress induction in enterocytes.

However, the data presented showing increased expression of PTG after 8h in CD patients' derived organoids have high standard deviations in all observed genes, highlighting high internal variability across samples. This suggests that the response to **PTG stimulation and the sensibility to it are heterogeneous across patients**: since also hTG2 have high standard deviation, this sensibility is not restricted to the ability of PTG to induce ER stress but it's the sensibility to PTG in a whole that is specific and varies from patient to patient.

Another important aspect of these results is the different intensity of increased gene expression between organoids and the CaCo-2, GEVS model and patients' biopsies. This could be a consequence of the composition of the organoid model since we differentiated intestinal stem cells mostly in enterocytes that, despite being the most abundant cell type in the intestine, are not the only one. Moreover, the lack of other intestinal components, like the immune system, could have a role in amplifying the effect of PTG to enterocytes: indeed, in the GEVS model it is used complete intestinal tissue from Balb/c mice, and CaCo-2 cell line derives from colon cancer cells that have their own limitations as a faithful CD model, while these organoids are generated from duodenal biopsies and their intestinal stem cells from this intestinal section. Considering patients' biopsies, they are collected from patients during their CD diagnosis, therefore these patients have active CD since gluten ingestion is still present; so, gluten peptides can continuously stimulate enterocytes and induce ER stress in them, reaching high intensity levels and uninterrupted UPR, as the high expression levels observed for all three ER stress markers suggests, possibly explaining why in our system, the expression levels of ATF4, ATF6 and Xbp1(s) in CD organoids are lower than the ones observed in the CaCo-2, GEVS model and patient's biopsies.

5. CONCLUSIONS

CD is an **autoimmune enteropathy** caused by the ingestion of gluten and is diffused worldwide, affecting patients of all ages with a wide variety of intestinal and extraintestinal symptoms. There is still no cure other than a lifelong GFD, which is difficult to follow and has side effects despite resolving CD symptomatology.

CD pathogenesis, although being extensively studied, is complex and still not fully understood. Other than a well-understood immune and genetic component, there are other factors responsible for this disease with unclear roles and mechanisms.

Among these, the **impact of gluten peptides directly on intestinal epithelial cells**, where the organism first encounters these peptides, hasn't been investigated: from literature it was mainly observed a promotion of an inflammatory status in intestinal epithelial cell lines by gliadin peptides and an enhancement of the immune response. Among these effects, it was observed the **mobilization of Ca^{2+}** from intracellular stores with a consequent induction of ER stress, a potential damaging mechanism for the cell, and influential on activating TG2.

In this PhD thesis we further investigated the relationship between ER stress and CD in our available model and set up an intestinal organoid model to study specifically ER stress induction in an enterocyte model by gliadin peptides.

Initially, we confirmed **ER stress induction by PTG in CaCo-2 cell line**, detecting UPR transcription factors (ATF4, ATF6 and Xbp1(s)) higher expressions in response to gliadin peptides together with a higher expression of CD markers (hTG2 and CLDN2). This connection between ER stress and PTG was further validated by inhibiting ER stress with 4PBA, a chemical chaperone, that shut down all increased expressions observed without it.

We performed a similar experiment in a more complex model using **intestines from Balb/c mice cultivated in GEVS as an *ex vivo* animal model for CD**, treating them with PTG and thapsigargin as an ER stress inducer. Here we confirmed what we observed in the CaCo-2 cell line model, detecting ER stress and CD markers increased expression in response to PTG stimulation. Moreover, thapsigargin caused increased expression of both TG2 and CLDN2 together with inducing ER stress as expected, confirming that both genes expressions are regulated by one or more of the transcription factors activated during ER

stress by UPR, and reinforcing the connection between ER stress and CD. These considerations were also verified by the complete inhibition of all genes when 4PBA was used together with PTG or thapsigargin treatments.

We also had the possibility to investigate ER stress levels in **CD patients' intestinal biopsies**, confronting them with intestinal biopsies from control patients: from this analysis, we detected specifically in CD patients increased expressions of all UPR transcription factors and CD markers as expected.

These results confirmed **the ability of gliadin peptides to induce ER stress** in cells and in addition to this, to induce the expression of marker genes of CD as indicated by our results in the cellular and animal model; our findings in patients biopsies indicate that **ER stress is present specifically in CD patients** and could have a role in the pathogenesis of the disease or in the damaging of the intestinal epithelium.

To further investigate how ER stress affects the intestinal epithelium, we needed a model of the human enterocytes, being the most abundant cell type constituting this tissue, in the context of CD: for this reason, we set up a patient derived organoid model generated from duodenal biopsies.

Starting from these biopsies, we successfully set up a protocol to isolate intestinal crypts from several patients, that after being seeded in matrigel, generated 3D staminal organoids that are patients specific and retain their genetic background. These organoids formed **spheric structures with a single cell border and a hollow on the inside**; they grow to an **average diameter of 134,7 ± 70,4µm**, the size shows only minor influences from the patient of origin and for the most part organoid cultures from different patients have organoids of similar sizes.

Keeping the generated organoids under staminal conditions to **preserve the stemness of the cells** (confirmed by high expression level of LGR5, marker of intestinal stem cells, detected by gene expression analysis on sequencing data and qPCR), we were able to expand organoid cultures through a passage protocol, with which staminal organoids are broken down into single cells, which are seeded in new matrigel drops and generate new organoids, increasing their available quantity. We were able to expand organoids culture on average to the 9th passage and **50% of organoid cultures reached the 12th passage**; even though some of them were kept for longer times, reaching the 20th or even higher passages,

being able to expand an organoid culture for several times allowed us to have enough organoids to perform our characterization and stimulation experiments.

After establishing staminal organoids, we successfully set up **protocols to differentiate them into the other intestinal cell types and to invert their polarity** to mimic more closely the intestinal epithelium.

We verified the effectiveness of the differentiation protocol by sequencing data and qPCR: we detected the presence of **high levels of enterocytes and Goblet cells in differentiated organoids** confronted with staminal ones, while Paneth cells did not show changes in abundance between differentiated and staminal organoids, an expected result since the factor necessary for their differentiation was absent from the differentiation medium; lastly, enteroendocrine cells were detected with low near absent presence in both conditions, in accordance with their low representation in the intestinal epithelium. These data, with a decreased expression of LGR5 in differentiated organoids, demonstrated the effectiveness of the differentiation protocol, especially to differentiate enterocytes. Additionally, when analyzing our differentiation data separating CD organoids from control ones, there were no big differences between the two groups, suggesting that patients' pathologies did not influence **organoid differentiation, which worked with the same effectiveness independently from the condition of the patient** from which it was generated.

Then we verified the inversion protocol by immunofluorescence, staining actin filaments on the apical side of the cells and observing their position relative to the nuclei. Analyzing multiple basal-out and apical-out organoids, we observed a shift of the apical side from the inside, facing the organoid's cavity, to the outside in both staminal and differentiated organoids, confirming the **successful inversion of organoids' polarity**.

With protocols set up, we generated apical-out differentiated organoids from control and CD patients and stimulated them with PTG for 1h and 8h to investigate the induction of ER stress in a model of human intestinal epithelium.

We evaluated ER stress level and hTG2 induced by PTG via qPCR. From these data, we did not observe differences between control and CD organoids after 1h of stimulation, but after 8h all ER stress markers and hTG2 have increased expressions in CD patients organoids compared to the control ones, suggesting that **ER stress induction is not immediate and it takes time to reach a stress level sufficient to activate UPR**. Moreover, our data showed high standard deviations only for the CD organoids sample at

the 8h timepoint, indicating **high heterogeneity across CD patients for their responsiveness to gliadin peptides.**

Our results in the organoid model, despite having a similar trend to the experiments on CaCo-2 cell line, the *ex vivo* animal model and patients' biopsies, show lower levels of ER stress and CD marker expression. Given the indication of a time-dependent induction of ER stress by gliadin peptides, it is possible that with higher incubation time, organoids could reach higher levels of ER stress and a correspondent higher activation of UPR; indeed, our organoids prior to the stimulation with PTG, were kept without gliadin for several passages, allowing them to return to a physiological state and needing more time with gliadin peptides to express CD symptoms. This would explain the heterogeneity for the responsiveness to PTG stimulation we observed in CD organoids, maybe some patients are more responsive to gliadin peptides and express CD symptoms quicker than others.

For this reason, other than **testing higher incubation times**, it is important to **increase our sample size**, to confirm if the heterogeneity we encountered corresponds to the heterogeneity of CD patients or it is a consequence of some limitations of our model. If our model can replicate patients heterogeneity, it would be interesting also to check if low responsive patients have a particular genetic background when confronted with more highly responsive ones through sequencing analysis.

Moreover, our organoid model is composed of enterocytes for the most part, even if other types are present, like Goblet cells and Paneth cells: it would be interesting to have **differentiated intestinal organoids with a more diverse cellular composition**, utilizing a differentiation protocol that allow higher differentiation for other cell types other than the enterocytes, on which ER stress induction could have higher impact, especially considering that secretory cell types could be more susceptible to it.

Additionally, new technologies are developing with which is possible the **co-culturing of patient derived intestinal organoids with the immune component from the patient**: this allow to study immune cells in the context of CD and how they interact with enterocytes upon PTG stimulation, investigating the role of ER stress in immune cells from CD patients and how its level changes when the immune component is present alongside with the enterocytes.

Regarding the **organoid model usage and limitations**, ours is in line with other intestinal organoids used to mimic other pathologies affecting the intestine like ulcerative colitis, Crohn disease and other inflamed bowel diseases (IBD). In these, patients' derived organoids can be generated from intestinal biopsies by isolating LGR5+ cells and then are cultured by embedding them in a 3D extracellular matrix, obtaining samples that recapitulate the intestinal architecture and key characteristics of the disease of interest. Organoids have been used as useful tools to explore new pathogenic mechanisms, like dysregulation of the epithelial barrier integrity and regeneration in colitis, or increased permeability in Crohn disease, in the same way we explored ER stress induction by PTG in our model [131].

Likewise organoid technology has **limitations** that are common among the various studies and **that characterize our model too**. First, there are no guidelines or standardized protocols for intestinal organoids generation, variations in matrix composition, growth factors and stem cell source cause different organoid phenotypes across laboratories and hindering reproducibility and the application of this technology to clinical research, to which there would be the additional problem of scaling organoid production due to the still high cost and intensive labor necessary to organoid culturing. Moreover, while intestinal organoid generation is diffusing as a technique, current methods are restricted to the epithelial component obtaining organoids that mimic only one aspect of the intestine, lacking all the other components present that have roles in the physiologic functions of this organ like blood vessels and vascularization, muscular tissues that are responsible for peristaltic movements, the immune component, as briefly mentioned before, that has a central role in IBD and the complex and diversified intestinal microbiota, which shows to be involved in several disease, like CD, at different levels: for this reason new techniques to co-culture organoids with other components are in development although still not being diffused enough and incurring in the same standardization problem that characterize the organoid technology [132].

6. BIBLIOGRAPHY

[1] M. K. Kowalski, D. Domżał-Magrowska, and E. Małecka-Wojciesko, 'Celiac Disease—Narrative Review on Progress in Celiac Disease', *Foods*, vol. 14, no. 6, p. 959, Mar. 2025, doi: 10.3390/foods14060959.

[2] G. Caio *et al.*, 'Celiac disease: a comprehensive current review', *BMC Med*, vol. 17, no. 1, p. 142, Dec. 2019, doi: 10.1186/s12916-019-1380-z.

[3] F. Perez, C. N. Ruera, E. Miculan, P. Carasi, and F. G. Chirdo, 'Programmed Cell Death in the Small Intestine: Implications for the Pathogenesis of Celiac Disease', *IJMS*, vol. 22, no. 14, p. 7426, July 2021, doi: 10.3390/ijms22147426.

[4] D. Karunaratne and N. Karunaratne, 'ENT Manifestations of Celiac Disease: A Scholarly Review', *Ear Nose Throat J*, vol. 101, no. 9, pp. 600–605, Nov. 2022, doi: 10.1177/0145561320972604.

[5] S. Husby *et al.*, 'European Society Paediatric Gastroenterology, Hepatology and Nutrition Guidelines for Diagnosing Coeliac Disease 2020', *J. pediatr. gastroenterol. nutr.*, vol. 70, no. 1, pp. 141–156, Jan. 2020, doi: 10.1097/MPG.0000000000002497.

[6] C. Catassi, E. F. Verdu, J. C. Bai, and E. Lionetti, 'Coeliac disease', *The Lancet*, vol. 399, no. 10344, pp. 2413–2426, June 2022, doi: 10.1016/S0140-6736(22)00794-2.

[7] E. M. Domsa, I. Berindan-Neagoe, I. Para, L. Munteanu, D. Matei, and V. Andreica, 'Celiac disease: a multi-faceted medical condition', *Journal of Physiology and Pharmacology*, 2019, doi: 10.26402/jpp.2020.1.01.

[8] L. Schøsler, L. A. Christensen, and C. L. Hvas, 'Symptoms and findings in adult-onset celiac disease in a historical Danish patient cohort', *Scandinavian Journal of Gastroenterology*, vol. 51, no. 3, pp. 288–294, Mar. 2016, doi: 10.3109/00365521.2015.1092576.

[9] S. P. Möller, B. Hayes, H. Wilding, P. Apputhurai, J. A. Tye-Din, and S. R. Knowles, 'Systematic review: Exploration of the impact of psychosocial factors on quality of life in adults living with coeliac disease', *Journal of Psychosomatic Research*, vol. 147, p. 110537, Aug. 2021, doi: 10.1016/j.jpsychores.2021.110537.

[10] P. Singh *et al.*, 'Global Prevalence of Celiac Disease: Systematic Review and Meta-analysis', *Clinical Gastroenterology and Hepatology*, vol. 16, no. 6, pp. 823-836.e2, June 2018, doi: 10.1016/j.cgh.2017.06.037.

[11] G. K. Makharia *et al.*, 'The global burden of coeliac disease: opportunities and challenges', *Nat Rev Gastroenterol Hepatol*, vol. 19, no. 5, pp. 313–327, May 2022, doi: 10.1038/s41575-021-00552-z.

[12] L. M. Sollid and K. E. A. Lundin, 'Celiac Disease', in *The Autoimmune Diseases*, Elsevier, 2020, pp. 849–869. doi: 10.1016/B978-0-12-812102-3.00045-2.

[13] J. F. Ludvigsson *et al.*, 'Diagnosis and management of adult coeliac disease: guidelines from the British Society of Gastroenterology', *Gut*, vol. 63, no. 8, pp. 1210–1228, Aug. 2014, doi: 10.1136/gutjnl-2013-306578.

[14] A. Rubio–Tapia *et al.*, 'Predictors of Family Risk for Celiac Disease: A Population-Based Study', *Clinical Gastroenterology and Hepatology*, vol. 6, no. 9, pp. 983–987, Sept. 2008, doi: 10.1016/j.cgh.2008.04.008.

[15] R. Kuja-Halkola, B. Lebwohl, J. Halfvarson, C. Wijmenga, P. K. E. Magnusson, and J. F. Ludvigsson, 'Heritability of non-HLA genetics in coeliac disease: a population-based study in 107 000 twins', *Gut*, vol. 65, no. 11, pp. 1793–1798, Nov. 2016, doi: 10.1136/gutjnl-2016-311713.

[16] A. D. Ramírez-Sánchez, I. L. Tan, B. C. Gonera-de Jong, M. C. Visschedijk, I. Jonkers, and S. Withoff, 'Molecular Biomarkers for Celiac Disease: Past, Present and Future', *IJMS*, vol. 21, no. 22, p. 8528, Nov. 2020, doi: 10.3390/ijms21228528.
[17] A. Fasano, 'Celiac Disease — How to Handle a Clinical Chameleon', *N Engl J Med*, vol. 348, no. 25, pp. 2568–2570, June 2003, doi: 10.1056/NEJMe030050.
[18] W. Dickey and N. Kearney, 'Overweight in Celiac Disease: Prevalence, Clinical Characteristics, and Effect of a Gluten-Free Diet', *Am J Gastroenterology*, vol. 101, no. 10, pp. 2356–2359, Oct. 2006, doi: 10.1111/j.1572-0241.2006.00750.x.
[19] D. A. Leffler, P. H. R. Green, and A. Fasano, 'Extraintestinal manifestations of coeliac disease', *Nat Rev Gastroenterol Hepatol*, vol. 12, no. 10, pp. 561–571, Oct. 2015, doi: 10.1038/nrgastro.2015.131.
[20] J. F. Ludvigsson *et al.*, 'The Oslo definitions for coeliac disease and related terms', *Gut*, vol. 62, no. 1, pp. 43–52, Jan. 2013, doi: 10.1136/gutjnl-2011-301346.
[21] S. Daum, C. Cellier, and C. J. J. Mulder, 'Refractory coeliac disease', *Best Practice & Research Clinical Gastroenterology*, vol. 19, no. 3, pp. 413–424, June 2005, doi: 10.1016/j.bpg.2005.02.001.
[22] J. E. Pizzorno, M. T. Murray, and H. Joiner-Bey, 'Celiac disease', in *The Clinician's Handbook of Natural Medicine*, Elsevier, 2016, pp. 188–193. doi: 10.1016/B978-0-7020-5514-0.00025-7.
[23] H. Wieser, P. Koehler, and K. A. Scherf, 'Chemistry of wheat gluten proteins: Qualitative composition', *Cereal Chem*, vol. 100, no. 1, pp. 23–35, Jan. 2023, doi: 10.1002/cche.10572.
[24] M. F. Gómez Castro *et al.*, 'p31-43 Gliadin Peptide Forms Oligomers and Induces NLRP3 Inflammasome/Caspase 1- Dependent Mucosal Damage in Small Intestine', *Front. Immunol.*, vol. 10, p. 31, Jan. 2019, doi: 10.3389/fimmu.2019.00031.
[25] I. Caputo *et al.*, 'Gliadin Peptides Induce Tissue Transglutaminase Activation and ER-Stress through Ca2+ Mobilization in Caco-2 Cells', *PLoS ONE*, vol. 7, no. 9, p. e45209, Sept. 2012, doi: 10.1371/journal.pone.0045209.
[26] S. Sposito *et al.*, 'Peculiar Ca2+ Homeostasis, ER Stress, Autophagy, and TG2 Modulation in Celiac Disease Patient-Derived Cells', *IJMS*, vol. 24, no. 2, p. 1495, Jan. 2023, doi: 10.3390/ijms24021495.
[27] M. G. Herrera *et al.*, 'Structural conformation and self-assembly process of p31-43 gliadin peptide in aqueous solution. Implications for celiac disease', *The FEBS Journal*, vol. 287, no. 10, pp. 2134–2149, May 2020, doi: 10.1111/febs.15109.
[28] M. Porpora *et al.*, 'Inflammation Is Present, Persistent and More Sensitive to Proinflammatory Triggers in Celiac Disease Enterocytes', *IJMS*, vol. 23, no. 4, p. 1973, Feb. 2022, doi: 10.3390/ijms23041973.
[29] L. Maiuri *et al.*, 'Association between innate response to gliadin and activation of pathogenic T cells in coeliac disease', *The Lancet*, vol. 362, no. 9377, pp. 30–37, July 2003, doi: 10.1016/S0140-6736(03)13803-2.
[30] R. E. Araya *et al.*, 'Mechanisms of innate immune activation by gluten peptide p31-43 in mice', *American Journal of Physiology-Gastrointestinal and Liver Physiology*, vol. 311, no. 1, pp. G40–G49, July 2016, doi: 10.1152/ajpgi.00435.2015.
[31] B. Frossi *et al.*, 'Mast cells are associated with the onset and progression of celiac disease', *Journal of Allergy and Clinical Immunology*, vol. 139, no. 4, pp. 1266-1274.e1, Apr. 2017, doi: 10.1016/j.jaci.2016.08.011.
[32] Y. L. Allegretti *et al.*, 'Broad MICA/B Expression in the Small Bowel Mucosa: A Link between Cellular Stress and Celiac Disease', *PLoS ONE*, vol. 8, no. 9, p. e73658, Sept. 2013, doi: 10.1371/journal.pone.0073658.

[33] E. Monguzzi *et al.*, 'Gliadin effect on the oxidative balance and DNA damage: An in-vitro, ex-vivo study', *Digestive and Liver Disease*, vol. 51, no. 1, pp. 47–54, Jan. 2019, doi: 10.1016/j.dld.2018.06.020.
[34] V. R. Villella *et al.*, 'A pathogenic role for cystic fibrosis transmembrane conductance regulator in celiac disease', *The EMBO Journal*, vol. 38, no. 2, p. e100101, Jan. 2019, doi: 10.15252/embj.2018100101.
[35] M. V. Barone and K. P. Zimmer, 'Endocytosis and transcytosis of gliadin peptides', *Mol Cell Pediatr*, vol. 3, no. 1, p. 8, Dec. 2016, doi: 10.1186/s40348-015-0029-z.
[36] M. Nanayakkara *et al.*, 'An undigested gliadin peptide activates innate immunity and proliferative signaling in enterocytes: the role in celiac disease', *The American Journal of Clinical Nutrition*, vol. 98, no. 4, pp. 1123–1135, Oct. 2013, doi: 10.3945/ajcn.112.054544.
[37] M. V. Barone *et al.*, 'Growth factor-like activity of gliadin, an alimentary protein: implications for coeliac disease', *Gut*, vol. 56, no. 4, pp. 480–488, Apr. 2007, doi: 10.1136/gut.2005.086637.
[38] R. Dieli-Crimi, M. C. Cénit, and C. Núñez, 'The genetics of celiac disease: A comprehensive review of clinical implications', *Journal of Autoimmunity*, vol. 64, pp. 26–41, Nov. 2015, doi: 10.1016/j.jaut.2015.07.003.
[39] B. Seliger, M. Kloor, and S. Ferrone, 'HLA class II antigen-processing pathway in tumors: Molecular defects and clinical relevance', *OncoImmunology*, vol. 6, no. 2, p. e1171447, Feb. 2017, doi: 10.1080/2162402X.2016.1171447.
[40] K. E. A. Lundin and C. Wijmenga, 'Coeliac disease and autoimmune disease—genetic overlap and screening', *Nat Rev Gastroenterol Hepatol*, vol. 12, no. 9, pp. 507–515, Sept. 2015, doi: 10.1038/nrgastro.2015.136.
[41] M. C. Mazzilli *et al.*, 'A Study of Italian Pediatric Celiac Disease Patients Confirms That the Primary HLA Association Is to the DQ(c I*0501,/ 1"0201) Heterodimer', 1991.
[42] S. Withoff, Y. Li, I. Jonkers, and C. Wijmenga, 'Understanding Celiac Disease by Genomics', *Trends in Genetics*, vol. 32, no. 5, pp. 295–308, May 2016, doi: 10.1016/j.tig.2016.02.003.
[43] Spanish Consortium on the Genetics of Coeliac Disease (CEGEC) *et al.*, 'Dense genotyping identifies and localizes multiple common and rare variant association signals in celiac disease', *Nat Genet*, vol. 43, no. 12, pp. 1193–1201, Dec. 2011, doi: 10.1038/ng.998.
[44] R. P. Anderson, 'Innate and adaptive immunity in celiac disease', *Current Opinion in Gastroenterology*, vol. 36, no. 6, pp. 470–478, Nov. 2020, doi: 10.1097/MOG.0000000000000672.
[45] M. Schumann, B. Siegmund, J. D. Schulzke, and M. Fromm, 'Celiac Disease: Role of the Epithelial Barrier', *Cellular and Molecular Gastroenterology and Hepatology*, vol. 3, no. 2, pp. 150–162, Mar. 2017, doi: 10.1016/j.jcmgh.2016.12.006.
[46] L. Lorand and R. M. Graham, 'Transglutaminases: crosslinking enzymes with pleiotropic functions', *Nat Rev Mol Cell Biol*, vol. 4, no. 2, pp. 140–156, Feb. 2003, doi: 10.1038/nrm1014.
[47] I. R. Korponay-Szabó *et al.*, 'Deamidated Gliadin Peptides Form Epitopes That Transglutaminase Antibodies Recognize', *J. pediatr. gastroenterol. nutr.*, vol. 46, no. 3, pp. 253–261, Mar. 2008, doi: 10.1097/MPG.0b013e31815ee555.
[48] T. Mayassi and B. Jabri, 'Human intraepithelial lymphocytes', *Mucosal Immunology*, vol. 11, no. 5, pp. 1281–1289, Sept. 2018, doi: 10.1038/s41385-018-0016-5.
[49] A. C. CherÑavsky, A. E. Rubio, S. Vanzulli, N. Rubinstein, S. D. Rosa, and L. Fainboim, 'Evidences of the Involvement of Bak, a member of the Bcl-2 Family of Proteins, in Active Coeliac Disease', *Autoimmunity*, vol. 35, no. 1, pp. 29–37, Jan. 2002, doi: 10.1080/08916930290005945.

[50] J. A. Tye-Din *et al.*, ‘Elevated serum interleukin-2 after gluten correlates with symptoms and is a potential diagnostic biomarker for coeliac disease’, *Aliment Pharmacol Ther*, vol. 50, no. 8, pp. 901–910, Oct. 2019, doi: 10.1111/apt.15477.
[51] Y. M. C. Kooy-Winkelaar *et al.*, ‘CD4 T-cell cytokines synergize to induce proliferation of malignant and nonmalignant innate intraepithelial lymphocytes’, *Proc. Natl. Acad. Sci. U.S.A.*, vol. 114, no. 6, Feb. 2017, doi: 10.1073/pnas.1620036114.
[52] B. Meresse *et al.*, ‘Reprogramming of CTLs into natural killer–like cells in celiac disease’, *The Journal of Experimental Medicine*, vol. 203, no. 5, pp. 1343–1355, May 2006, doi: 10.1084/jem.20060028.
[53] M. F. Du Pré and L. M. Sollid, ‘T-cell and B-cell immunity in celiac disease’, *Best Practice & Research Clinical Gastroenterology*, vol. 29, no. 3, pp. 413–423, June 2015, doi: 10.1016/j.bpg.2015.04.001.
[54] R. Iversen and L. M. Sollid, ‘The Immunobiology and Pathogenesis of Celiac Disease’, *Annu. Rev. Pathol. Mech. Dis.*, vol. 18, no. 1, pp. 47–70, Jan. 2023, doi: 10.1146/annurev-pathmechdis-031521-032634.
[55] S. M. Kim, T. Mayassi, and B. Jabri, ‘Innate immunity: Actuating the gears of celiac disease pathogenesis’, *Best Practice & Research Clinical Gastroenterology*, vol. 29, no. 3, pp. 425–435, June 2015, doi: 10.1016/j.bpg.2015.05.001.
[56] M. Nanayakkara *et al.*, ‘P31–43, an undigested gliadin peptide, mimics and enhances the innate immune response to viruses and interferes with endocytic trafficking: a role in celiac disease’, *Sci Rep*, vol. 8, no. 1, p. 10821, July 2018, doi: 10.1038/s41598-018-28830-y.
[57] G. Paolella *et al.*, ‘The toxic alpha-gliadin peptide 31–43 enters cells without a surface membrane receptor’, *Cell Biology International*, vol. 42, no. 1, pp. 112–120, Jan. 2018, doi: 10.1002/cbin.10874.
[58] Y. Junker *et al.*, ‘Wheat amylase trypsin inhibitors drive intestinal inflammation via activation of toll-like receptor 4’, *Journal of Experimental Medicine*, vol. 209, no. 13, pp. 2395–2408, Dec. 2012, doi: 10.1084/jem.20102660.
[59] J. A. Gilbert, M. J. Blaser, J. G. Caporaso, J. K. Jansson, S. V. Lynch, and R. Knight, ‘Current understanding of the human microbiome’, *Nat Med*, vol. 24, no. 4, pp. 392–400, Apr. 2018, doi: 10.1038/nm.4517.
[60] E. F. Verdu and D. Schuppan, ‘Co-factors, Microbes, and Immunogenetics in Celiac Disease to Guide Novel Approaches for Diagnosis and Treatment’, *Gastroenterology*, vol. 161, no. 5, pp. 1395-1411.e4, Nov. 2021, doi: 10.1053/j.gastro.2021.08.016.
[61] G. Marasco *et al.*, ‘Gut Microbiota and Celiac Disease’, *Dig Dis Sci*, vol. 61, no. 6, pp. 1461–1472, June 2016, doi: 10.1007/s10620-015-4020-2.
[62] G. De Palma, I. Nadal, M. C. Collado, and Y. Sanz, ‘Effects of a gluten-free diet on gut microbiota and immune function in healthy adult human subjects’, *Br J Nutr*, vol. 102, no. 8, pp. 1154–1160, Oct. 2009, doi: 10.1017/S0007114509371767.
[63] A. Caminero *et al.*, ‘Duodenal Bacteria From Patients With Celiac Disease and Healthy Subjects Distinctly Affect Gluten Breakdown and Immunogenicity’, *Gastroenterology*, vol. 151, no. 4, pp. 670–683, Oct. 2016, doi: 10.1053/j.gastro.2016.06.041.
[64] J. Petersen *et al.*, ‘T cell receptor cross-reactivity between gliadin and bacterial peptides in celiac disease’, *Nat Struct Mol Biol*, vol. 27, no. 1, pp. 49–61, Jan. 2020, doi: 10.1038/s41594-019-0353-4.
[65] K. L. Olshan, M. M. Leonard, G. Serena, A. R. Zomorrodi, and A. Fasano, ‘Gut microbiota in Celiac Disease: microbes, metabolites, pathways and therapeutics’, *Expert Review of Clinical Immunology*, vol. 16, no. 11, pp. 1075–1092, Nov. 2020, doi: 10.1080/1744666X.2021.1840354.

[66] M. Schumann *et al.*, ‘Mechanisms of epithelial translocation of the 2-gliadin-33mer in coeliac sprue’, *Gut*, vol. 57, no. 6, pp. 747–754, Feb. 2008, doi: 10.1136/gut.2007.136366.
[67] A. L. Sheppard *et al.*, ‘Systematic review with meta-analysis: the accuracy of serological tests to support the diagnosis of coeliac disease’, *Aliment Pharmacol Ther*, vol. 55, no. 5, pp. 514–527, Mar. 2022, doi: 10.1111/apt.16729.
[68] A. Fasano and C. Catassi, ‘Celiac Disease’, *N Engl J Med*, vol. 367, no. 25, pp. 2419–2426, Dec. 2012, doi: 10.1056/NEJMcp1113994.
[69] N. R. Lewis and B. B. Scott, ‘Meta-analysis: deamidated gliadin peptide antibody and tissue transglutaminase antibody compared as screening tests for coeliac disease’, *Aliment Pharmacol Ther*, vol. 31, no. 1, pp. 73–81, Jan. 2010, doi: 10.1111/j.1365-2036.2009.04110.x.
[70] G. Caio and U. Volta, ‘Coeliac disease: changing diagnostic criteria?’, *Gastroenterology and Hepatology from Bed to Bench*, 2012.
[71] D. C. Adelman, J. Murray, T.-T. Wu, M. Mäki, P. H. Green, and C. P. Kelly, ‘Measuring Change In Small Intestinal Histology In Patients With Celiac Disease’, *American Journal of Gastroenterology*, vol. 113, no. 3, pp. 339–347, Mar. 2018, doi: 10.1038/ajg.2017.480.
[72] G. Oberhuber, ‘Histopathology of celiac disease’, 2000.
[73] A. S. Oxentenko and J. A. Murray, ‘Celiac Disease: Ten Things That Every Gastroenterologist Should Know’, *Clinical Gastroenterology and Hepatology*, vol. 13, no. 8, pp. 1396–1404, Aug. 2015, doi: 10.1016/j.cgh.2014.07.024.
[74] A. Al-Toma *et al.*, ‘European Society for the Study of Coeliac Disease (ESsCD) guideline for coeliac disease and other gluten-related disorders’, *UEG Journal*, vol. 7, no. 5, pp. 583–613, June 2019, doi: 10.1177/2050640619844125.
[75] M. D. L. Moreno *et al.*, ‘Detection of gluten immunogenic peptides in the urine of patients with coeliac disease reveals transgressions in the gluten-free diet and incomplete mucosal healing’, *Gut*, vol. 66, no. 2, pp. 250–257, Feb. 2017, doi: 10.1136/gutjnl-2015-310148.
[76] A. Lanzini *et al.*, ‘Complete recovery of intestinal mucosa occurs very rarely in adult coeliac patients despite adherence to gluten-free diet’, *Aliment Pharmacol Ther*, vol. 29, no. 12, pp. 1299–1308, June 2009, doi: 10.1111/j.1365-2036.2009.03992.x.
[77] S. Lechuga, M. B. Braga-Neto, N. G. Naydenov, F. Rieder, and A. I. Ivanov, ‘Understanding disruption of the gut barrier during inflammation: Should we abandon traditional epithelial cell lines and switch to intestinal organoids?’, *Front. Immunol.*, vol. 14, Feb. 2023, doi: 10.3389/fimmu.2023.1108289.
[78] K. Lenaerts, F. G. Bouwman, W. H. Lamers, J. Renes, and E. C. Mariman, ‘Comparative proteomic analysis of cell lines and scrapings of the human intestinal epithelium’, *BMC Genomics*, vol. 8, no. 1, p. 91, 2007, doi: 10.1186/1471-2164-8-91.
[79] A. Polvi, O. A. Garden, R. S. Houlston, M. Maki, R. M. Batt, and J. Partanen, ‘Genetic susceptibility to gluten sensitive enteropathy in Irish setter dogs is not linked to the major histocompatibility complex’, *Tissue Antigens*, vol. 52, no. 6, pp. 543–549, Dec. 1998, doi: 10.1111/j.1399-0039.1998.tb03085.x.
[80] K. Mazumdar *et al.*, ‘Visualization of Transepithelial Passage of the Immunogenic 33-Residue Peptide from α-2 Gliadin in Gluten-Sensitive Macaques’, *PLoS ONE*, vol. 5, no. 4, p. e10228, Apr. 2010, doi: 10.1371/journal.pone.0010228.
[81] D. Sblattero *et al.*, ‘Characterization of the Anti-Tissue Transglutaminase Antibody Response in Nonobese Diabetic Mice’, *The Journal of Immunology*, vol. 174, no. 9, pp. 5830–5836, May 2005, doi: 10.4049/jimmunol.174.9.5830.

[82] T. L. Freitag *et al.*, 'Gliadin-primed CD4+CD45RBlowCD25- T cells drive gluten-dependent small intestinal damage after adoptive transfer into lymphopenic mice', *Gut*, vol. 58, no. 12, pp. 1597–1605, Dec. 2009, doi: 10.1136/gut.2009.186361.
[83] E. F. Verdu *et al.*, 'Gliadin-dependent neuromuscular and epithelial secretory responses in gluten-sensitive HLA-DQ8 transgenic mice', *American Journal of Physiology-Gastrointestinal and Liver Physiology*, vol. 294, no. 1, pp. G217–G225, Jan. 2008, doi: 10.1152/ajpgi.00225.2007.
[84] R. W. DePaolo *et al.*, 'Co-adjuvant effects of retinoic acid and IL-15 induce inflammatory immunity to dietary antigens', *Nature*, vol. 471, no. 7337, pp. 220–224, Mar. 2011, doi: 10.1038/nature09849.
[85] N. Ohta *et al.*, 'IL-15-Dependent Activation-Induced Cell Death- Resistant Th1 Type CD8+NK1.1+ T Cells for the Development of Small Intestinal Inflammation', *The Journal of Immunology*.
[86] M. Gagliardi *et al.*, 'Gut-Ex-Vivo system as a model to study gluten response in celiac disease', *Cell Death Discov.*, vol. 7, no. 1, Mar. 2021, doi: 10.1038/s41420-021-00430-2.
[87] M. Gagliardi *et al.*, 'A Gut-Ex-Vivo System to Study Gut Inflammation Associated to Inflammatory Bowel Disease (IBD)', *Biology*, vol. 10, no. 7, p. 605, June 2021, doi: 10.3390/biology10070605.
[88] R. Monzani *et al.*, 'The Gut-Ex-Vivo System (GEVS) Is a Dynamic and Versatile Tool for the Study of DNBS-Induced IBD in BALB/C and C57BL/6 Mice, Highlighting the Protective Role of Probiotics', *Biology*, vol. 11, no. 11, p. 1574, Oct. 2022, doi: 10.3390/biology11111574.
[89] Z. Zhao *et al.*, 'Organoids', *Nat Rev Methods Primers*, vol. 2, no. 1, p. 94, Dec. 2022, doi: 10.1038/s43586-022-00174-y.
[90] H. K. Kleinman and G. R. Martin, 'Matrigel: Basement membrane matrix with biological activity', *Seminars in Cancer Biology*, vol. 15, no. 5, pp. 378–386, Oct. 2005, doi: 10.1016/j.semcancer.2005.05.004.
[91] S. Yang *et al.*, 'Organoids: The current status and biomedical applications', *MedComm*, vol. 4, no. 3, p. e274, June 2023, doi: 10.1002/mco2.274.
[92] A. Barbáchano *et al.*, 'Organoids and Colorectal Cancer', *Cancers*, vol. 13, no. 11, p. 2657, May 2021, doi: 10.3390/cancers13112657.
[93] C. Corrò, L. Novellasdemunt, and V. S. W. Li, 'A brief history of organoids', *American Journal of Physiology-Cell Physiology*, vol. 319, no. 1, pp. C151–C165, July 2020, doi: 10.1152/ajpcell.00120.2020.
[94] X.-Y. Tang *et al.*, 'Human organoids in basic research and clinical applications', *Sig Transduct Target Ther*, vol. 7, no. 1, May 2022, doi: 10.1038/s41392-022-01024-9.
[95] C. Günther, B. Winner, M. F. Neurath, and T. S. Stappenbeck, 'Organoids in gastrointestinal diseases: from experimental models to clinical translation', *Gut*, vol. 71, no. 9, pp. 1892–1908, Sept. 2022, doi: 10.1136/gutjnl-2021-326560.
[96] A. Fatehullah, S. H. Tan, and N. Barker, 'Organoids as an in vitro model of human development and disease', *Nat Cell Biol*, vol. 18, no. 3, pp. 246–254, Mar. 2016, doi: 10.1038/ncb3312.
[97] S. Rahmani, N. M. Breyner, H.-M. Su, E. F. Verdu, and T. F. Didar, 'Intestinal organoids: A new paradigm for engineering intestinal epithelium in vitro', *Biomaterials*, vol. 194, pp. 195–214, Feb. 2019, doi: 10.1016/j.biomaterials.2018.12.006.
[98] M. Stelzner *et al.*, 'A nomenclature for intestinal in vitro cultures', *American Journal of Physiology-Gastrointestinal and Liver Physiology*, vol. 302, no. 12, pp. G1359–G1363, June 2012, doi: 10.1152/ajpgi.00493.2011.
[99] V. Kriz and V. Korinek, 'Wnt, RSPO and Hippo Signalling in the Intestine and Intestinal Stem Cells', *Genes*, vol. 9, no. 1, p. 20, Jan. 2018, doi: 10.3390/genes9010020.

[100] C. Pleguezuelos-Manzano, J. Puschhof, S. Van Den Brink, V. Geurts, J. Beumer, and H. Clevers, 'Establishment and Culture of Human Intestinal Organoids Derived from Adult Stem Cells', *CP in Immunology*, vol. 130, no. 1, Sept. 2020, doi: 10.1002/cpim.106.

[101] W. Dieterich, M. F. Neurath, and Y. Zopf, 'Intestinal ex vivo organoid culture reveals altered programmed crypt stem cells in patients with celiac disease', *Sci Rep*, vol. 10, no. 1, Feb. 2020, doi: 10.1038/s41598-020-60521-5.

[102] J. Y. Co, M. Margalef-Català, D. M. Monack, and M. R. Amieva, 'Controlling the polarity of human gastrointestinal organoids to investigate epithelial biology and infectious diseases', *Nat Protoc*, vol. 16, no. 11, pp. 5171–5192, Nov. 2021, doi: 10.1038/s41596-021-00607-0.

[103] C. A. Thorne, I. W. Chen, L. E. Sanman, M. H. Cobb, L. F. Wu, and S. J. Altschuler, 'Enteroid Monolayers Reveal an Autonomous WNT and BMP Circuit Controlling Intestinal Epithelial Growth and Organization', *Developmental Cell*, vol. 44, no. 5, pp. 624-633.e4, Mar. 2018, doi: 10.1016/j.devcel.2018.01.024.

[104] D. S. Schwarz and M. D. Blower, 'The endoplasmic reticulum: structure, function and response to cellular signaling', *Cell. Mol. Life Sci.*, vol. 73, no. 1, pp. 79–94, Jan. 2016, doi: 10.1007/s00018-015-2052-6.

[105] W. Huang, Y. Gong, and L. Yan, 'ER Stress, the Unfolded Protein Response and Osteoclastogenesis: A Review', *Biomolecules*, vol. 13, no. 7, p. 1050, June 2023, doi: 10.3390/biom13071050.

[106] Y. Guo, D. W. Sirkis, and R. Schekman, 'Protein Sorting at the*trans*-Golgi Network', *Annu. Rev. Cell Dev. Biol.*, vol. 30, no. 1, pp. 169–206, Oct. 2014, doi: 10.1146/annurev-cellbio-100913-013012.

[107] M. Wang and R. J. Kaufman, 'Protein misfolding in the endoplasmic reticulum as a conduit to human disease', *Nature*, vol. 529, no. 7586, pp. 326–335, Jan. 2016, doi: 10.1038/nature17041.

[108] D. E. Clapham, 'Calcium Signaling', *Cell*, vol. 131, no. 6, pp. 1047–1058, Dec. 2007, doi: 10.1016/j.cell.2007.11.028.

[109] I. Caputo *et al.*, 'Anti-tissue transglutaminase antibodies activate intracellular tissue transglutaminase by modulating cytosolic Ca2+ homeostasis', *Amino Acids*, vol. 44, no. 1, pp. 251–260, Jan. 2013, doi: 10.1007/s00726-011-1120-y.

[110] A. Ruggiano, O. Foresti, and P. Carvalho, 'ER-associated degradation: Protein quality control and beyond', *Journal of Cell Biology*, vol. 204, no. 6, pp. 869–879, Mar. 2014, doi: 10.1083/jcb.201312042.

[111] M. A. McGuckin, R. D. Eri, I. Das, R. Lourie, and T. H. Florin, 'ER stress and the unfolded protein response in intestinal inflammation', *American Journal of Physiology-Gastrointestinal and Liver Physiology*, vol. 298, no. 6, pp. G820–G832, June 2010, doi: 10.1152/ajpgi.00063.2010.

[112] K. Zhang and R. J. Kaufman, 'From endoplasmic-reticulum stress to the inflammatory response', *Nature*, vol. 454, no. 7203, pp. 455–462, July 2008, doi: 10.1038/nature07203.

[113] N. M. PeÃ, 'The endoplasmic reticulum stress/unfolded protein response in gliomagenesis, tumor progression and as a therapeutic target in glioblastoma', *Biochemical Pharmacology*, 2016.

[114] R. Huang *et al.*, 'IRE1 signaling regulates chondrocyte apoptosis and death fate in the osteoarthritis', *Journal Cellular Physiology*, vol. 237, no. 1, pp. 118–127, Jan. 2022, doi: 10.1002/jcp.30537.

[115] P. Walter and D. Ron, 'The Unfolded Protein Response: From Stress Pathway to Homeostatic Regulation', *Science*, vol. 334, no. 6059, pp. 1081–1086, Nov. 2011, doi: 10.1126/science.1209038.

[116] F. He, X. Ru, and T. Wen, 'NRF2, a Transcription Factor for Stress Response and Beyond', *IJMS*, vol. 21, no. 13, p. 4777, July 2020, doi: 10.3390/ijms21134777.
[117] H. Tang, R. Kang, J. Liu, and D. Tang, 'ATF4 in cellular stress, ferroptosis, and cancer', *Arch Toxicol*, vol. 98, no. 4, pp. 1025–1041, Apr. 2024, doi: 10.1007/s00204-024-03681-x.
[118] R. F. Hillary and U. FitzGerald, 'A lifetime of stress: ATF6 in development and homeostasis', *J Biomed Sci*, vol. 25, no. 1, Dec. 2018, doi: 10.1186/s12929-018-0453-1.
[119] S. A. Oakes and F. R. Papa, 'The Role of Endoplasmic Reticulum Stress in Human Pathology', 2017.
[120] S. Yuan, D. She, S. Jiang, N. Deng, J. Peng, and L. Ma, 'Endoplasmic reticulum stress and therapeutic strategies in metabolic, neurodegenerative diseases and cancer', *Mol Med*, vol. 30, no. 1, p. 40, Mar. 2024, doi: 10.1186/s10020-024-00808-9.
[123] '2020 New Guidelines for the Diagnosis of Paediatric Coeliac Disease. ESPGHAN Advice Guide.pdf'. ESPGHAN, 2020.
[122] T. Sato *et al.*, 'Single Lgr5 stem cells build crypt-villus structures in vitro without a mesenchymal niche', *Nature*, vol. 459, no. 7244, pp. 262–265, May 2009, doi: 10.1038/nature07935.
[123] N. Lugli *et al.*, 'R-spondin 1 and noggin facilitate expansion of resident stem cells from non-damaged gallbladders', *EMBO Reports*, vol. 17, no. 5, pp. 769–779, May 2016, doi: 10.15252/embr.201642169.
[124] A. Treveil *et al.*, 'Regulatory network analysis of Paneth cell and goblet cell enriched gut organoids using transcriptomics approaches', *Mol. Omics*, vol. 16, no. 1, pp. 39–58, 2020, doi: 10.1039/C9MO00130A.
[125] N. Barker *et al.*, 'Identification of stem cells in small intestine and colon by marker gene Lgr5', *Nature*, vol. 449, no. 7165, pp. 1003–1007, Oct. 2007, doi: 10.1038/nature06196.
[126] G. D. Wu, W. Wang, and P. G. Traber, 'Isolation and characterization of the human sucrase-isomaltase gene and demonstration of intestine-specific transcriptional elements.', *Journal of Biological Chemistry*, vol. 267, no. 11, pp. 7863–7870, Apr. 1992, doi: 10.1016/S0021-9258(18)42593-8.
[127] A. Tawiah *et al.*, 'High MUC2 Mucin Expression and Misfolding Induce Cellular Stress, Reactive Oxygen Production, and Apoptosis in Goblet Cells', *The American Journal of Pathology*, vol. 188, no. 6, pp. 1354–1373, June 2018, doi: 10.1016/j.ajpath.2018.02.007.
[128] S. Yu *et al.*, 'Paneth Cell-Derived Lysozyme Defines the Composition of Mucolytic Microbiota and the Inflammatory Tone of the Intestine', *Immunity*, vol. 53, no. 2, pp. 398-416.e8, Aug. 2020, doi: 10.1016/j.immuni.2020.07.010.
[129] M. S. Engelstoft *et al.*, 'Research Resource: A Chromogranin A Reporter for Serotonin and Histamine Secreting Enteroendocrine Cells', *Molecular Endocrinology*, vol. 29, no. 11, pp. 1658–1671, Nov. 2015, doi: 10.1210/me.2015-1106.
[130] R. B. Doctor, 'The Actin Cytoskeleton in the Apical Domain of Epithelial Cells', in *Advances in Molecular and Cell Biology*, vol. 37, Elsevier, 2006, pp. 25–47. doi: 10.1016/S1569-2558(06)37002-6.
[131] J. Ren and S. Huang, 'Intestinal organoids in inflammatory bowel disease: advances, applications, and future directions', *Front. Cell Dev. Biol.*, vol. 13, p. 1517121, May 2025, doi: 10.3389/fcell.2025.1517121.
[132] C. Tian *et al.*, 'Stem cell-derived intestinal organoids: a novel modality for IBD', *Cell Death Discov.*, vol. 9, no. 1, p. 255, July 2023, doi: 10.1038/s41420-023-01556-1.